

Division of Cardiology, Department of Medicine  
Helsinki University Central Hospital  
Helsinki, Finland



**MULTICHANNEL MAGNETOCARDIOGRAPHY  
AND BODY SURFACE POTENTIAL MAPPING  
IN EXERCISE-INDUCED MYOCARDIAL ISCHEMIA**

by

Helena Hänninen

Academic Dissertation

To be publicly discussed, by permission of the Medical Faculty  
of the University of Helsinki, in Auditorium 4 of the Meilahti Hospital,  
on October 18, 2002, at 1 o'clock noon.

**HELSINKI 2002**

**Supervised by:**

Docent Lauri Toivonen, M.D., Ph.D.

Docent Markku Mäkijärvi, M.D., Ph.D.

Division of Cardiology, Department of Medicine

Helsinki University Central Hospital

Helsinki, Finland

**Reviewed by:**

Docent Juhani Airaksinen, M.D., Ph.D.

Division of Cardiology, Department of Medicine

Turku University Hospital

Turku, Finland

Professor Hannu Eskola, D.Sc. (Tech.)

Digital Media Institute

Tampere University of Technology

Tampere, Finland

ISBN 952-91-4882-8 (Print)

ISBN 952-10-0617-X (PDF)

Yliopistopaino

Helsinki 2002

**To Petri**

CONTENTS	Page
ABBREVIATIONS .....	8
LIST OF ORIGINAL PUBLICATIONS .....	9
1. ABSTRACT .....	10
2. INTRODUCTION .....	11
3. REVIEW OF THE LITERATURE .....	12
3.1. Electrophysiology of myocardial ischemia.....	12
3.1.1. Ischemic changes at cellular level .....	12
3.1.2. Injury currents.....	13
3.1.2.1. Direct-current magnetocardiography .....	13
3.1.2.2. Diastolic injury currents.....	13
3.1.2.3. Systolic injury currents .....	15
3.1.2.4. Relation of injury currents to myocardial blood flow .....	15
3.1.2.5. Influence of injury currents on electro- and magnetocardiography ...	15
3.1.3. Epicardium and endocardium in experimental transmural ischemia .....	16
3.2. Electrocardiography (ECG).....	17
3.2.1. Theory.....	17
3.2.2. Genesis of cardiac repolarization .....	17
3.2.3. Differences between depolarization and repolarization .....	18
3.2.4. Types of ECG leads.....	18
3.3. Stress testing.....	19
3.3.1. Exercise types .....	19
3.3.2. Objectives of exercise testing.....	19
3.3.3. Myocardial oxygen uptake .....	19
3.3.4. Safety of exercise testing.....	20
3.3.5. Pharmacological stress testing.....	20
3.4. 12-lead ECG in exercise testing .....	20
3.4.1. Diagnostic aspects .....	20
3.4.1.1. Lead sensitivity .....	20
3.4.1.2. Measurement of the ST amplitude.....	20

3.4.1.3.	Criteria for a positive exercise test.....	21
3.4.1.4.	Ischemia localization.....	21
3.4.2.	Sensitivity and specificity.....	21
3.4.2.1.	ST-segment analysis.....	21
3.4.2.2.	Exercise capacity.....	22
3.4.2.3.	ST/HR index, ST/HR slope, and ST/HR hysteresis.....	22
3.4.3.	Prognostic significance of exercise ECG .....	22
3.4.4.	Limitations of the 12-lead ECG.....	24
3.5.	Magnetocardiography (MCG) .....	24
3.5.1.	History .....	24
3.5.2.	Main differences between MCG and ECG.....	24
3.5.3.	Clinical applications of MCG.....	25
3.5.4.	MCG ischemia studies at rest .....	25
3.5.5.	MCG stress studies .....	27
3.5.5.1.	Healthy volunteers .....	27
3.5.5.2.	Coronary artery disease (CAD) patients .....	27
3.5.6.	Current density estimations .....	28
3.6.	Body surface potential mapping (BSPM).....	28
3.6.1.	Theory.....	28
3.6.2.	Clinical applications of BSPM .....	28
3.6.3.	BSPM ischemia studies at rest.....	30
3.6.4.	BSPM stress studies .....	30
3.6.4.1.	Types of stress testing and time phases analyzed .....	30
3.6.4.2.	Map analysis .....	31
3.6.4.3.	Localization of exercise-induced ischemia .....	32
3.6.5.	Acute coronary occlusion .....	32
4.	AIMS OF THE STUDY .....	33
5.	MATERIALS AND METHODS .....	33
5.1.	Study subjects .....	33
5.1.1.	Group I: Single-vessel CAD without prior myocardial infarction.....	33
5.1.2.	Group II: Triple-vessel CAD with prior myocardial infarction.....	34
5.1.3.	Healthy controls.....	35
5.1.4.	Patient distribution in separate studies .....	35
5.2.	Exercise testing.....	36

5.3.	MCG recording and data processing .....	36
5.4.	BSPM recording and data processing.....	38
5.5.	MCG and BSPM data analysis .....	38
5.5.1.	Signal averaging, interpolation, and data conversion .....	38
5.5.2.	Exercise test phases analyzed .....	39
5.5.3.	Repolarization parameters .....	39
5.5.4.	Signal-to-noise ratio and reproducibility of the signal analysis .....	40
5.6.	Magnetic field polarity and orientation .....	41
5.7.	Discriminant index analysis .....	41
5.8.	Map illustrations.....	42
5.9.	Assessment of coronary artery disease .....	42
5.9.1.	Symptom-limited upright bicycle ergometry.....	42
5.9.2.	Transthoracic echocardiography.....	42
5.9.3.	Coronary angiography and left ventriculography .....	43
5.9.4.	Thallium ( <sup>201</sup> Tl) single-photon emission computed tomography.....	43
5.10.	Statistical analysis .....	43
6.	RESULTS OF THE STUDIES.....	44
6.1.	MCG in detection of exercise-induced myocardial ischemia.....	44
6.1.1.	Magnetic field orientation and rotation (I, IV) .....	44
6.1.1.1.	ST segment .....	44
6.1.1.2.	T-wave .....	44
6.1.2.	ST segment and T-wave parameters in MCG (II, IV) .....	46
6.1.2.1.	Spatial evaluation of ischemic changes .....	46
6.1.2.2.	Optimal recording locations.....	48
6.1.3.	Performance of the ischemia parameters evaluated in MCG (IV) .....	50
6.2.	BSPM in detection of exercise-induced myocardial ischemia .....	51
6.2.1.	Spatial evaluation of ischemic changes .....	51
6.2.2.	Optimal recording locations .....	56
6.2.4.	Performance of ischemia parameters in BSPM (III, V).....	58
6.3.	Spatial comparison of MCG and BSPM .....	59
6.4.	Optimal time phases of exercise testing .....	59

6.5.	12-lead ECG in detection of exercise-induced myocardial ischemia .....	59
7.	DISCUSSION.....	61
7.1.	Main findings.....	61
7.2.	Contribution to previous investigations.....	62
7.2.1.	Myocardial ischemia in MCG .....	62
7.2.1.1.	Magnetic field orientation.....	62
7.2.1.2.	QRST analysis in MCG .....	63
7.2.1.3.	ST-segment- and T-wave parameters in MCG .....	63
7.2.1.4.	Optimal locations of ST-segment and T-wave parameters .....	64
7.2.2.	Myocardial ischemia in BSPM.....	64
7.2.2.1.	ST-segment parameters in BSPM.....	64
7.2.2.2.	T-wave parameters in BSPM .....	65
7.2.2.3.	Optimal locations of ST-segment and T-wave parameters .....	65
7.2.3.	Comparison of MCG and BSPM.....	66
7.2.4.	Time scale of ST-segment and T-wave parameters.....	66
7.3.	Methodological considerations.....	67
7.4.	Clinical implications.....	70
8.	CONCLUSIONS .....	71
9.	ACKNOWLEDGEMENTS.....	72
10.	REFERENCES .....	75

## **ABBREVIATIONS**

AP	action potential
BSPM	body surface potential mapping
CAD	coronary artery disease
ECG	electrocardiography, electrocardiogram, electrocardiographic
LAD	left anterior descending coronary artery
LCX	left circumflex coronary artery
LV	left ventricle, left ventricular
MCG	magnetocardiography, magnetocardiogram, magnetocardiographic
MI	myocardial infarction
PCI	percutaneous coronary intervention
RCA	right coronary artery
SD	standard deviation
SPECT	single-photon emission computed tomography
SQUID	superconducting quantum interference device

## LIST OF ORIGINAL PUBLICATIONS

This thesis is based on the following original publications:

**I** Hänninen H, Takala P, Mäkijärvi M, Montonen J, Korhonen P, Oikarinen L, Nenonen J, Katila T, Toivonen L. Detection of exercise-induced myocardial ischemia by multichannel magnetocardiography in single vessel coronary artery disease. *Ann Noninvasive Electrocardiol* 2000; 5: 147-157.

**II** Hänninen H, Takala P, Mäkijärvi M, Montonen J, Korhonen P, Oikarinen L, Simelius K, Nenonen J, Katila T, Toivonen L. Recording locations in multichannel magnetocardiography and body surface potential mapping sensitive for regional exercise-induced myocardial ischemia. *Basic Res Cardiol* 2001; 96: 405-414.

**III** Hänninen H, Takala P, Mäkijärvi M, Korhonen P, Oikarinen L, Simelius K, Nenonen J, Katila T, Toivonen L. ST-segment level and slope in exercise-induced myocardial ischemia evaluated with body surface potential mapping. *Am J Cardiol* 2001; 88: 1152-1156.

**IV** Hänninen H, Takala P, Korhonen P, Oikarinen L, Mäkijärvi M, Nenonen J, Katila T, Toivonen L. Features of ST segment and T-wave in exercise-induced myocardial ischemia evaluated with multichannel magnetocardiography. *Ann Med* 2002; 34: 120-129.

**V** Hänninen H, Takala P, Rantonen J, Mäkijärvi M, Virtanen K, Nenonen J, Katila T, Toivonen L. ST-T integral and T-wave amplitude in detection of exercise-induced myocardial ischemia evaluated with body surface potential mapping. Submitted.

These studies are referred to in the text by their Roman numerals.

Publications I, II, and III constitute a part of the Doctor of Science in Technology thesis, "Cardiac exercise studies with bioelectromagnetic mapping", by Panu Takala, Helsinki University of Technology, Department of Engineering Physics and Mathematics, Laboratory of Biomedical Engineering, 2001.

## 1. ABSTRACT

The aim of the present series of studies was to examine the capability of multichannel magnetocardiography (MCG) and body surface potential mapping (BSPM) to detect and localize exercise-induced myocardial ischemia. Particular emphasis was given to the diagnostic performance of various repolarization parameters, despite variation in the ischemic vessel branch and the presence of single- or multi-vessel disease or of a history of remote myocardial infarction (MI). The optimal recording locations to detect ischemia-induced changes in these repolarization parameters were identified by use of discriminant index analysis.

A pilot study was conducted in 27 patients with single-vessel coronary artery disease (CAD) without prior MI and in 17 healthy controls to evaluate the capability of MCG to detect exercise-induced myocardial ischemia. To identify the optimal recording locations of MCG and BSPM to this detection, 24 patients with single-vessel CAD without prior MI and the 17 healthy controls underwent examinations. In BSPM, the optimal recording sites and time-phases of an exercise test of ST amplitude, ST slope, ST-T integral, and T-wave amplitude to detect exercise-induced myocardial ischemia were studied in 45 patients with CAD, including the 27 patients with single-vessel CAD without prior MI, 18 patients with triple-vessel CAD and a history of prior MI, and in 25 healthy controls. In another MCG pilot study, ST amplitude, ST slope, T-wave amplitude, and ST-T integral were examined in detection of exercise-induced myocardial ischemia in 27 patients with single-vessel CAD without prior MI, in 17 patients with triple-vessel CAD and prior remote MI, and in 26 healthy controls.

The results showed that MCG and BSPM are able to detect exercise-induced myocardial ischemia caused by stenosis in any of the main coronary artery branches, regardless of the presence or absence of a history of remote MI. The exercise-induced myocardial ischemia caused a change in the orientation of the magnetic field during the ST segment and T-wave. In addition to ST depression and elevation, changes in ST slope, T-wave amplitude, and ST-T integral were associated with exercise-induced myocardial ischemia. The optimal locations for ischemia-induced ST depression and decrease in ST slope, in T-wave amplitude and in ST-T integral area were in MCG over the middle inferior thorax and abdomen, and in BSPM over the left anterior and posterior thorax. In BSPM, the variation in these optimal sites in patient subgroups with different ischemia regions was more extensive for T-wave than for ST-segment parameters. The ST-segment and T-wave parameters performed best in different phases of the formal exercise test: ST segment at last workload phase and immediately after cessation of exercise, and T-wave two to four minutes after cessation of exercise.

In conclusion, MCG and BSPM can detect exercise-induced myocardial ischemia in a heterogeneous CAD patient population. In MCG and in BSPM, several ST-segment and T-wave parameters as well as ST amplitude are able to detect ischemia. Spatial evaluation of ischemia-induced postexercise T-wave changes may be useful in localization of the ischemic myocardial region. ST-segment and T-wave parameters may contain information on separate physiological stages of the ischemia development and resolution during exercise testing. Thus, combining the observations over different phases of exercise testing may enhance the electromagnetic detection of clinically relevant myocardial ischemia.

## 2. INTRODUCTION

Coronary artery disease (CAD) is the leading cause of natural death in adults in industrialized countries. Despite the development of novel noninvasive diagnostic tests for CAD, 12-lead electrocardiography (ECG) exercise testing is still the most common means of clinical investigation in evaluation of patients with chest pain (Goraya et al. 2000). In addition to the value of ECG exercise testing as a diagnostic tool, exercise capacity evaluated in this way is a strong and independent predictor of the cardiovascular and all-cause mortality in patients with CAD and in the healthy population (Weiner et al. 1995, Roger et al. 1998, Goraya et al. 2000, Myers et al. 2002)

Magnetocardiography (MCG) is a novel noninvasive technique to register the extracorporeal magnetic fields of the heart generated by the same bioelectric currents as the ECG. The first human MCG recording was recorded in 1963 (Baule and McFee). The development of superconducting quantum interference device (SQUID) magnetometers has allowed the recording of real-time MCGs (Cohen et al. 1970). Early direct-current MCG recordings have made a significant contribution to understanding of the ischemic diastolic TP shifts and systolic “true” ST shifts (Cohen et al. 1971, Cohen et al. 1983, Savard et al. 1983). Presently, MCG is used mainly as a research tool, and most MCG studies so far have focused on arrhythmia risk assessment (Nenonen et al. 2002b). MCG is most sensitive to tangential currents, and chest leads of ECG to radial currents with respect to chest surface. MCG is also able to detect circular vortex currents, which give no ECG signal (Siltanen 1989). Since MCG may show pathological deviations from the normal depolarization and repolarization in a different manner than does ECG, application of MCG to ischemia research is inviting.

Body surface potential mapping (BSPM) is aimed at improving the noninvasive characterization and use of cardiac generated potentials by increased sampling of body surface ECG over the whole thorax. In BSPM, the widespread direct torso sampling of ECG emphasizes its sensitivity in detection of local cardiac events (Mirvis 1987). BSPM is superior to 12-lead ECG in detection and localization of acute and remote myocardial infarctions (MI) (Kornreich et al. 1993, Menown et al. 2000a,b). In patients with non-Q-

wave MIs, minor potential losses during the QRS complex can be identified in BSPM, which are not detectable in 12-lead ECG (Medvegy et al. 2000). Some BSPM studies show marked overlap of the patterns of exercise-induced ST deviation (Kubota et al. 1985 and 1989), others modest success (Wada et al. 1981, Yanowitz et al. 1982), and some improved ischemia localization capacity (Fox et al. 1979a) compared to that of 12-lead ECG. The capability of BSPM to localize acute exercise-induced myocardial ischemia is as yet, however, not established.

Novel, less invasive revascularization techniques will be applicable to a larger proportion of CAD patients in the future, thus enhancing the importance of accurate detection and localization of myocardial ischemia. This requires detailed knowledge of the presence of ischemia. In the present series of investigations, the aim was to examine the ability of MCG and BSPM to detect and localize exercise-induced myocardial ischemia.

At first, a pilot study tested a method to quantify the ischemia-induced changes in the magnetic field orientation. Then, various repolarization parameters, calculated from ST-segment and T-wave data, were applied to ischemia analysis in MCG and BSPM. The capability of the optimal recording locations and optimal time-phases was examined for these repolarization variables in detecting exercise-induced myocardial ischemia in MCG and in BSPM.

### **3. REVIEW OF THE LITERATURE**

#### **3.1. Electrophysiology of myocardial ischemia**

##### **3.1.1. Ischemic changes at cellular level**

**Action potential (AP) changes during acute coronary occlusion.** The development of glass microelectrodes has permitted the description of ischemia-induced changes in transmembrane APs (Downar et al. 1977). The first detectable change, 15 to 30 seconds after experimental coronary occlusion, is the depolarization of the resting membrane potential (Fozzard and Makielski 1985). In the minutes that follow, the resting membrane potential decreases further, and the upstroke velocity, amplitude, and duration of the AP diminish (Surawicz 1995a) (Figure 1). In animal studies, the cells in subepicardial layers of the heart depolarize from -90 to -80 mV to about -65 mV within 4 to 10 minutes after coronary occlusion, and the membrane excitability at this level is lost (Kléber et al. 1978).

**Possible mechanisms of extracellular potassium (K<sup>+</sup>) accumulation.** The most important determinant of the changing electrical activity in acute ischemia is net cellular loss and the following extracellular accumulation of potassium ions (K<sup>+</sup>) (Kléber et al. 1995, Surawicz 1995a). Although several mechanisms appear to be involved in the net cellular loss of K<sup>+</sup> during acute ischemia, the exact mechanism is still controversial. A

decreased active  $K^+$  influx, owing to inhibition of the  $Na^+/K^+$  pump, does not alone explain the potassium loss, since in early ischemia only a small decrease in the rate of the active  $Na^+/K^+$  pumping occurs (Weiss and Shine 1982). Increased passive efflux, by opening of specific  $K^+$  channels, such as the adenosine triphosphate-sensitive  $K^+$  channel or  $Na^+$ -activated  $K^+$  channel has been suggested (Janse and Wit 1989). Intracellular acidification, by stimulation of anaerobic glycolysis, may lead to redistribution of freely movable anions and a cotransport or secondary redistribution of cations (Janse and Wit 1989, Kléber et al. 1995).

**Metabolic changes.** The insufficient catabolism of phospholipids leads to accumulation of specific amphipathic lipid metabolites, contributing to the decrease in the upstroke velocity of the AP, the depolarization of the resting membrane potential, and the shortening of AP duration. In myocardial hypoxia, a large  $K^+$  efflux has been reported in the absence of AP shortening; the latter is observed only at lower levels of oxygen. The primary event inducing  $K^+$  loss may therefore be acidification instead of opening of the  $K_{atp}$  channel (Yan et al. 1993). Osmotic cell swelling, resulting in reduction in extracellular space, may also contribute to the increase in extracellular  $K^+$  concentration (Janse and Opthof 1995). It has also been proposed that depolarization occurs as a direct consequence of intracellular  $Ca^{2+}$  overload in ischemic myocardium, although limited information exists to support the increase in intracellular  $Ca^{2+}$  during the first minutes of ischemia (Janse and Wit 1989).

### 3.1.2. Injury currents

#### 3.1.2.1. *Direct-current magnetocardiography*

Direct-current MCG and ECG studies have clarified the difference between systolic injury currents flowing during the ST segment and diastolic injury currents flowing during the TQ segment and the contribution of these currents to ST shifts in ECG. Direct-current MCG has proven to be useful as a research tool, but thus far not to be practical for clinical purposes (Cohen et al. 1983, Savard et al. 1983).

#### 3.1.2.2. *Diastolic injury currents*

The difference in resting membrane potential between ischemic and normal cells creates a diastolic injury current which flows during the entire cardiac cycle, except that it is interrupted during the S-T interval ("apparent" S-T shift) (Vincent et al. 1977, Cohen et al. 1983, Savard et al. 1983). During the TQ segment, the intracellular potential of the ischemic cells is higher (less negative, i.e., depolarized) than in the normal cells (Figure 1a), causing the diastolic injury current to flow from the ischemic toward the normal tissue. This current causes elevation of the TQ segment in subendocardial ischemia, and depression of the TQ segment in transmural ischemia in spatial areas adjacent to the ischemic region. The differences between the spatial geometry of the ischemic region and

the normal tissues contribute markedly to the manifestations of the injury current in the body surface ECG (Holland and Brooks 1977, Surawicz and Saito 1978, Savard et al. 1983).

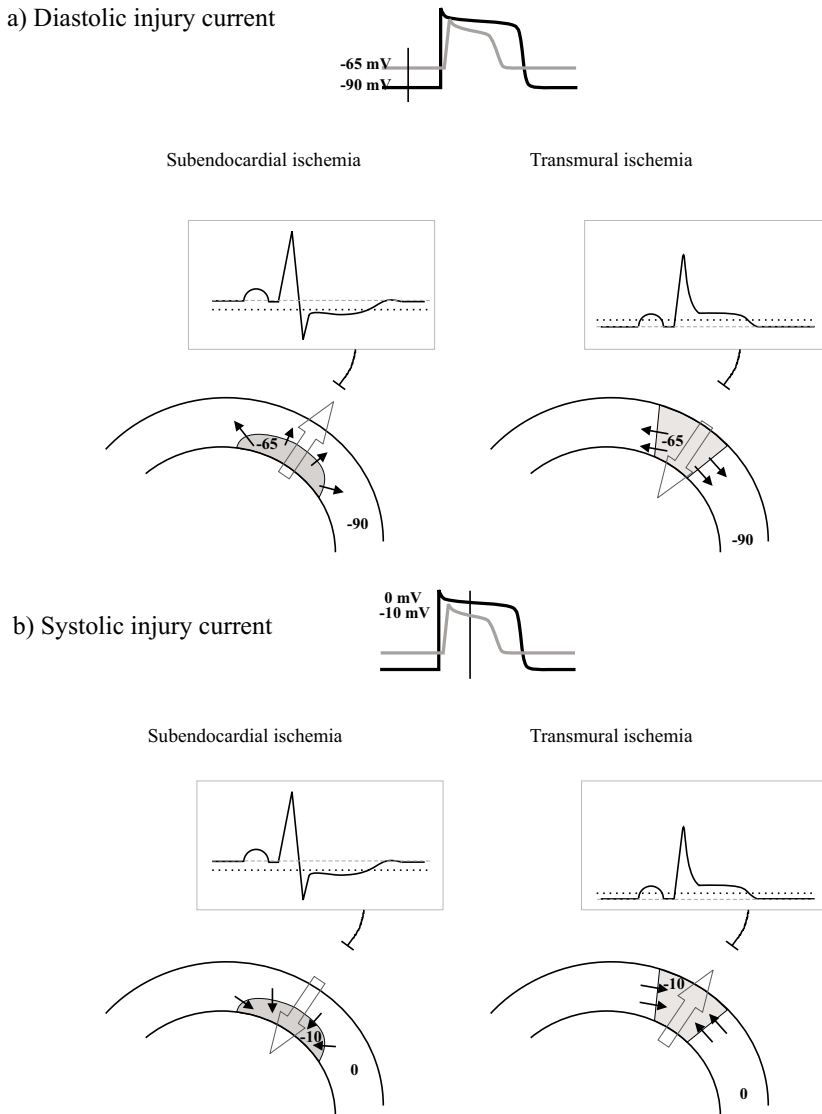


**Figure 1.** Schematic illustration of ischemia-induced changes in cardiac cell action potential (AP) and effect of cardiac spatial geometry between the ischemic region and normal tissues on the body-surface electrocardiogram (ECG). AP of ischemic myocardial cell (grey line), normal myocardial cell (black line). In the ischemic cell, resting membrane potential decreases, and upstroke velocity, amplitude, and duration of AP decrease. a) Diastolic injury current. During the

*TQ segment, the ischemic cell intracellular potential is higher (less negative) than in normal cells. The diastolic injury current flows from ischemic toward normal tissue (small black arrows); net injury current depicted as large white arrow. Left: In subendocardial ischemia, the injury current causes TQ-segment elevation. Right: In transmural ischemia, the injury current causes TQ-segment depression. b) Systolic injury current. During the ST segment, normal-cell intracellular potential is higher (less negative) than ischemic-cell potential. This induces the systolic injury current from normal to ischemic myocardium (small black arrows). Net injury current depicted as large white arrow. Left: In subendocardial ischemia, the current causes ST-segment depression. Right: In transmural ischemia, the injury current causes ST-segment elevation. The opposite ST segment deviations in ECG in subendocardial and transmural ischemia are due to the difference in spatial geometry between the ischemic region and normal tissues. In all four ECG curves, dashed lines indicate the actual baseline due to high-pass filtering; dotted lines depict the baseline that would be evident in direct-current measurements.*

### **3.1.2.3.        *Systolic injury currents***

The difference in AP amplitude between ischemic and normal cells creates the systolic injury current flowing during the plateau of the AP, corresponding to the ST segment of the ECG (Holland and Brooks 1977, Vincent et al. 1977, Cohen et al. 1983, Savard et al. 1983). Furthermore, the ischemic cells may become non-excitabile and fail to depolarize due to diminished resting potential, also leading to the systolic injury current (Cohen et al. 1983). In both conditions, during the ST segment the intracellular potential of the normal cells is higher (less negative) than the potential of the ischemic cells (Figure 1b). This induces the systolic injury current to flow from the normal to the ischemic myocardium ("true" S-T shift). This current causes depression of the ST segment in subendocardial ischemia, and elevation of the ST segment in transmural ischemia (Holland and Brooks 1977, Surawicz and Saito 1978, Savard et al. 1983).

### **3.1.2.4.        *Relation of injury currents to myocardial blood flow***

In experimental models simulating exercise-induced ischemia, development of ECG changes indicative of ischemia has corresponded to a predictable degree of blood flow distribution, and the magnitude of the ST shift has correlated with the intensity of the myocardial blood flow abnormality (Mirvis et al. 1986).

### **3.1.2.5.        *Influence of injury currents on electro- and magnetocardiography***

The ECG recorded on the body surface does not reveal the displacement of the TQ baseline, because the baseline is filtered out to eliminate skin interference (Cohen et al. 1975). The ECG thus does not differentiate between the ST segment displacement caused by the systolic and diastolic injury currents (Vincent et al. 1977, Cohen et al. 1983, Savard et al. 1983). The TQ shift can, however, be measured by use of direct-current MCG, which is insensitive to skin interference and hence able to distinguish between the two types of injury currents (Cohen et al. 1983).

**Spatial and nonspatial influences.** The magnitude and the polarity of the deflection between TQ and ST segments are determined by the orientation of the recording electrode with respect to the boundary of the normal and ischemic tissue, the spatial geometry of the ischemic region, and the nature and extent of the conductor with which both the electrode and the heart are in contact (Holland and Brooks 1977, Holland and Arnsdorf 1977). The TQ-ST segment deflection is a function not only of the electrode location and ischemic geometry (spatial influences), but also of the difference in transmembrane voltage between the ischemic and normal tissues during both systole and diastole (nonspatial influences) (Holland and Brooks 1977, Holland and Arnsdorf 1977). In ECG, experimental studies have demonstrated the significance of the spatial relationship between the cardiac source and the location of the recording electrode on the body surface (MacLeod et al. 1998).

### **3.1.3. Epicardium and endocardium in experimental transmural ischemia**

**Differences between epicardium and endocardium.** Acute myocardial ischemia elicits more severe electrophysiological disturbances in epicardium than in endocardium. Epicardium exhibits more pronounced changes in monophasic APs and greater prolongation of conduction time and of refractory period than does endocardium during acute ischemia (Taggart et al. 1988). Lukas and Antzelevitch (1993) found that in acute myocardial ischemia, the presence of a prominent transient outward current in ventricular epicardium, but not in endocardium, contributes to more pronounced electrophysiological disturbances in epicardium than in endocardium. In a canine model, simulated ischemia in epicardium shortened AP duration and led to loss of AP spike-and-dome morphology. This loss of the AP dome morphology in ischemic epicardium gives rise to a transmural voltage gradient underlying ST-segment elevation in ECG during transmural ischemia (Yan and Antzelevitch 1999).

**The M cell theory.** The discovery of the M cells in deep subepicardial layers of the ventricular wall has changed the concept of T-wave genesis. Yan and Antzelevitch (1998) compared transmural ECGs with transmembrane AP recordings from epicardial, M region, and endocardial sites. They showed that the morphology of the T-wave appears to be due in large part to currents flowing down voltage gradients present on either side of the M-cell region during both phases 2 and 3 of the ventricular AP. The T-wave begins when the epicardial AP separates from that of M cells. As the epicardium repolarizes, the gradient between epicardium and M cells grows, giving rise to the ascending limb of the T-wave. The peak of the T-wave marks the time of the full repolarization of the epicardium. When the endocardial plateau deviates from that of M cells it generates the opposite voltage gradient, limiting the amplitude of the T-wave, and thus contributes to the initial part of the descending limb of the T-wave. The full repolarization of the M-cell region marks the end of the T-wave.

**Electrical coupling of ventricular wall layers.** Epicardium and endocardium serve to electrically stabilize and abbreviate the AP duration of the M cells (Antzelevitch et al. 1999). Removal or infarction of either would be expected to lead to a prolongation of the AP duration of the M cells (Yan and Antzelevitch 1996). Supporting this hypothesis, QT interval and QT dispersion are reported to increase in some patients presenting with non-Q-wave infarction, in which a thin margin of the endocardium is infarcted (Antzelevitch et al. 1999).

## **3.2. Electrocardiography (ECG)**

### **3.2.1. Theory**

**Genesis of ECG.** The heart beat is accompanied by the development and spread of ionic currents through the body, resulting in the establishment of electric potentials on the body surface. This current flow arises from ion movement across myocardial cell membranes and from subsequent ion movement throughout the extracellular space of the various tissues of the body. All normal and abnormal deflections recorded by the ECG depend upon the origin and behavior of this chain of ionic activity. One may view the ECG as a study of ionic current flow: 1) across excitable cell membranes (the transmembrane events of single myocardial cells), 2) between aggregates of cells (the temporal and spatial patterns of activation and recovery), and 3) throughout the entire body (the properties of the volume conductor and boundaries of the body) (Holland and Arnsdorf 1977). This flow of current creates voltages between sites on the body surface where electrodes may be placed. These voltages, measured as a function of time, are called electrocardiograms (Barr 1989).

### **3.2.2. Genesis of cardiac repolarization**

The basic shape of the ventricular action potential (AP), the local difference between AP shapes and durations, and the sequence of activation all contribute to the patterns of ventricular repolarization. The ST segment corresponds to the early, slow phase of repolarization (AP plateau, phase 2), whereas the T-wave represents the more rapid, terminal portion of repolarization (AP phase 3). The duration of the AP roughly correlates with the duration of the QT interval, and the duration of the plateau of the AP with the duration of the ST segment in the ECG (Surawicz 1995b).

**ST segment.** Absence of ST-segment deviation from baseline implies an absence of significant potential differences during the plateau of ventricular repolarization. Small differences at the very onset of repolarization in various parts of the left ventricle may be expected to cause deviation in the QRS and ST-T junction (i.e., depression of the J point) and the early portion of the ST segment. This provides the rationale of measuring the ST deviation 60 ms to 80 ms after the end of the QRS complex (Surawicz and Saito 1978).

**T-wave.** The concordance (same polarity) of the normal QRS and T-waves has been explained by the inverse correlation between their activation times and refractory periods (Burgess et al. 1972) and between their activation times and AP durations transmurally (Franz et al. 1987) and epicardially (Cowan et al. 1988). In patients with T-wave inversion caused by aortic stenosis or left ventricular hypertrophy, no relation exists between the duration of the AP and activation time, and the repolarization sequence has closely resembled the activation sequence (Cowan et al. 1988, Franz et al. 1991). It has been thought that exercise-induced ischemia shortens the AP duration in the endocardium, and reverses the normal repolarization sequence thus taking place from endocardium to epicardium, demonstrated as T-wave changes in ECG (Surawicz 1995c, Lukas and Antzelevitch 1993). During exercise testing, more pronounced shortening of the interval from the apex of the T-wave to the end of the T-wave occurs in patients with CAD than in healthy controls, with no significant change in QT interval between these groups (O'Donnell et al. 1985). In patients with abnormal T-waves at rest, the presence or absence of exercise-induced T-wave normalization has not distinguished patients with CAD from those without (Aravindakshan et al. 1977).

### **3.2.3. Differences between depolarization and repolarization**

Depolarization and repolarization differ in some fundamental aspects. Repolarization is not propagated in the same sense as depolarization, and the current emerges from a much wider region at the same time-point (Barr 1989). In BSPM, detection of multiple potential maxima or minima during repolarization has indicated that some information about local myocardial repolarization events may be detected on the body surface, challenging the concepts of single dipole analysis of ECG (Abildskov et al. 1977). Since the potential decline in any volume conductor with the properties of the human thorax is approximately in proportion to the square of the distance, the remoteness of the electrodes placed on the patient's extremities is sufficient to minimize the nondipolar components of the ECG caused by the proximity effect. In contrast, the anterior precordial leads are influenced by the local potentials generated in the structures lying directly beneath the corresponding electrodes (Surawicz 1995c).

### **3.2.4. Types of ECG leads**

When an electrode is in contact with the heart, ECG leads are called direct; when they are placed at a distance greater than two cardiac diameters from the heart, they are called indirect. When ECG leads are in close proximity to the heart (but not in contact), they are called semidirect. In bipolar leads, both electrodes face sites with similar potential variations, whereas in unipolar leads, potential variation in one electrode is negligible in comparison with the other. In the standard 12-lead ECG used in clinical practice, leads I, II, and III are indirect and bipolar; leads aVR, aVL, and aVF are indirect and unipolar; and leads from V<sub>1</sub> to V<sub>6</sub> are semidirect and unipolar (Surawicz 1995c). If any two of the six

limb leads are recorded simultaneously, the other four can be mathematically derived from them (Macfarlane 1989). To reduce motion and muscle artifacts in exercise testing, modified limb leads according to Mason and Likar (1966) are usually applied.

### **3.3. Stress testing**

#### **3.3.1. Exercise types**

Three types of muscular contraction or exercise can be applied as a stress to the cardiovascular system: static (isometric), dynamic (isotonic or locomotory), and resistive (a combination of static and dynamic) (Bruce 1974, MacDougall 1994).

#### **3.3.2. Objectives of exercise testing**

The objectives of exercise testing are: 1) to determine the functional aerobic capacity (maximal oxygen uptake), 2) to assess cardiovascular response to exercise (chronotropic and inotropic reserve), 3) to assess the balance of forces at the cell membrane between increasing myocardial demand for oxygen and available supply by the coronary circulation, reflected in the ST displacement of the ECG, and 4) to consider the exercise test as an important extension of the clinical history and physical examination (Bruce 1971).

#### **3.3.3. Myocardial oxygen uptake**

The intramyocardial wall stress, contractility, and heart rate primarily determine myocardial oxygen uptake, which can be estimated during clinical exercise testing as the product of heart rate and systolic blood pressure, called the rate-pressure product or double product. A linear relationship exists between myocardial oxygen uptake and coronary blood flow. During exercise, coronary blood flow increases as much as five-fold above the resting value. A subject with obstructive CAD cannot often maintain adequate coronary blood flow to the affected region and supply the metabolic demands of the myocardium during exercise; consequently, myocardial ischemia occurs (Fletcher et al. 2001). The aerobic capacity,  $\dot{V}O_2$  max, is not only greater in men than in women, but is greater in athletes than in sedentary persons; it increases with physical training and diminishes with bed-rest or semi-starvation (Bruce 1971). Cardiopulmonary exercise-testing involves measurement during a symptom-limited exercise test of respiratory oxygen uptake ( $\dot{V}O_2$ ), carbon dioxide production ( $\dot{V}CO_2$ ), and ventilatory parameters (Chaitman 1997). Maximal oxygen uptake ( $\dot{V}O_2$  max) is equal to the product of cardiac output and of arterial-mixed venous oxygen difference at maximal exercise, representing the liters of oxygen transported from the lungs per minute and used by skeletal muscle at peak effort (Bruce 1977).

### **3.3.4. Safety of exercise testing**

Although exercise testing is generally considered a safe procedure, acute MI and death have occurred. Multiple surveys have confirmed that as many as 10 MIs or deaths or both can be expected per 10 000 exercise tests. Estimates of sudden cardiac death during exercise testing revealed rates from 0 to 5 per 100 000 tests (Fletcher et al. 1998).

### **3.3.5. Pharmacological stress testing**

Instead of exercise, pharmacological agents can serve to increase cardiac work or serve to cause coronary arterial vasodilation in order to increase myocardial blood flow. Patients unable to undergo exercise testing for reasons such as deconditioning, peripheral vascular disease, orthopedic disability, neurological disease, or concomitant illnesses can benefit from pharmacological stress imaging. Adrenergic agents such as dobutamine and vasodilators such as adenosine or dipyridamole can be applied to challenge flow in stenosed vessels, and the functional consequences can be analyzed with echocardiography or nuclear perfusion imaging (Fletcher et al. 2001).

## **3.4. 12-lead ECG in exercise testing**

### **3.4.1. Diagnostic aspects**

#### **3.4.1.1. *Lead sensitivity***

In 12-lead ECG, the chest lead V<sub>5</sub> is the most sensitive single unipolar electrode position for detection of exercise-induced myocardial ischemia (Blackburn and Katigbak 1963, Viik et al. 1998 and 1999). The bipolar lead CM<sub>5</sub>, applied between the manubrium and lead V<sub>5</sub> chest location, has been suggested as the most sensitive single bipolar lead for its detection (Chaitman et al. 1978, Quyyumi et al. 1986). Multiple lead systems improve the accuracy of exercise treadmill testing compared to a unipolar lead V<sub>5</sub> or bipolar lead CM<sub>5</sub> alone (Mason et al. 1967, Chaitman et al. 1978). ST deviation in right precordial leads improves the detection of exercise-induced transient ischemia caused by stenosis of the right coronary artery (RCA) (Braat et al. 1985, Chouhan et al. 1989, Michaelides et al. 1999).

In resting ECG recorded during chest pain, the number of leads with ST-segment deviations and the amount of total ST-segment deviation has shown a positive correlation with the number of diseased coronary arteries. The left main and triple vessel CAD frequently show ST depression in leads I, II, and V<sub>4</sub>-V<sub>6</sub>, ST elevation in lead aVR, and a total amount of ST-segment changes of > 12 mm (Gorgels et al. 1993).

#### **3.4.1.2. *Measurement of the ST amplitude***

ST level is measured relative to the P-Q junction, because during exercise the U-P segment often disappears. The three key measurements are the identification of the P-Q junction (isoelectric line), the J point (i.e., J junction), and the time-point 60 ms or 80 ms after the J

point. At ventricular rates > 130 beats/min, the optimal instant to determine the extent of ST-segment displacement is at 60 ms after the J junction. When the J point relative to the P-Q junction is depressed at baseline, the net difference from the J junction determines the magnitude of exercise-induced displacement. When the J junction is elevated at rest and progressively becomes more depressed during exercise, the magnitude of ST-segment displacement is determined from the P-Q junction and not from the resting elevated J junction (Fletcher et al. 2001).

#### **3.4.1.3.        *Criteria for a positive exercise test***

ST-segment depression is the most common manifestation of exercise-induced myocardial ischemia, representing subendocardial ischemia. The standard criterion for abnormal ST depression is a horizontal or downsloping ST-segment depression of  $\geq 0.10$  mV lasting for 80 ms. Horizontal ST slope < 0.7 mV/s during exercise and ST slope < 0.3 mV/s during recovery in addition to ST depression has improved the accuracy of exercise testing (Ribisl et al. 1993). Other factors related to the probability and severity of CAD include the degree, time of appearance, duration, and number of leads with ST-segment depression. The development of > 0.10 mV of J point elevation, persistently elevated at 60 ms after the J point, is considered an abnormal response (Fletcher et al. 2001). Prior MI is the most frequent cause of ST-segment elevation during exercise and is related to the presence of severe hypokinetic or akinetic left ventricular (LV) segmental wall motion (Mark et al. 1987a, Yasumura et al. 1987, Bruce et al. 1988). In patients without a previous MI, ST-segment elevation frequently localizes the site of severe transient ischemia (Mark et al. 1987a, Fletcher et al. 2001).

#### **3.4.1.4.        *Ischemia localization***

The site of ST depression in exercise 12-lead ECG does not identify the anatomic site of coronary artery obstruction (Dunn et al. 1981, Fuchs et al. 1982, Mark et al. 1987a, Chaitman 1997).

### **3.4.2. Sensitivity and specificity**

#### **3.4.2.1.        *ST-segment analysis***

The sensitivity of exercise ECG for single-vessel disease ranges from 25% to 71%. The exercise-induced ST-segment displacement is most frequent in patients with left anterior descending coronary artery (LAD) disease, followed by those with RCA disease, and then by those with isolated left circumflex coronary artery (LCX) disease (Chaitman 1997). Meta-analysis, comparing the results of exercise testing and coronary angiography, has demonstrated that ST depression has a mean sensitivity and mean specificity of 68% and 77% for detection of CAD in general (Gianrossi et al. 1989), and 81% and 66% for detection of multi-vessel disease (Detrano et al. 1989). The predictive accuracy of a test is

greatly influenced by the prevalence of disease in the population tested (Selzer 1981, Diamond 1986).

#### **3.4.2.2. *Exercise capacity***

Patients with exercise-induced ST depression of 0.20 mV or more and who were unable to complete stage II of the Bruce exercise protocol had a post-test risk for CAD and multi-vessel disease of 0.97 and 0.88. In patients with work capacity exceeding stage III of the Bruce protocol the corresponding post-test risk was 0.76 and 0.44 (Chaitman 1986).

#### **3.4.2.3. *ST/HR index, ST/HR slope, and ST/HR hysteresis***

Improved performance in the exercise ECG for detection of CAD and assessment of the anatomical, functional, and prognostic severity of CAD can come from relating the magnitude of ST-segment depression to heart rate changes during effort (Elamin et al. 1982, Okin and Kligfield 1995). Heart-rate adjustment of ST depression increases the predictive value of the exercise ECG for coronary events and for cardiovascular mortality in asymptomatic men and women (Okin et al. 1991) and for higher-risk asymptomatic men (Okin et al. 1996).

The ST/HR index represents the average rate of change in ST depression over the entire course of exercise. In contrast, the linear regression-based ST/HR slope quantifies the maximal rate of ST-segment change relative to heart rate during the period of active ischemia that occurs at the end of exercise. Advantages of the ST/HR index include its arithmetic simplicity, which allows retrospective application in populations that have used standard exercise protocols; the ST/HR slope, on the other hand, is more useful in detection of triple-vessel disease and for evaluating the anatomic extent of coronary obstruction (Okin and Kligfield 1995). ST/HR hysteresis, integrating the ST/HR analysis during both the exercise and postexercise recovery phases of the exercise ECG test, has improved the diagnostic performance of exercise testing compared to the end-exercise or recovery ST depression or the ST/HR index (Lehtinen et al. 1996, Viik et al. 1997).

#### **3.4.3. Prognostic significance of exercise ECG**

**Epidemiological studies.** In a multivariate analysis of the resting routine electrocardiogram, the most significant correlates of ST-T-wave abnormalities were LV contraction abnormalities, followed by age, gender, presence of LAD disease, elevated end-systolic volume index, and diagnosis of hypertension (Mirvis et al. 1990). Epidemiological studies have shown that degree of exercise-induced ST deviation is a very strong and independent predictor of future coronary death and other clinical endpoints in three groups: high-risk men with no history of CAD (Rautaharju et al. 1986, Laukkanen et al. 2001a), heterogeneous CAD inpatients referred for cardiac catheterization (Mark et al. 1987b), and outpatients with suspected CAD referred for exercise testing (Mark et al. 1991).

**Significance of ST depression and chest pain.** Exercise-induced ST depression has been the most significant variable in relation to the amount of ischemic myocardium evaluated with stress echocardiography, whereas no relation has been noted between exercise-induced chest pain and amount of ischemic myocardial dysfunction. Those patients with neither chest pain nor ST depression constitute almost 50% of patients with CAD, and have less ischemia than do patients with ECG-documented ischemia (Hecht et al. 1994).

**Prognostic factors.** Exercise capacity is a strong predictor of all-cause mortality in healthy males (Goraya et al. 2000, Laukkanen et al. 2001b, Myers et al. 2002) and in patients with CAD (Roger et al. 1998, Goraya et al. 2000, Myers et al. 2002). Abnormal heart-rate recovery, which may be a reflection of decreased vagal activity and impaired chronotropic response, has been associated with increased overall mortality (Cole et al. 1999). Since beta blockers slow heart-rate recovery (Desai et al. 2001), its predictive value in patients taking beta blockers is controversial; some studies showing predictive value (Cole et al. 1999), not found in the others (Nishime et al. 2000). In patients with an exercise-induced horizontal or downsloping ST depression of 0.20 mV or more, the annual survival rate decreases with decreasing duration of exercise performance (Dagenais et al. 1982). The time of onset of 0.20 mV of ST depression during exercise has been inversely related to coronary events (Ellestad and Wan 1975). A systolic blood pressure less than 130 mm Hg during maximal exercise, exercise duration less than 3 minutes (Bruce 1977), and chronotropic incompetence (Ellestad and Wan 1975) have each been related to poor prognosis. In contrast, patients with CAD showing a negative exercise electrocardiogram reaching Bruce stage III, or 85% of the maximal age-predicted heart rate, had a respective annual mortality rate of only 1.5%, 2.5%, and 3.5% per year for single, double, and triple-vessel disease (Weiner et al. 1982).

**Mortality.** The annual mortality rate in asymptomatic patients or in patients with mild angina appears to be lower than in more symptomatic patients (Ryan et al. 1985). Exercise-induced ST depression, angina, or both have correlated in some studies with clinical endpoints, including unstable angina, recurrent MI, sudden death, and overall mortality after MI (Théroux et al. 1979, Froelicher 1994), whereas several other studies have failed to demonstrate a significant relation between ST depression and clinical outcome (Pilote et al. 1989, Arnold et al. 1993, Mickley et al. 1993, Moss et al. 1993). The abnormal ST-segment baseline often impairs the interpretation of the exercise ECG in post-MI patients (Fletcher et al. 1998). Revascularization procedures may influence the natural history of the patients after MI and alter the prognosis associated with abnormalities observed during exercise testing (Chaitman et al. 1993). However, such factors as the presence of inducible ischemia, severity of LV dysfunction, and the extent of CAD do associate with adverse post-MI outcome (Marcovitz 1997).

#### **3.4.4. Limitations of the 12-lead ECG**

The diagnostic power of 12-lead ECG in acute transient ischemia and in MI may not be optimal, due to limited coverage of the standard precordial leads over the thorax (Selker 1989). Such failure of 12-lead ECG in detection of cardiac abnormalities is primarily a result of inadequate spatial sampling of ECG information relative to the localized distributions specific to those abnormalities (Kornreich et al. 1991 and 1993, Lux et al. 1995). During percutaneous coronary intervention (PCI), because the standard 12-lead ECG does not sample the ST amplitude extrema, their magnitude, or location, the 12-lead ECG often underestimates ischemic response (Lux et al. 1995).

### **3.5. Magnetocardiography (MCG)**

#### **3.5.1. History**

MCG is a technique to register the extracorporeal magnetic field of the heart which is generated by the same currents as the ECG (Nenonen 2002a, Tavarozzi et al. 2002a). First detected in the early 1960's, the cardiac magnetic field has a peak amplitude of only about 50 pT, one millionth of the earth's magnetic field (Baule and McFee, 1963). Cohen (1967) was the first to use a shielded measuring chamber for MCG recordings. The development of the SQUID magnetometer allowed the recording of real-time MCGs (Cohen et al. 1970, Cohen and McCaughan 1972). The development of second-order SQUID gradiometers and low-cost aluminum shielding has allowed MCG recordings to be made in a hospital environment (Nenonen 2002a, Nenonen et al. 2002b, Tavarozzi et al. 2002b).

#### **3.5.2. Main differences between MCG and ECG**

MCG has morphological features similar to the P-wave, QRS complex, and T- and U-waves of the ECG, and the temporal relationships between them are generally the same (Saarinen et al. 1978). Almost all MCG studies are based on measurement of the magnetic-field component perpendicular (radial or z-component) to the anterior chest ( $B_z$ ). MCG is thus most sensitive to currents tangential to the chest surface, whereas especially chest leads of ECG are more sensitive to radial currents. MCG may therefore show any pathological deviation from the normal direction of depolarization and repolarization in a different manner than does ECG (Siltanen 1989). MCG is also less affected than is ECG by conductivity variations caused by the lungs, pericardial effusion, muscles, and skin (Plonsey 1972, Siltanen 1989).

The ischemic diastolic TP shifts and systolic "true" ST shifts can be distinguished from each other in direct-current MCG, since there are no potentials generated by the skin-electrode interface needing to be filtered out, as in body surface ECG. The main difference between spatial ECG and MCG ( $B_z$ ) patterns is the spatial angle of 90° between them, an essential feature of the MCG and ECG maps (Siltanen 1989). With increasing distance  $r$

from the source, the magnetic field attenuates rapidly in proportion to  $1 / r^2$  (Saarinen et al. 1974, Siltanen 1989).

### 3.5.3. Clinical applications of MCG

In addition to ischemia research (Table 1), MCG has been applied mainly in the following clinical settings:

**Localization of pre-excitation and other cardiac sources.** MCG has proven accurate in localization of accessory pathways causing pre-excitation in Wolff-Parkinson-White syndrome (Mäkijärvi et al. 1992), as well as in localization of the tachycardia points of origin (Moshage et al. 1996, Leder et al. 1998a) and premature ectopic complexes (Oeff and Burghoff 1994). MCG has proven more accurate than BSPM in three-dimensional localization of an amagnetic pacing catheter in the heart (Pesola et al. 1999a).

**Arrhythmia-risk stratification.** Late fields of MCG have been superior to late potentials of signal-averaged ECG in post-MI patients in indicating a propensity toward life-threatening arrhythmias (Mäkijärvi et al. 1993, Korhonen et al. 2000). Magneto-cardiographic intra-QRS fragmentation (Korhonen et al. 2001) and QT dispersion (Oikarinen et al. 2001) have identified post-MI patients prone to ventricular arrhythmias, the former being independent of the extent of LV dysfunction.

**LV hypertrophy.** MCG can detect patients with LV hypertrophy (Fujino et al. 1984) and quantify its degree in patients with increased LV mass (Karvonen et al. 2002).

**Fetal rhythm assessment.** In fetal MCG, parameters concerning the electrical excitation of the fetal heart such as AV conduction, repolarization period, or morphology of the QRS complex can be determined, leading to more profound analysis of fetal arrhythmias (van Leeuwen et al. 1999a, Menéndez et al. 2001). Moreover, prenatal diagnosis of QT prolongation has been made feasible by fetal MCG (Menéndez et al. 2000).

### 3.5.4. MCG ischemia studies at rest

**Depolarization and repolarization.** At rest, the largest differences between post-MI patients and controls have occurred in MCG during repolarization, whereas in BSPM they have been found during depolarization. The repolarization changes in MCG have been more prominent in patients with inferior than in those with anterior Q-wave MI (Lant et al. 1990). Tsukada et al. (2000) studied 10 patients with CAD, of which 7 had a history of remote myocardial infarction, and 12 healthy subjects with MCG at rest. The ratio of the maximum repolarization and depolarization values, found by comparison between ST-T and QRS isointegral maxima, was reduced in patients with CAD compared to values in healthy controls. Kandori et al. (2001a) used 64-channel MCG at rest to study 20 patients with CAD and 29 healthy controls, and parameters calculated from the current-arrow maps

of their ST-segment data were able to differentiate their CAD patients from healthy controls. The equivalent current dipole calculation during depolarization and repolarization has also allowed separation of patients with CAD from healthy controls (van Leeuwen et al. 1997).

**QT dispersion.** The spatial evaluation of QT dispersion at rest has separated patients with CAD without MI from healthy controls (van Leeuwen et al. 1996 and 1999b).

**Magnetic field orientation.** The magnetic field orientation of a heterogeneous CAD patient group comprising both non-MI patients with normal ECGs and post-MI patients has differed from that of healthy controls at rest, with more prominent changes in severe disease (van Leeuwen et al. 1999c). The authors defined field orientation as the angle between the line joining the field extrema and the right-left line of the torso (van Leeuwen et al. 1999c).

**Table 1.** *Human magnetocardiographic studies on coronary artery disease and ischemia.*

Author	Year	Journal	No. of patients	No. of controls	Type of stress testing	QRS analysis y/n
<b>With stress testing</b>						
Saarinen	1974	Cardiovasc Res	1	24	Physical	n
Cohen	1976	J Electrocardiol	-	1	Physical	n
Cohen	1983	Circ Res	1	-	Physical	n
Brockmeier	1994	J Electrocardiol	-	20	Physical	n
Brockmeier	1997	J Cardiovasc Electrophysiol	-	3	Orciprenaline	n
Hailer	1999	J Electrocardiol	7	8	Arbutamine	n
Pesola	1999	BioMed Tech (Berl)	13	-	Physical	n
Kandori	2001	Med Biol Eng Comput	8	4	Physical	y
Takala	2001	Ann Biomed Eng	-	12	Physical	n
Takala	2001	Phys Med Biol	3	2	Physical	n
Takala	2002	Basic Res Cardiol	24	17	Physical	n
<b>No. of subjects</b>			<b>57</b>	<b>91</b>		
<b>Without stress testing</b>						
Lant	1990	J Electrocardiol	22	9	None	y
Van Leeuwen	1996	Pacing Clin Electrophysiol	10	10	None	n
Van Leeuwen	1997	Biomed Tech (Berl)	20	10	None	y
Leder	1998	Int J Cardiol	2	2	None	y
Van Leeuwen	1999	BioMed Tech (Berl)	42	20	None	n
Tsukada	2000	Int J Card Imaging	10	12	None	y
Kandori	2001	Med Biol Eng Comput	20	29	None	n
<b>No. of subjects</b>			<b>126</b>	<b>92</b>		

### 3.5.5. MCG stress studies

#### 3.5.5.1. *Healthy volunteers*

In 1976 Cohen and coworkers reported pronounced ST depressions in MCG of a healthy subject after physical exercise, whereas ECG showed only slight ST depression (Cohen et al. 1976). ST-segment shifts and T-wave inversions in MCG not visible in simultaneous ECG mapping have been evident in healthy subjects after both physical exercise and pharmacological stress (Brockmeier et al. 1994 and 1997). In healthy subjects, physical exercise leads to an increase in the magnetic field component outward from the precordium and a decrease in the minimal value of the MCG signal during ST segment and T-wave, neither of which were found in ECG mapping (Takala et al. 2001a). It has been suggested that the difference between these MCG and ECG findings may be explained by the higher sensitivity of MCG to junctional ST shifts and circular vortex currents, the latter giving no ECG signal (Brockmeier et al. 1997).

#### 3.5.5.2. *Coronary artery disease (CAD) patients*

**Exercise stress studies.** Saarinen et al. (1974) reported performing the first single-channel MCG on a CAD patient after exercise testing. Ischemic ST depression appeared in MCG, and the ST amplitude shift/R amplitude ratio was greater in MCG than in ECG. In a direct-current MCG study, Cohen et al. (1983) found TQ baseline elevation and ST depression after a two-step exercise test of a patient with CAD. The ratio of the diastolic to the systolic injury current was 70% to 30% during exercise, and during recovery, the diastolic "apparent" ST shift disappeared more rapidly than did the "true" ST shift. Kandori et al. (2001b) found distinct patterns for each stenosed main coronary artery in current-ratio maps and different maximum current ratios in six patients with CAD compared to patterns in four healthy controls after a two-step exercise test. After PCI treatment, these abnormalities were reduced. Heart-rate adjustment of the rotation of the magnetic field has improved ischemia detection during the recovery phase of a bicycle exercise test (Takala et al. 2001b and 2002). The magnetic field orientation was defined as the two-dimensional orientation of the maximum spatial field gradient, a method closely resembling the method presented by van Leeuwen et al. (1999c).

**Pharmacological stress studies.** Hailer et al. (1999) studied seven CAD patients with normal 12-lead ECGs, and eight healthy controls with 37-channel MCG and 12-lead ECG at rest and under pharmacological stress induced with arbutamine. The evaluation of spatial distribution of QT dispersion in MCG, reflecting regional heterogeneity of repolarization, enhanced the sensitivity of detection of CAD both at rest and during stress compared to the QT dispersion assessed in 12-lead ECG.

### **3.5.6. Current density estimations**

During QRS complex, inverse calculation of the current distribution has revealed reduced current density over the infarcted region of the myocardium (Leder et al. 1998b). Current density estimation by use of the injury current during ST segment has been able to localize regions of transient exercise-induced ischemia, then verified by coronary angiography and thallium ( $^{201}\text{Tl}$ ) single-photon emission computed tomography (SPECT) (Pesola et al. 1999b). The need for accurate thorax geometry and the need to use several constraints in the calculation process, however, limit the applicability of this method (Nenonen 1994, MacLeod et al. 1995, Leder et al. 1998b).

## **3.6. Body surface potential mapping (BSPM)**

### **3.6.1. Theory**

BSPM, defined as the temporal sequence of potential distributions observed on the thorax throughout one or more electrical cardiac cycles, is an extension of conventional ECG aimed at refining the noninvasive characterization and use of cardiac-generated potentials. The improved characterization is accomplished by increased spatial sampling of body surface ECG, recorded as tens or even hundreds of unipolar ECGs either simultaneously or individually with subsequent time alignment (Lux 1989, Flowers and Horan 1995). Complete body surface-mapping sampling systems utilize leads ranging from 128 to 242 body surface recording sites (Lux 1989, Simelius et al. 1996). Interpolation techniques allow a 32-lead recording array to show an average correlation of 97% with respect to actual recordings of a complete body surface map, over 92% accuracy in estimating low amplitude signals, and a root mean square error of 20  $\mu\text{V}$  for ST-segment distributions (Lux et al. 1979, Green et al. 1987a, Fuller et al. 1996).

**Comparison to vectorcardiography.** Vectorcardiography is designed for the detection of cardiac electrical activity compressed into a single dipole source (Hoffman 1980, Macfarlane 1989), whereas BSPM is sensitive to regional cardiac events (Mirvis et al. 1980, Mirvis 1987). Electrocardiographic examination of specific cardiac regions is excluded by any approaches in which the heart is represented as a single fixed-location dipole (Abildskov et al. 1977). Whereas vectorcardiography conceptualizes all forces into three vectoral terms, body surface mapping permits widespread direct torso sampling which emphasizes detection of local cardiac events (Mirvis 1987).

### **3.6.2. Clinical applications of BSPM**

In addition to ischemia research (Table 2), BSPM has been mainly applied in the following clinical settings:

**Localization of pre-excitation and other cardiac sources.** BSPM is useful in localization of the accessory pathways in Wolff-Parkinson-White syndrome (Dubuc et al. 1993), and the origin sites of ectopic atrial activation (SippensGroenewegen et al. 1998). Abnormal activation sequences in right bundle branch block (Sohi et al. 1980) and in left bundle branch block (Sohi et al. 1983) have also been investigated by use of BSPM.

**Table 2.** *Human body surface potential mapping studies on myocardial ischemia.*

Author	Year	Journal	No. of patients	No. of controls	Type of stress testing	QRS analysis y/n
<b>With stress testing</b>						
Mirvis	1977	Circulation	-	15	Bicycle	y
Fox	1978	Br Heart J	20	20	Bicycle	n
Fox	1978	Br Med J	85	24	Bicycle	n
Fox	1979	Am J Cardiol	85	24	Bicycle	n
Fox	1979	Am J Cardiol	80	20	Bicycle	n
Simoons & Block	1981	Am J Cardiol	25	25	Bicycle	y
Wada	1981	Jpn Circ J	22	-	Bicycle	n
Yanowitz	1982	Am J Cardiol	25	-	Treadmill	n
Kubota	1985	Am Heart J	61	-	Treadmill	n
Ikeda	1986	J Electrocardiol	41	-	Dipyridamole	n
Farr	1987	Am J Cardiol	40	-	Bicycle	n
Yasumura	1987	Am Heart J	24	-	Treadmill	n
Montague	1988	Am J Cardiol	14	8	Bicycle	n
Nakajima	1988	Am Heart J	28	10	Treadmill	n
Kubota	1989	Circulation	21	-	Treadmill	n
Hosoya	1990	Am Heart J	52	-	Treadmill	n
Montague	1990	Chest	51	8	Bicycle	n
Bosimini	1991	Circulation	31	22	Mental	n
Miyakoda	1999	J Electrocardiol	99	15	Bicycle	y
Takala	2001	Ann Biomed Eng	-	12	Bicycle	n
Boudik	2002	J Electrocardiol	44	17	Dipyridamole	n
<b>No. of subjects</b>			<b>848</b>	<b>220</b>		
<b>Without stress testing</b>						
Green	1987	Circulation	41	644	None	y
Ishikawa	1988	Circulation	48	120	None	n
Kittnar	1993	Physiol Res	69	-	None	n
Tseng	1999	Jpn Heart J	108	-	None	n
<b>No. of subjects</b>			<b>266</b>	<b>764</b>		

**Detection and localization of acute and remote myocardial infarctions.** BSPM is superior to 12-lead ECG in detection of acute (Menown et al. 2000a,b and 2001) and of acute or remote (Kornreich et al. 1991 and 1993) myocardial infarctions.

**LV hypertrophy.** BSPM has showed higher correlation coefficients to the LV mass determined by other clinical methods than has 12-lead ECG or vectorcardiography (Holt et al. 1978).

### **3.6.3. BSPM ischemia studies at rest**

When mathematically or statistically derived basis functions were applied in feature extraction, BSPM map characterization has separated 41 patients with angiographically documented CAD and normal 12-lead ECGs from 644 healthy subjects with a sensitivity and specificity greater than 94% (Green et al. 1987b). During evaluation of the whole QRST interval, the majority of the discriminating information was present in the QRS complex, not in the ST-T interval usually the focus in ischemia analysis. Because the map coefficients used to perform statistical comparison were not actual physiological variables, the electrophysiological basis of these QRS abnormalities thus remains uncertain. Repolarization changes at rest have been found in CAD patients with normal wall motion in echocardiography, but not found in healthy controls (Kittnar et al. 1993).

### **3.6.4. BSPM stress studies**

#### **3.6.4.1. *Types of stress testing and time phases analyzed***

**Types of stress.** Most stress BSPM studies have applied physical exercise (Fox et al. 1978a,b and 1979a,b, Wada et al. 1981, Yanowitz et al. 1982, Farr et al. 1987, Montague et al. 1988 and 1990, Hosoya et al. 1990, Nakajima et al. 1988, Kubota et al. 1985 and 1989, Miyakoda et al. 1999). In addition, mental (Bosimini et al. 1991) and pharmacological (Ikeda et al. 1986, Boudik et al. 2002) stress have also been utilized (Table 2). The number of patients studied thus far is limited, probably due to the technical complexity and extensive preparation needed for electrode attachment.

**Exercise-testing position.** Pilot studies with the upright ergometer or treadmill exercise systems have documented poorer signal quality than with the supine posture, especially when recorded from lower chest sites (Mirvis et al. 1977). The supine bicycle-exercise test has been selected in several studies to improve the signal-to-noise ratio of the data collected during exercise (Mirvis et al. 1977, Wada et al. 1981, Montague et al. 1988 and 1990, Miyakoda et al. 1999). Upright exercise-testing uses either bicycle (Fox et al. 1978a,b and 1979a,b, Simoons and Block 1981) or treadmill (Kubota et al. 1985 and 1989, Yasumura et al. 1987, Nakajima et al. 1988, Hosoya et al. 1990) exercise. Supine exercise represents an equal or greater stress to the circulatory system than does exertion in a seated or upright posture (McGregor et al. 1961, Epstein et al. 1969). In the supine position, the maximal work capacity is lower, angina develops at a lower double product rate, and due to

increased LV filling pressure and greater LV volume, the ischemic ST depression is usually greater than in the upright position (Currie et al. 1983). Evidence exists that false-positive ST changes may normalize more rapidly in the supine position (Murayama et al. 1985).

**Time phase of exercise test analyzed.** In most studies, instead of maximal exercise, the time period immediately after cessation of exercise has been analyzed in order to improve the signal-to-noise ratio (Fox et al. 1978a,b and 1979a,b, Wada et al. 1981, Yanowitz et al. 1982, Kubota et al. 1985 and 1989, Farr et al. 1987, Nakajima et al. 1987, Yasumura et al. 1987, Montague et al. 1988, Hosoya et al. 1990, Miyakoda et al. 1999). In BSPM, correlation has been high between ST changes at cessation of exercise and recovery, showing that ST integral changes reflective of myocardial ischemia persist well after exercise into the immediate recovery period (Montague et al. 1988 and 1990). Of patients with CAD, 6% to 8% present with ST-segment depression only during the recovery phase of an exercise test (Savage et al. 1987, Lachterman et al. 1990).

#### **3.6.4.2. Map analysis**

Map analysis in many of the early exercise BSPM studies has been qualitative, describing the various map features in patients with different ischemia regions (Kubota et al. 1985 and 1989, Nakajima et al. 1988). Miyakoda et al. (1999) have applied correlation coefficient analysis to evaluate exercise-induced changes in the QRST integral maps at rest and after exercise. The sum of the ST integral decrease over the mapping area has separated patients with isolated LAD stenosis from healthy controls (Montague et al. 1988). ST integral analysis of the difference maps and departure maps in BSPM has improved the detection of mental stress-induced ischemia compared to use of the standard criterion of 0.1 mV of ST depression (Bosimini et al. 1991).

**Correlation with severity of CAD.** Exercise BSPM has provided quantitative discrimination among individual patients and patient groups with single- and multi-vessel CAD. Patients with multi-vessel CAD and angina-limited exercise have demonstrated a significantly greater decrease in exercise ST integral than do patients with single-vessel CAD and angina (Montague et al. 1990). Montague et al. (1990) also found a significant correlation between peak ST ischemic changes and quantitative coronary angiographic scores. Another study with 100 subjects demonstrated a positive correlation between number of obstructed coronary arteries and severity of exercise ST depression and over the area of its occurrence (Fox et al. 1979b).

**Comparison to standard precordial leads.** In patients with independently documented CAD, standard precordial leads do not sample the maximal ST depression in 25% (Yanowitz et al. 1982), and in 10% to 16% of patients with CAD the ST depression occurs exclusively outside the conventional precordial leads (Kubota et al. 1985, Fox et al. 1979b). This suggests that improved sensitivity of exercise testing may be possible with BSPM, especially in single-vessel disease.

### 3.6.4.3. *Localization of exercise-induced ischemia*

Since exercise-induced ischemia has been supposed to be regional in nature, and BSPM sensitive to such regional myocardial changes (Mirvis 1987), the anticipation has been that BSPM will aid in localizing ischemic zones in exercise testing.

**ST segment.** Experimental studies on ischemia localization vary from modest success (Wada et al. 1981, Yanowitz et al. 1982, Kubota et al. 1989) to improved localizing accuracy compared to results from 12-lead ECG (Fox et al. 1979b, Farr et al. 1987). Fox et al. (1979b) found ST depression mainly over the superior part of the thorax in patients with LAD stenosis (n = 12), over the inferior torso in patients with RCA stenosis (n = 5), and over the left lateral thorax in patients with LCX stenosis (n = 2). Of the 6 patients with triple-vessel disease, 66% had ECG signs of ischemia in all three defined sites of the precordial mapping (Fox et al. 1979a). The capability of BSPM to identify the culprit vessel is, however, to be established. Marked overlap of the patterns of exercise-induced ST deviation on the body surface has been observed among patients with stenosis in the three main coronary branches (Simoons and Block 1981, Kubota et al. 1985 and 1989, Nakajima et al. 1988, Hosoya et al. 1990, Montague et al 1990).

**ST-T integral and T-wave.** Some evidence exists that body surface T-wave potential or combined ST-T isointegral distribution may be more sensitive in localizing the ischemia region than is ST-segment mapping alone (Ishikawa et al. 1988, Nakajima et al. 1988, Kubota et al. 1989, Tseng et al. 1999). Anterior, inferior, and lateral T-wave changes have been evident in patients with evidence of anterior, inferoposterior, or lateral ischemia, respectively, assessed by <sup>201</sup>Tl SPECT and coronary angiography (Ishikawa et al. 1988, Nakajima et al. 1988, Kubota et al. 1990, Tseng et al. 1990). In BSPM, spatial and temporal T-wave changes have separated patients with remote anterior MI from patients with LV hypertrophy (Yamaki et al. 1992).

### 3.6.5. **Acute coronary occlusion**

When compared to the 12-lead ECG, BSPM has markedly improved the detection of acute (Menown et al. 2000a,b and 2001) and acute plus remote myocardial infarctions (Kornreich et al. 1991 and 1993, Medvegy et al. 2000). BSPM studies in patients undergoing PCI and in patients having both acute and remote MIs, distributions of body surface ST deviations (Kornreich et al. 1991 and 1993, Shenasa et al. 1993, Lux et al. 1995, MacLeod et al. 1995; Horáček et al. 2001, Horáček and Wagner 2002), and changes in QRS maps (Montague et al. 1986, Montague and Witkowski 1989, Horan et al. 1990) have all differed markedly in patients with anatomically different ischemia regions.

The six optimal thoracic locations for detection of myocardial infarction (Kornreich et al. 1991 and 1993) have been less valuable than has 18-lead ECG (12-lead ECG, right precordial leads V<sub>3R</sub>-V<sub>5R</sub>, and posterior leads V<sub>7</sub>-V<sub>9</sub>) in monitoring acute transmural

ischemia during PCI (Wung and Drew 1999). In that PCI monitoring study, the baseline ECG served as a reference point for measuring ST deviation between periods of acute ischemia and no ischemia in the same individual. In patients presenting with acute MI, the baseline ECG was unavailable, possibly explaining some of the differences they reported in ECG lead sensitivity (Wung and Drew 1999).

#### **4. AIMS OF THE STUDY**

The studies reported in this thesis were designed to investigate the detection and localization of exercise-induced myocardial ischemia by MCG and BSPM. The specific aims were:

1. To study detection and localization of exercise-induced myocardial ischemia by use of MCG and BSPM in well-defined CAD, represented by patients with single-vessel disease and anginal pain in the standard exercise test and no history of MI.
2. To study detection and localization of exercise-induced ischemia by MCG and BSPM in a heterogeneous CAD population selected to represent CAD patients in general, including subsets of patients with ischemia in any of the main coronary artery branch regions and also with healed MI.
3. To compare the capability of MCG and BSPM to detect exercise-induced myocardial ischemia in the same study population.
4. To study and compare the performance of various repolarization parameters, calculated from ST-segment and T-wave signals, in detection of exercise-induced myocardial ischemia in MCG and BSPM.
5. To identify the optimal spatial recording locations and the optimal temporal phases of exercise testing for various ischemia parameters for detection of exercise-induced ischemia in MCG and in BSPM.

#### **5. MATERIALS AND METHODS**

##### **5.1. Study subjects**

A total of 47 patients with CAD and 26 healthy controls were included in the present series of investigations. Of the 47 CAD patients, 3 were excluded from MCG analysis and 2 from BSPM analysis due to insufficient quality of the data in visual observation.

##### **5.1.1. Group I: Single-vessel CAD without prior myocardial infarction**

Study Group I comprised 27 CAD patients with single-vessel disease and no history of MI (Table 3). In coronary angiography, all patients had significant ( $\geq 50\%$  of the luminal

diameter) stenosis in one of the main coronary artery branches. At screening, all patients were required to have anginal pain, and to show 12-lead ECG documented evidence of ischemia with  $\geq 0.1$  mV ST-segment depression in symptom-limited upright bicycle ergometry. Inclusion also required that the patients had no history of MI, abnormal Q-waves, or bundle branch block in 12-lead ECG, or wall-motion abnormalities or LV hypertrophy in rest echocardiography. All patients were clinically stable and under appropriate medication during the study.

### 5.1.2. Group II: Triple-vessel CAD with prior myocardial infarction

Study Group II comprised 18 CAD patients with at least one documented remote MI and triple-vessel disease. Of these 18, 10 had Minnesota code Q-waves in 12-lead ECG, 15 had wall hypokinesia in cine angiography, and all had  $\geq 50\%$  narrowing of all 3 main coronary arteries (Table 4). The patients underwent  $^{201}\text{Tl}$  SPECT exercise test imaging with redistribution imaging at four hours, and coronary angiography for definition of the main ischemia region and the culprit vessel. Classification was based on a reversible thallium perfusion defect supplied by a stenotic ( $\geq 70\%$  luminal diameter) coronary artery. Two investigators independently classified the patients into three groups according to main ischemia region. All patients were clinically stable and under appropriate medication.

**Table 3.** *Clinical characteristics of study groups, Studies I and II.*

	Study	Group				
		CAD	LAD stenosis	LCX stenosis	RCA stenosis	Controls
Number of subjects	I/II	27/24	12/11	7/6	8/7	17/17
Age (years)	I	58 $\pm$ 10	57 $\pm$ 10	61 $\pm$ 7	58 $\pm$ 12	55 $\pm$ 7
	II	57 $\pm$ 10	53 $\pm$ 7	59 $\pm$ 7	57 $\pm$ 13	55 $\pm$ 7
Gender (male/female)	I	15/12	6/6	4/3	5/3	12/5
	II	14/10	6/5	3/3	5/2	12/5
LV ejection fraction (%)	I	65 $\pm$ 8	64 $\pm$ 6	70 $\pm$ 8	62 $\pm$ 8	66 $\pm$ 7
	II	64 $\pm$ 8	63 $\pm$ 6	70 $\pm$ 9	60 $\pm$ 7	66 $\pm$ 7
Stenosis (%)	I	86 $\pm$ 13	81 $\pm$ 15	91 $\pm$ 12	92 $\pm$ 5	-
	II	86 $\pm$ 13	82 $\pm$ 15	90 $\pm$ 13	92 $\pm$ 5	-

Values expressed as mean  $\pm$  SD or number of patients. Abbreviations: CAD = coronary artery disease patients, LV = left ventricular, LAD = patients with left anterior descending coronary artery stenosis, LCX = patients with left circumflex coronary artery stenosis, RCA = patients with right coronary artery stenosis, Stenosis = degree of coronary artery stenosis as percentage luminal narrowing of vessel diameter.

**Table 4.** *Clinical characteristics of study groups, Studies III, IV, and V.*

Group	Study	Number of subjects	Age (years)	Gender (male/female)	LV ejection fraction (%)	Stenosis (%)
CAD All	III,V	45	59 ± 9	32/13	57 ± 14	87 ± 13
	IV	44	57 ± 9	31/13	58 ± 14	87 ± 13
No MI single-vessel	III, V	27	57 ± 10	16/11	64 ± 8	86 ± 12
	IV	27	58 ± 10	15/12	65 ± 9	87 ± 13
Post-MI multivessel	III, V	18	61 ± 8	16/2	47 ± 15	88 ± 13
	IV	17	61 ± 8	15/2	47 ± 15	88 ± 13
LAD area ischemic	III, V	18	59 ± 9	12/6	56 ± 13	81 ± 14
	IV	16	58 ± 9	10/6	57 ± 12	79 ± 14
LAD 1-vessel CAD	III, V	13	57 ± 10	7/6	63 ± 6	81 ± 14
	IV	12	57 ± 10	6/6	64 ± 6	81 ± 15
LCX area ischemic	III, V	14	60 ± 7	10/4	57 ± 19	92 ± 11
	IV	15	60 ± 7	11/4	57 ± 18	92 ± 10
LCX 1-vessel CAD	III, V	6	59 ± 7	3/3	70 ± 9	90 ± 13
	IV	7	61 ± 7	4/3	67 ± 9	91 ± 12
RCA area ischemic	III, V	13	58 ± 11	10/3	59 ± 11	92 ± 8
	IV	13	59 ± 11	9/4	61 ± 12	92 ± 8
RCA 1-vessel CAD	III, V	8	57 ± 12	6/2	60 ± 7	92 ± 5
	IV	8	58 ± 12	5/3	64 ± 11	92 ± 5
Controls	III, V	25	55 ± 7	19/6	66 ± 7	-
	IV	26	51 ± 10	20/6	66 ± 7	-

Values expressed as mean ± SD or number of patients. MI = myocardial infarction. For abbreviations, see Table 3.

### 5.1.3. Healthy controls

The 26 healthy controls had no history of hypertension, smoking, or of heart disease in the family, and had normal findings in rest echocardiography as well as in standard upright 12-lead ECG exercise testing (Tables 3 and 4).

### 5.1.4. Patient distribution in separate studies

The study subjects were distributed among Studies I to V in the following manner:

**Studies I and II.** Study I comprised 27 patients, and Study II 24 patients, all without previous MI but with single-vessel CAD (Group I), plus the same 17 healthy controls (Table 3). Of the 27 patients in Study I, 25 were on beta blockers, 6 on Ca<sup>2+</sup> antagonists, and 21 on long-acting nitrates. Of the 24 patients in Study II, 21 were on beta blockers, 5 on Ca<sup>2+</sup> antagonists, and 19 on long-acting nitrates.

**Studies III and V.** These studies each comprised 27 patients, all without previous MI but with single-vessel disease (Group I), 18 patients with a history of one or more MIs and with triple-vessel disease (Group II), and 25 healthy controls (Table 4). Of these 45 patients, 41 were on beta blockers, 11 on  $\text{Ca}^{2+}$  antagonists, 36 on long-acting nitrates, and 9 on angiotensin-converting enzyme inhibitors.

**Study IV.** This study comprised 27 patients without previous MI and single-vessel disease (Group I), 17 patients with a history of  $\geq 1$  MIs and triple-vessel disease (from Group II), and 26 healthy controls (Table 4). Of the 44 study patients, 40 were on beta blockers, 10 on  $\text{Ca}^{2+}$  antagonists, 35 on long-acting nitrates, and 9 on angiotensin-converting enzyme inhibitors.

## **5.2. Exercise testing**

Study subjects underwent two separate exercise tests for MCG and BSPM recordings in random order on the same day.

First, a baseline recording was performed in a resting state for 5 minutes. A non-magnetic ergometer, designed and constructed for exercise MCG recordings performed in a supine position, was used for the bicycle exercise test. The ergometer was calibrated against a standard bicycle exercise ergometer (Siemens Ergomed 840L, Germany), used in the cardiac catheterization laboratory for supine exercise testing. During exercise, the workload was increased stepwise and blood pressure monitored every 2 minutes. The cessation criteria were severe fatigue or dyspnoea, severe chest pain, progressive decrease or abnormal elevation in systolic blood pressure, or repetitive ventricular arrhythmias. MCG and BSPM were continuously recorded during the exercise and for up to 10 minutes in the recovery phase.

## **5.3. MCG recording and data processing**

Patients and controls underwent the measurements in a magnetically shielded room (Euroshield Ltd., Eura, Finland) in a biomagnetic research laboratory in a hospital environment with a 67-channel cardiomagnetometer (Neuromag Ltd., Helsinki, Finland). This cardiomagnetometer was equipped with seven hardware axial and 60 planar dc-SQUID gradiometers, arranged on a slightly curved surface with a diameter of 30 cm (Figure 2). The gradiometers record the component of the magnetic field perpendicular to the anterior chest ( $B_z$ ). The 60 planar gradiometers are arranged in pairs, detecting the x and y components of the registered magnetic field.

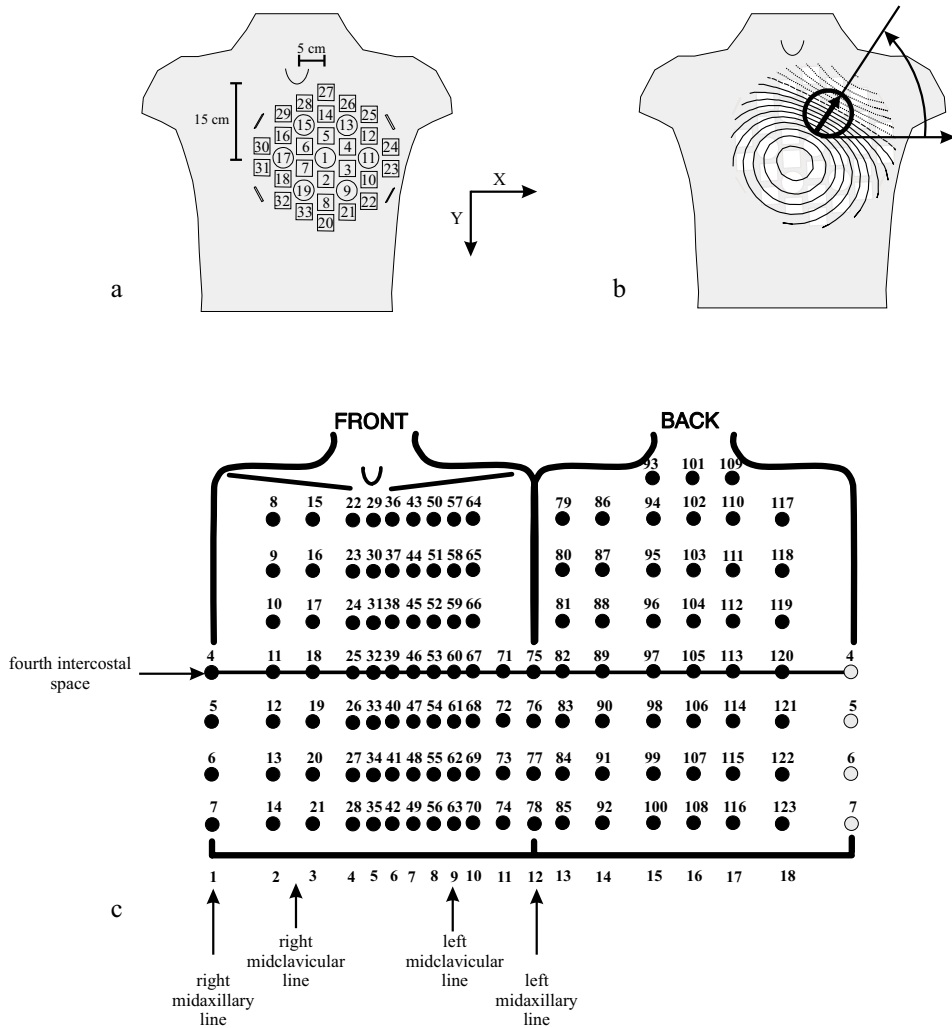


**Figure 2.** a) Sensor arrangement of the cardiomagnetometer. The  $XY$ -plane is parallel to the sensor surface, whereas the  $Z$ -coordinate would point into the chest. The circles represent the seven co-axial gradiometers, and each rectangle denotes two orthogonal planar gradiometers. Numbers refer to measurement locations. b) Distribution of the normal component ( $B_z$ ) of the magnetic field. The peak gradient is indicated by the thick arrow. Orientation of the magnetic field was measured as the angle between direction of the peak gradient and the patient's right-left line ( $X$ -axis). c) BSPM electrode layout. The 120 electrodes are mounted on 18 vertical strips. The dimensions of the upper body determine horizontal spacing of the electrodes. Strip 1 is located on the right and strip 12 on the left midaxillary line, respectively. Strip 9 is located on the left midclavicular line. The right midclavicular line is between strips 2 and 3. In all strips, the fourth electrode from the inferior end of the strip was placed at the level of the fourth intercostal space determined at the border of the sternum. (Reprinted with permission from *Annals of Medicine*.)

The patients lay on a non-magnetic bed, and the center of the gradiometer grid was placed in a position 15 cm caudally from the jugular notch and 5 cm left of the midline (Figure 2). The grid was always brought as close to the chest as possible without touching it, allowing tilting of the grid up to 20° in respect to the frontal plane.

The standard 12-lead ECG was recorded simultaneously with MCG. The arm electrodes were attached at the base of the shoulders against the deltoid border, below the clavicle according to “correct” Mason-Likar placement (Gamble et al. 1984). The left leg electrode was placed in the anterior axillary line halfway between the costal margin and the crest of the ilium (Mason and Likar 1966).

Recordings were band-pass filtered at 0.03-300 Hz, digitized with a sampling frequency of 1 kHz, and stored on a computer disk.

#### **5.4. BSPM recording and data processing**

In the BSPM measurements, unipolar potentials were recorded at 120 locations covering the whole thorax (Figure 2). In addition, three limb leads were recorded with electrodes on the right and left shoulder and on the left hip, as in MCG measurements. A Wilson central terminal served as a reference for the unipolar leads. The 120 Ag/AgCl electrodes were attached to 18 flexible plastic strips, each pair with a vertical inter-electrode distance of 5 cm. These strips were attached on the subject’s thorax vertically with the highest electrode density at the left anterior thorax. For all strips, the fourth electrode from the inferior end of the strip was placed at the level of the fourth intercostal space, determined at the border of the sternum. Horizontal distances between the strips were determined individually according to the dimensions of the thorax (Figure 2).

Recordings were band-pass filtered at 0.16 Hz to 300 Hz, digitized with a sampling frequency of 1 kHz, and stored on a computer disk.

#### **5.5. MCG and BSPM data analysis**

##### **5.5.1. Signal averaging, interpolation, and data conversion**

**Averaging.** The MCG and BSPM data were baseline-corrected and signal-averaged. First, a template beat of raw data with good signal quality in visual observation was selected. A line fitted to the PQ- and TP-intervals was then subtracted from the raw data of each cardiac cycle to define the baseline level. In the case of a high heart rate with a shortened TP-segment, a line connecting two consecutive PQ-intervals served as a baseline. Signals judged invalid in visual observation were excluded before averaging. A range of acceptable data values, called the tube, was formed around the template. The template was compared with the first baseline-corrected cardiac cycle of raw data. If the candidate beat did not fit inside the tube in all axial channels, it was excluded from the average. The cumulative

average served as the template for the next candidate beat. The amplitude shift of the template was adjusted to include approximately 20 of the 40 candidate beats in the average. The 12-lead ECG, recorded simultaneously with MCG, was baseline-corrected and signal-averaged concomitantly with the MCG signal.

**Interpolation.** After averaging, all signals judged invalid by visual observation were deleted and replaced by data interpolated from other leads. The details of this signal conversion, based on minimum-norm estimation, have been presented by Burghoff et al. (2000).

**MCG data conversion.** The 67-channel measurement data, containing signals of axial and planar gradiometers and the interpolated channels, was converted to a 33-channel set-up of axial gradiometers only. This conversion was performed in order to make the signals in different measurement locations comparable. This minimum-norm based transformation method has yielded an average correlation of 93% between the simulated and measured MCG signals recorded by different sensor configurations (Burghoff et al. 2000).

### 5.5.2. Exercise test phases analyzed

Five phases of the exercise test were analyzed: 1) at rest, 2) in the last workload phase (Studies III and V), 3) immediately after cessation of exercise, 4) after two minutes of recovery, and 5) after four minutes of recovery.

### 5.5.3. Repolarization parameters

**Defining the J point, T-wave apex, and end of T-wave.** The J point, the T-wave apex, and the end of the T-wave were manually determined from the signals of the seven co-axial gradiometers in MCG, and from the signals of the leads equivalent to standard precordial leads  $V_1$ - $V_6$  in BSPM. This was performed for each study subject in all exercise test phases evaluated. For further analysis, these time instances were selected to represent the J point, T-wave apex, and the end of the T-wave in all MCG channels and BSPM leads.

**Amplitudes.** In Studies I and II, the ST amplitude was measured as an average amplitude over the second time quarter from the J point on to the T-wave apex (Figure 3). In Studies III, IV, and V, the ST amplitude was measured at 60 ms after the J point (Chaitman 1997). In Studies I and II, the ST amplitude in the 12-lead ECG, recorded simultaneously with MCG, was measured at 60 ms after the J point.

**ST slope.** In Studies III and IV, the ST slope was calculated by fitting a regression line to the signal from the J point on to 60 ms after it (Figure 3).

**Integrals.** Integrals were calculated as an integration of the area under the curve from the J point on to the end of the T-wave. In Study IV, the ST-T isointegral (positive minus absolute negative area) was measured. In Study V, the ST-T isointegral and the positive ST-T area were measured (Figure 3).

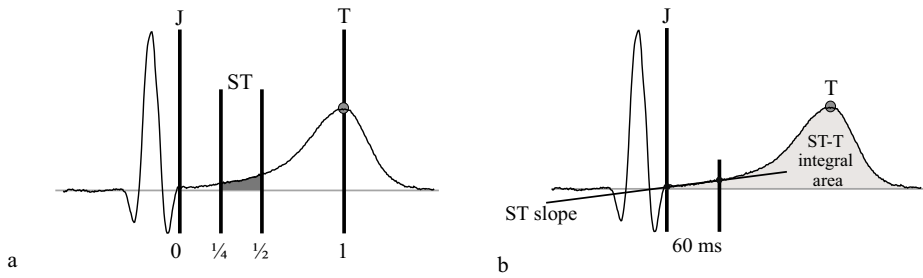


**Figure 3.** a) Studies I and II. Instants of the cardiac cycle analyzed were: 1) an interval of the ST segment defined as the second quarter from the J point to the T-wave apex, and 2) the T-wave apex. b) Studies III to V. ST amplitude was measured 60 ms after the J point. ST slope was calculated by fitting a regression line to the signal from the J point to point 60 ms after it. Integrals were calculated as an integration of the area under the curve from the J point to the end of the T-wave. The ST-T isointegral (positive minus absolute negative area) and the positive ST-T area were measured. (Reprinted with permission from *Basic Research in Cardiology*.)

#### 5.5.4. Signal-to-noise ratio and reproducibility of the signal analysis

**Signal-to-noise ratio.** The signal-to-noise ratio of different MCG and ECG sensors (the 7 hardware axial gradiometers, the 60 hardware planar gradiometers, the 33 simulated axial gradiometers, the 12-lead ECG recorded simultaneously with MCG, and the 123 BSPM leads) was compared in a subset of 10 patients at cessation of stress. The mean QRS amplitude and the root mean square noise as an average over 20 to 40 ms baseline in the P-Q interval was evaluated for each channel. The mean amplitudes and signal-to-noise ratios are summarized in Table 5.

**Table 5.** Mean values of baseline root mean square noise, QRS amplitude, and mean QRS signal-to-noise ratio in ten patients with CAD at cessation of stress.

Sensors	Mean root mean square noise	Mean QRS amplitude	Mean QRS signal-to-noise ratio
7 hardware axial gradiometers (fT)	45	2990	66
60 planar gradiometers (fT/cm)	19	490	26
33 simulated axial gradiometers (fT)	85	3440	41
12-lead ECG ( $\mu$ V)	4,3	274	65
123 BSPM leads ( $\mu$ V)	5,5	170	31

**Reproducibility of the signal analysis.** Reproducibility of the data analysis was tested in the same subset of 10 CAD patients by analyzing twice the MCG and BSPM signals at rest and immediately after cessation of stress, the second analysis without detailed knowledge of the previous analysis parameters. Signals were averaged, invalid signals

interpolated, MCG data converted to 33 axial channels, and the evaluated time instances determined. ST amplitude at 60 ms after the J point and T-wave apex amplitude were determined. Variation coefficients were calculated by first subtracting the amplitudes of the second analysis from the corresponding ones in the first analysis in each location, and then calculating the means of these differences over all channels in all subjects. In MCG, the variation coefficients for ST amplitude and T-wave amplitude were at rest  $91 \pm 96$  fT and  $82 \pm 89$  fT, and at cessation of stress  $86 \pm 77$  fT and  $155 \pm 160$  fT, respectively. In BSPM, the variation coefficients for ST amplitude and T-wave amplitude were at rest  $4.9 \pm 5.3$   $\mu$ V and  $12.9 \pm 14.2$   $\mu$ V, and at cessation of stress  $7.3 \pm 13.2$   $\mu$ V and  $17.6 \pm 19.6$   $\mu$ V, respectively.

## 5.6. Magnetic field polarity and orientation

**Manual determination of magnetic field polarity.** In Study I, the magnetic field polarity of the isofield maps was manually determined by first drawing a line from the magnetic field minimum to the field maximum. Then, the orientation of the magnetic field was defined as the angle between the line connecting the field minimum and maximum and the patient's right-to-left line (X-axis) on the measurement plane (Figures 2 and 4).

**Computerized measurement of the magnetic field orientation.** In Studies I and IV, a computerized method called the surface gradient method was developed to determine the magnetic field orientation. This method is based on the arrow maps introduced by Cohen and Hosaka (1976). First, the spatial difference of the magnetic field perpendicular to the measurement plane ( $B_z$ ), called the surface gradient, was calculated. Then, the two-dimensional orientation of the largest peak surface gradient was determined. The orientation of the magnetic field was defined as the angle between the direction of the peak gradient and the right-left line (X-axis) of the patient (Figures 2 and 4).

## 5.7. Discriminant index analysis

A discriminant index, suggested by Flowers et al. (1976) and Kornreich et al. (1991), indicates the capability of each recording site to separate each patient subgroup from other patients and controls.

In Studies III to V, the discriminant index analysis was applied to MCG and BSPM data. The discriminant index was calculated for each patient subgroup in each MCG and BSPM recording location. First, the mean value of the parameter of the control group was subtracted from the corresponding mean of the patient subgroup. This difference was then divided by the standard deviation of the parameter in all subjects at the same recording site. The analysis was performed for all evaluated parameters for the phases of the exercise test examined.

The smallest negative discriminant index indicates the optimal recording location for ST depression, for the decrease in T-wave amplitude, and for the decrease in ST slope and ST-T integral area. The highest positive discriminant index indicates the optimal recording locations for the reciprocal increase in the parameters examined.

## **5.8. Map illustrations**

**Group mean isofield, isopotential, isoslope, and isointegral maps.** The group mean isofield maps of the MCG signal, isopotential maps of the BSPM signal, and isoslope and isointegral maps of the MCG and BSPM signal were calculated. These group mean ST amplitude, T-wave amplitude, ST slope, and ST-T integral maps allowed evaluation of typical spatial patterns of the various ischemia parameters in the study groups.

**Spatial field gradient maps.** In Study I, the spatial field gradient maps were calculated to visualize the orientation of the spatial field gradient.

**Discriminant index maps.** The discriminant index maps were created for the CAD patient groups to illustrate the capability of different recording sites to separate a patient subgroup from other patients and controls by means of various parameters. The optimal locations of MCG and of BSPM to detect ischemia, projected on the torso surface, were visually compared by use of the discriminant index maps.

**Phase-difference maps.** In Study V, the phase-difference maps were created by calculating the difference between the group mean amplitudes for the ST segment or for T-wave apex at two phases of the exercise test. These were formed to illustrate spatial patterns of ischemia-induced amplitude changes during the exercise test.

## **5.9. Assessment of coronary artery disease**

### **5.9.1. Symptom-limited upright bicycle ergometry**

Upright bicycle exercise tests were carried out by starting from a load of 50 W and increasing it by 25 W to 50 W every 3 minutes. The test was considered positive if the patient experienced any anginal chest pain and if the ECG showed ST-segment depression of  $\geq 0.1$  mV measured at 60 ms or 80 ms after the J point.

### **5.9.2. Transthoracic echocardiography**

The patient was placed in the left lateral decubitus position, and two-dimensional echocardiograms were performed. Four views were obtained: parasternal long-axis and short-axis, apical four-chamber and two-chamber. The parasternal long-axis view M-mode image served for measuring LV wall thickness, LV diameter, and ejection fraction by use of the Teichholz formula.

### **5.9.3. Coronary angiography and left ventriculography**

A stenosis of  $\geq 50\%$  of luminal diameter was considered significant in routine coronary angiography. The LV ejection fraction was determined from contrast left ventriculography in the right anterior oblique projection by use of the area-length method.

### **5.9.4. Thallium ( $^{201}\text{Tl}$ ) single-photon emission computed tomography**

The  $^{201}\text{Tl}$  SPECT exercise test imaging was performed with a symptom-limited bicycle exercise test and redistribution imaging at 4 hours. The main ischemia region was defined as the largest myocardial region with a reversible or partially reversible perfusion defect. The territory of a vessel was defined according to Brunken et al. (1987).

## **5.10. Statistical analysis**

Continuous variables in all studies are presented as mean  $\pm$  standard deviation (SD). The differences in mean levels of continuous variables between the groups were estimated by the Mann-Whitney U-test.

Sensitivity was defined as the percentage of CAD patients classified by a test to the CAD group, and specificity as the percentage of healthy controls classified to the control group. Cut-off values were dichotomized for various parameters by selecting the parameter value resulting in the maximum sum of sensitivity and specificity in classification of subjects to the CAD and the control groups. In Studies III, IV, and V, the receiver operating characteristic curves were created for various parameters to assess their performance in identification of patients with CAD. The areas under the curves were given as percentages of the maximal value, which would be the result of a test yielding a 100% sensitivity and specificity. In Study III, the areas under the receiver operating characteristic curves were compared statistically by means of a two-tailed z test of the difference between the areas under two performance curves (Hanley and McNeil 1982 and 1983).

In Studies IV and V, multivariate analyses were performed to evaluate the relative information content of individual variables in classifying subjects to the CAD group and to the control group by use of stepwise logistic regression analysis and a p-value of 0.05 as the limit for entry into the equation.

A two-tailed p-value  $< 0.05$  was considered statistically significant. The biostatistic software used was SPSS for Windows (version 8.0 or 10.0).

## 6. RESULTS OF THE STUDIES

### 6.1. MCG in detection of exercise-induced myocardial ischemia

#### 6.1.1. Magnetic field orientation and rotation (I, IV)

##### 6.1.1.1. *ST segment*

**Manual determination of field polarity (I).** Manual measurement of the magnetic field polarity of the ST segment separated the pooled CAD patient group from the control group immediately after cessation of exercise (ST-segment field orientation CAD group:  $170 \pm 50^\circ$  vs. control group:  $100 \pm 50^\circ$ ;  $p < 0.005$ ) and also at 4 minutes of recovery ( $p < 0.01$ ) (Figure 4).

**Peak gradient orientation (I, IV).** In Study I, the CAD group was separated from the control group by the orientation of the peak gradient of the ST segment immediately after cessation of exercise and also at 4 minutes of recovery (Figures 4 and 5, Table 6). In Study IV, the orientation of the peak gradient of the ST segment separated the pooled CAD group and all patient subgroups from the control group immediately after cessation of exercise ( $p < 0.001$  for the pooled CAD group).

##### 6.1.1.2. *T-wave*

**Manual determination of field polarity (I).** The manually measured magnetic field polarity of the T-wave apex at 4 minutes of recovery separated the CAD group from the control group (T-wave field polarity CAD group:  $80 \pm 50^\circ$  vs. control group:  $60 \pm 20^\circ$ ;  $p < 0.05$ ). The difference in magnetic field polarity (e.g., rotation of the field polarity) between rest and 4-minute recovery separated the CAD group from the control group.

**Peak gradient orientation (I, IV).** In Study I, the orientation of the peak gradient of the T-wave apex differed in the CAD group from that of the control group at 4 minutes' recovery (Table 6). Moreover, the difference in magnetic field orientation (e.g., rotation of the field) of the T-wave apex between rest and 4 minutes of recovery was larger in the CAD group than in the control group (T-wave field rotation CAD group:  $30 \pm 40^\circ$  vs. control group:  $10 \pm 10^\circ$ ;  $p < 0.05$ ). In Study IV, the orientation of the T-wave peak gradient separated the pooled CAD group, and the LAD and RCA subgroups, but not the LCX subgroup from the control group at 2 minutes' recovery ( $p < 0.001$  for the pooled CAD group).

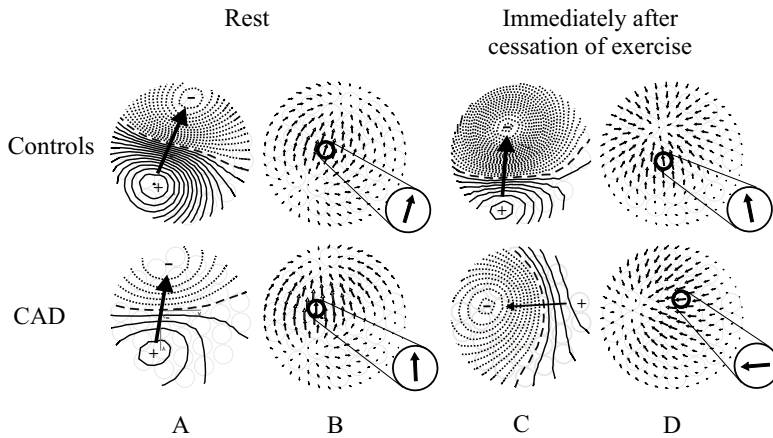


**Figure 4.** Study I. Group mean ST-segment magnetic field distribution and interpolated spatial field gradient of healthy Controls and of patients with coronary artery disease (CAD) at rest and immediately after cessation of exercise. Spatial distribution of the magnetic field component  $B_z$  at rest (A) and immediately after cessation of exercise (C). Large black arrow is the line connecting the magnetic field maximum and minimum. Any change in magnetic field orientation is apparent as arrow rotation. Interpolated gradient arrows at rest (B) and immediately after cessation of exercise (D). Peak gradients marked by the circled arrows, also shown enlarged. The large arrow direction in each A and C parallels the maximal field gradients in B and D, respectively. The step between any two consecutive lines is 100 fT. — positive, ..... negative, - - - - zero line. (Reprinted with permission from *The Annals of Noninvasive Electrocardiology*.)

**Table 6.** Orientation of MCG peak gradient of the ST segment and T-wave apex, Study I.

Group	Rest	At cessation of exercise	4 minutes recovery
<b>ST segment</b>			
Controls (°)	88 ± 60	106 ± 49	112 ± 50
CAD (°)	119 ± 94	167 ± 68†	160 ± 43†
LAD stenosis (°)	102 ± 73	191 ± 56**	150 ± 41*
LCX stenosis (°)	92 ± 119	130 ± 79	184 ± 38**
RCA stenosis (°)	168 ± 91*	165 ± 66*	157 ± 48
<b>T-wave apex</b>			
Controls (°)	56 ± 12	61 ± 19	58 ± 18
CAD (°)	65 ± 61	66 ± 44	87 ± 60*
LAD stenosis (°)	54 ± 15	57 ± 22	82 ± 61
LCX stenosis (°)	48 ± 16	50 ± 21	86 ± 82
RCA stenosis (°)	97 ± 109	94 ± 68	97 ± 42*

\*  $p < 0.05$ , \*\*  $p < 0.01$ , and †  $p < 0.005$  between patients and controls, Mann-Whitney U-test. Mean ± SD. For abbreviations, see Table 3.

## 6.1.2. ST segment and T-wave parameters in MCG (II, IV)

### 6.1.2.1. Spatial evaluation of ischemic changes

**ST amplitude (II, IV).** The pooled CAD group and the patient subgroups showed ST depression over the sternum, middle inferior thorax, and abdomen at cessation of exercise, and reciprocal ST elevation over the left parasternal area and over the left anterior shoulder at cessation of exercise (Figures 4 and 5, Tables 7 and 8).

**ST slope (IV).** The pooled CAD group and the patient subgroups showed decrease in the ST slope over the inferior thorax and abdomen, and reciprocal increase in the ST slope over the left parasternal area and left shoulder (Figure 5, Table 8).

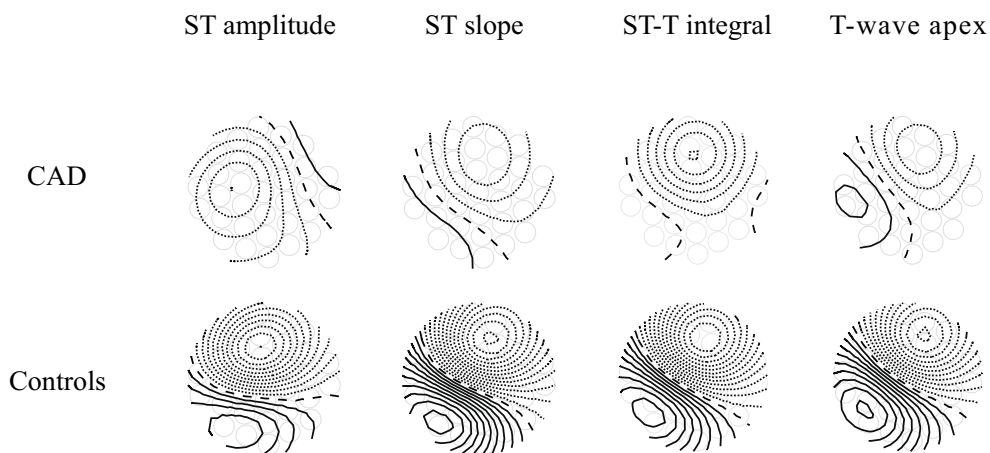


**Figure 5.** Study IV. From left to right: Group mean magnetic isofield maps of ST amplitude and ST slope immediately after cessation of exercise, and ST-T integral and T-wave apex amplitude at 2 minutes' recovery. Top: patients with coronary artery disease (CAD), bottom: healthy Controls. The ST amplitude map in the CAD group was rotated compared to that of the Controls. ST slope was more horizontal in the CAD than in the Control group. The ST-T integral and T-wave apex amplitude decreased over the abdomen and increased over the left shoulder in the CAD group compared to values in Controls. The step between two isocontour lines is 200 fT in ST amplitude maps, 2 pT/s in ST slope maps, 50 fTs in ST-T integral maps, and 500 fT in T-wave maps. In MCG, positive values indicate flux towards the chest. — positive, ..... negative, - - - zero line. (Reprinted with permission from *Annals of Medicine*.)

**Table 7.** ST-segment amplitudes at cessation of stress in the optimal MCG channels for ST elevation and depression, Study II.

Group	ST amplitude increase			ST amplitude decrease		
	DI	Patients (fT)	Controls (fT)	DI	Patients (fT)	Controls (fT)
CAD	0.98	-70 ± 470†	-700 ± 680	-1.14	-80 ± 360‡	610 ± 660
LAD	0.95	-270 ± 510**	-1050 ± 880	-1.05	-23 ± 330†	610 ± 660
LCX	0.75	-240 ± 420	-710 ± 650	-1.49	-350 ± 370†	470 ± 520
RCA	1.46	240 ± 500**	-700 ± 680	-1.17	-270 ± 480**	490 ± 710

\*\* p < 0.01, † p < 0.005, and ‡ p < 0.001 comparing patient groups to control group, Mann-Whitney U-test. Mean ± SD. DI = discriminant index. Abbreviations as in Table 3.

**Table 8.** ST-segment amplitudes and ST slopes in the optimal MCG channels at cessation of stress, Study IV.

Group	All CAD patients	LAD area ischemic	LCX area ischemic	RCA area ischemic
ST amplitude increase				
Discriminant index	0.94	1.07	0.68	1.19
Patients (fT)	-440 ± 1370‡	210 ± 1860‡	-330 ± 1210**	25 ± 980‡
Controls (fT)	-2170 ± 1880	-1910 ± 1970	-1240 ± 1410	-2170 ± 1870
ST amplitude decrease				
Discriminant index	-0.96	-0.88	-1.13	-0.98
Patients (fT)	-570 ± 980‡	-270 ± 1100**	-830 ± 1210‡	-610 ± 940**
Controls (fT)	920 ± 1680	1020 ± 1500	920 ± 1680	920 ± 1680
ST slope increase				
Discriminant index	1.21	1.25	1.08	1.46
Patients (pT/s)	-7.5 ± 6.6‡	-5.4 ± 3.5‡	-9.3 ± 7.8**	-2.4 ± 4.4‡
Controls (pT/s)	-25 ± 17	-26 ± 20	-25 ± 17	-24 ± 17
ST slope decrease				
Discriminant index	-1.12	-0.98	-1.27	-1.29
Patients (pT/s)	1.3 ± 3.7‡	5.4 ± 5.2**	-0.95 ± 5.3‡	-1.1 ± 7.7‡
Controls (pT/s)	10.7 ± 9.6	21 ± 18	13 ± 13	13 ± 13

\*\* p < 0.01 and ‡ p < 0.001 comparing patient group to control group; Mann-Whitney U-test. Mean ± SD. Abbreviations as in Table 3.

**T-wave amplitude (II, IV).** The pooled CAD group and the patient subgroups showed T-wave amplitude decrease over the sternum, middle inferior thorax, and abdomen, and reciprocal T-wave amplitude increase over the left parasternal area and over the left anterior shoulder at 2 and 4 minutes' recovery (Figure 5, Tables 9 and 10).

**ST-T integral (IV).** In the pooled CAD group and in the patient subgroups, the ST-T integral area became negative over the mapped area with the zero area line over the abdomen (Figure 5, Table 10).

#### **6.1.2.2. Optimal recording locations**

**ST amplitude (II, IV).** The optimal location for detecting ST depression was over the inferior thorax and abdomen for the pooled CAD group and also for the LAD, RCA, and LCX subgroups, except in Study II for the LCX subgroup, in which the optimal site was more lateral on the left. The optimal location for detecting reciprocal ST elevation was over the left parasternal area and left anterior shoulder for the pooled CAD group and for the LAD and RCA subgroups. For the LCX subgroup the optimal site was more cranial (Figure 6, Tables 7 and 8).

**ST slope (IV).** In all CAD groups, the optimal location for the decrease in ST slope was over the inferior thorax and abdomen, and for reciprocal increase in ST slope over the left parasternal area and left anterior shoulder (Figure 6, Table 8).

**T-wave amplitude (II, IV).** The optimal location for decrease in T-wave amplitude was over the inferior thorax and abdomen for the pooled CAD group and for the LAD, RCA, and LCX subgroups, except in Study II for the LCX subgroup, in which the optimal site was more lateral on the left. The optimal location for reciprocal increase in T-wave amplitude was over the left parasternal area and left anterior shoulder for the pooled CAD group and for the LAD, RCA, and LCX subgroups, except in Study II for the LCX subgroup, in which the optimal site was more cranial and medial (Figure 6, Tables 9 and 10).

**ST-T integral (IV).** In all CAD groups, the optimal location for the decrease in ST-T integral area was over the inferior thorax and abdomen, and for the reciprocal increase in ST-T integral area over the left parasternal area and left anterior shoulder (Figure 6, Table 10).

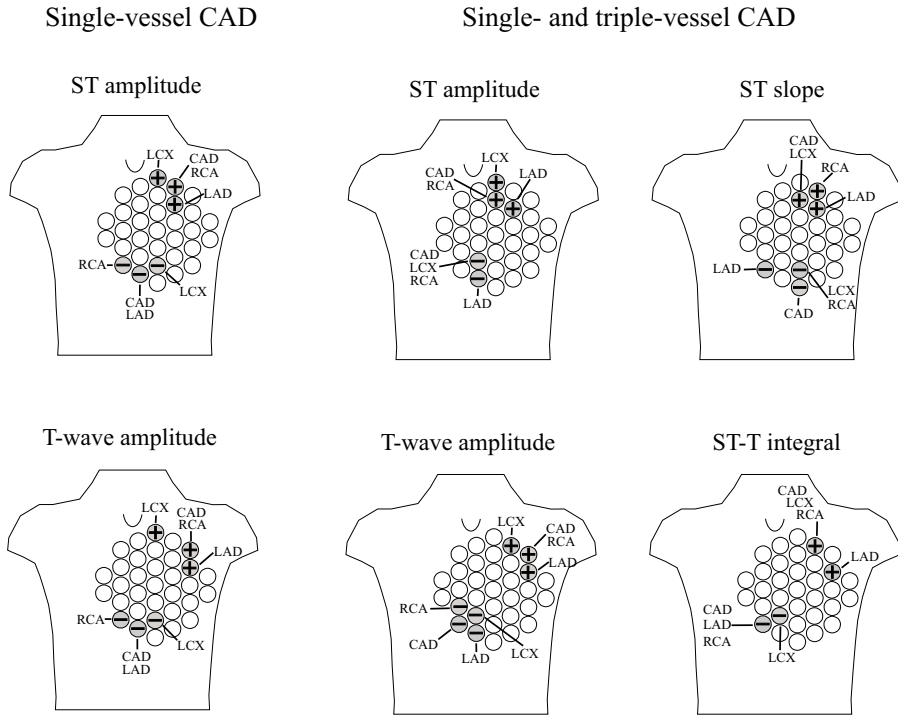


**Figure 6.** Studies II and IV. Optimal recording locations of MCG for ischemia-induced changes in ST amplitude, ST slope, ST-T integral area, and T-wave amplitude for patients with single-vessel coronary artery disease (Study II) and with single- and triple-vessel CAD (Study IV). Plus-signs indicate the highest discriminant index values considered as the optimal location for the ischemia-induced increase in the parameters. Minuses indicate the most negative discriminant index values, and thus the optimal location for ischemia-induced decrease in the parameters. The optimal locations for decrease in ST amplitude, ST slope, T-wave amplitude and ST-T integral area were over the abdomen and for the reciprocal increase in parameters over the left parasternal area and shoulder. Patients with anterior (LAD), posterior (LCX), and inferior (RCA) ischemia.

**Table 9.** T-wave apex amplitudes at 4 minutes of recovery in the optimal MCG channels for T-wave amplitude increase and decrease, Study II.

T-wave amplitude				T-wave amplitude		
Group	DI	Patients (fT)	Controls (fT)	DI	Patients (fT)	Controls (fT)
CAD	1.06	-1810 ± 1460†	-3790 ± 1840	-0.92	1470 ± 1130**	2780 ± 1460
LAD	1.15	-1010 ± 920†	-3160 ± 1990	-0.79	1660 ± 1100	2780 ± 1460
LCX	0.63	-2320 ± 1300	-3400 ± 1860	-1.30	560 ± 1970	2400 ± 1140
RCA	1.40	-1180 ± 1230†	-3790 ± 1840	-1.26	1060 ± 850**	3340 ± 2010

\*\* p < 0.01 and † p < 0.005 comparing patient group to controls group, Mann-Whitney U-test. Mean ± SD. Abbreviations as in Table 3.

**Table 10.** *T-wave amplitudes and ST-T integral areas in the optimal MCG channels at 2 minutes of recovery, Study IV.*

Group	All CAD patients	LAD area ischemic	LCX area ischemic	RCA area ischemic
<b>T-wave amplitude increase</b>				
Discriminant index	1.10	1.24	1.10	1.25
Patients (fT)	-1300 ± 2100‡	-580 ± 2100‡	-1700 ± 2900**	-880 ± 1400‡
Controls (fT)	-4500 ± 2700	-4000 ± 2600	-5200 ± 2700	-4500 ± 2700
<b>T-wave amplitude decrease</b>				
Discriminant index	-1.05	-0.87	-1.26	-1.17
Patients (fT)	720 ± 2500‡	860 ± 2300**	-150 ± 3600**	470 ± 2100‡
Controls (fT)	4200 ± 3000	3400 ± 2200	4000 ± 2800	4600 ± 3400
<b>Increase in ST-T integral</b>				
Discriminant index	1.01	1.26	0.69	1.22
Patients (fTs)	-240 ± 260‡	-30 ± 280*	-340 ± 290*	-170 ± 170‡
Controls (fTs)	-570 ± 340	-430 ± 330	-570 ± 340	-570 ± 340
<b>Decrease in ST-T integral</b>				
Discriminant index	-1.00	-0.87	-1.15	-1.08
Patients (fTs)	40 ± 300‡	90 ± 190*	-50 ± 450**	5 ± 200‡
Controls (fTs)	410 ± 380	410 ± 380	370 ± 350	410 ± 380

\*  $p < 0.05$ , \*\*  $p < 0.01$ , and ‡  $p < 0.001$  comparing patient groups to control group; Mann-Whitney U-test. Mean ± SD. Abbreviations as in Table 3.

### 6.1.3. Performance of the ischemia parameters evaluated in MCG (IV)

**Receiver operating characteristic curves.** For the pooled CAD group, all ST-segment parameters and the T-wave amplitude performed equally well in ischemia detection (area under the receiver operating characteristic curve from 82% to 86%) (Table 14). In non-MI patients, ST elevation and the increase in ST slope performed best. In contrast, in post-MI patients, decrease in ST slope, and decrease or reciprocal increase in T-wave amplitude performed best. The peak gradient of the ST segment showed a trend toward performing slightly better than did the peak gradient of the T-wave in the pooled CAD group (Table 11).

**Stepwise logistic regression analysis.** A forward stepwise logistic regression analysis was performed to study the independent discriminative value of the parameters in separation of the CAD patients from the controls. When all the variables were tested by the presence of CAD as the dependent variable, the ST slope increase ( $p < 0.001$ ) and the peak gradient orientation of the ST segment ( $p < 0.005$ ) were the only parameters that entered the model. When the ST peak gradient orientation was removed from the model, the ST slope increase ( $p < 0.005$ ) and T-wave amplitude increase ( $p < 0.05$ ) entered the model.

**Table 11.** Areas under the receiver operating characteristic curves for ST- and T-wave amplitude changes in MCG, Study IV.

Group	CAD	No MI single- vessel	Post-MI multi- vessel	LAD area ischemic	LCX area ischemic	RCA area ischemic
At cessation of stress						
ST elevation	83 %	90 %	80 %	83 %	75 %	91 %
ST depression	82 %	82 %	84 %	77 %	86 %	83 %
ST slope increase	83 %	92 %	83 %	84 %	80 %	86 %
ST slope decrease	84 %	85 %	91 %	77 %	88 %	88 %
ST peak gradient	83 %	87 %	75 %	86 %	78 %	84 %
At 2 minutes recovery						
T-wave increase	86 %	83 %	90 %	84 %	80 %	94 %
T-wave decrease	82 %	74 %	91 %	78 %	82 %	88 %
Increase in ST-T integral	80 %	81 %	80 %	88 %	72 %	89 %
Decrease in ST-T integral	79 %	76 %	85 %	77 %	75 %	87 %
T-wave peak gradient	75 %	77 %	72 %	73 %	65 %	90 %

Abbreviations as in Table 3. (Reprinted with permission from *Annals of Medicine*.)

## 6.2. BSPM in detection of exercise-induced myocardial ischemia

### 6.2.1. Spatial evaluation of ischemic changes

**ST amplitude (II, III, V).** The pooled CAD group and the patient subgroups showed ST depression over the left anterior and inferior thorax and over the left side. Reciprocal ST elevation took place over the middle anterior thorax and over the right shoulder (Figures 7 and 8, Tables 12 and 13).

**ST slope (III).** The pooled CAD group and the patient subgroups showed decrease in ST slope over the left anterior thorax and over the left side. The reciprocal increase in ST slope took place over the right shoulder (Figure 8, Table 13).

**T-wave amplitude (II, V).** In Studies II and V, the pooled CAD group and the LAD and LCX subgroups showed a decrease in T-wave amplitude over the left anterior thorax and over the left side. In the RCA subgroup, the decrease in T-wave amplitude was more caudal than in the other groups over the inferior thorax and abdomen, where the T-waves' amplitude turned negative. In the RCA subgroup, the decrease in T-wave amplitude was more caudal in Study II than in Study V. The reciprocal increase in T-wave amplitude took place over the right shoulder (Figure 9, Tables 12 and 14).

**ST-T integral (V).** The pooled CAD group and the LAD and LCX subgroups showed decrease in ST-T isointegral area and decrease in positive ST-T area over the left side on the midaxillary line. The decrease in ST-T isointegral was more caudal in the RCA than in the other subgroups (Table 14).

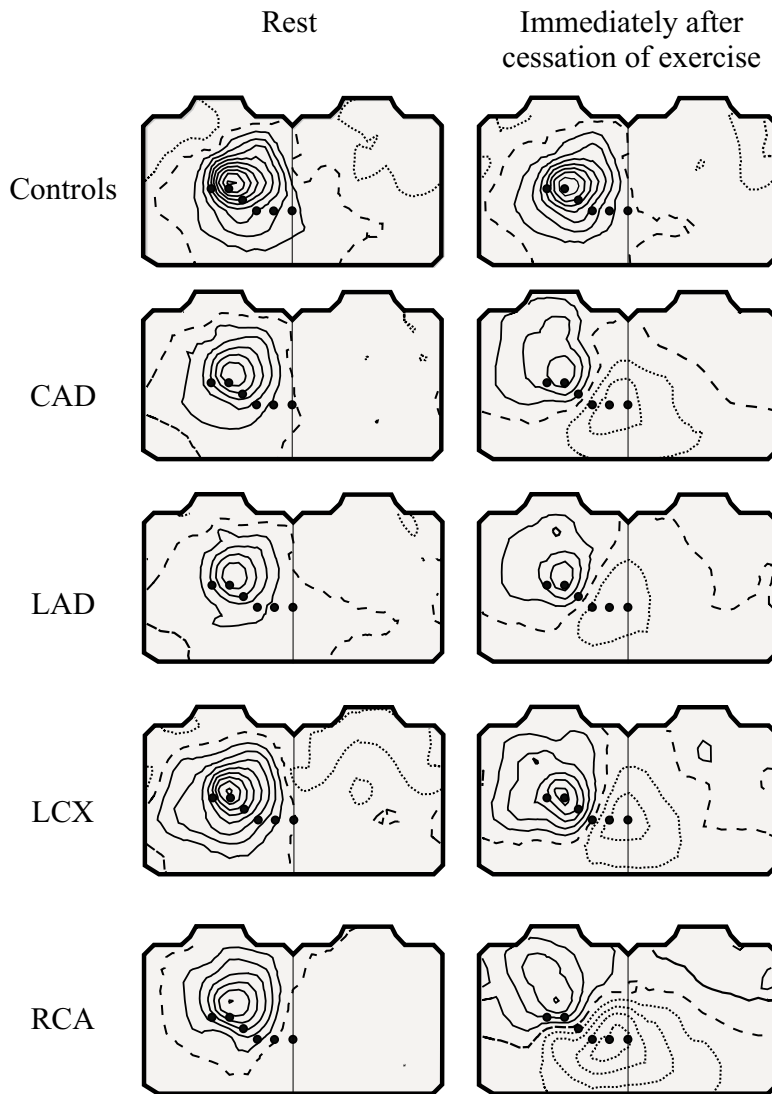


**Figure 7.** Study II. Group mean electric isopotential maps of ST-segment amplitudes. Left to right: Spatial distribution of the electric potential at rest and immediately after cessation of exercise. Top to bottom: Healthy Controls, patients with coronary artery disease (CAD), with stenosis in the left anterior descending (LAD), left circumflex (LCX), or right (RCA) coronary artery. All CAD groups showed ST depression over the left side. Location of maximal ST depression was most caudal in the RCA subgroup. Torso silhouettes represent the potential and slope over the anterior chest (left) and over the back (right). The step between two isocontour lines is  $25 \mu\text{V}$ . — positive, ..... negative, - - - zero line, • leads  $V_1$ - $V_6$ .

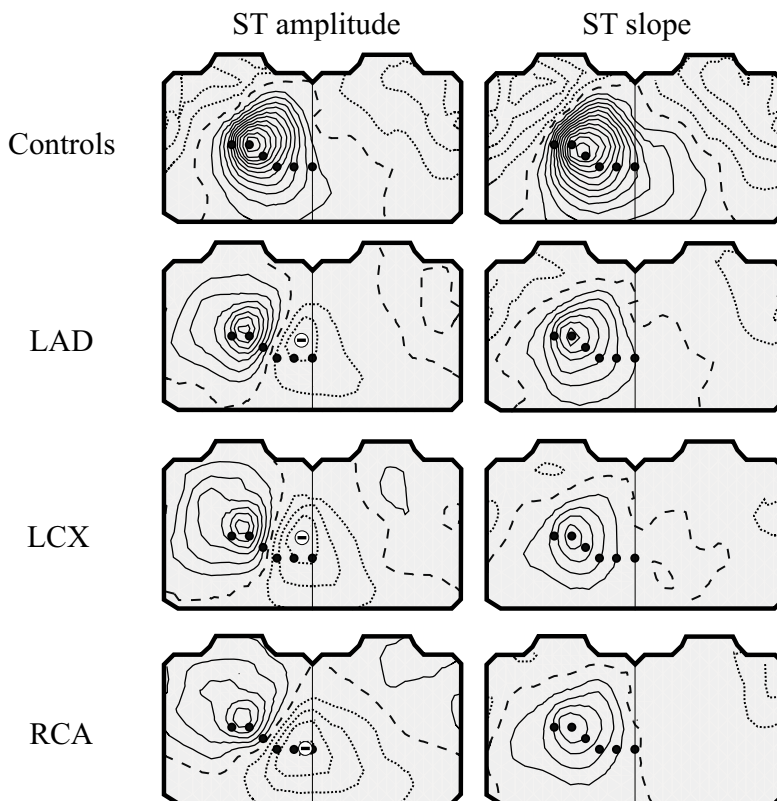


**Figure 8.** Study III. Group mean BSPM maps of ST amplitude and ST slope immediately after cessation of exercise. See Fig. 7 for subjects. Healthy Controls have a large potential maximum over the anterior thorax. In anterior and posterior ischemia the maximal ST depression is found in adjacent locations on the left side of the thorax, whereas in inferior ischemia the maximal ST depression is further down. The reciprocal ischemic ST elevation is found over the right shoulder, where the healthy Controls have negative ST amplitude. An ascending ST slope is found over the left precordium both in patients and in Controls. The ST slope is more horizontal in CAD patients than in Controls. Torso silhouettes represent the potential and slope over the anterior chest (left) and over the back (right). The step between any two isocontour lines is  $25 \mu\text{V}$  in amplitude maps and  $300 \mu\text{V/s}$  in ST-slope maps. Locations of maximal ST depression are marked with a minus sign in a white circle. — positive, ..... negative, - - - zero line, • leads  $V_1$ - $V_6$ . (Reprinted with permission from *The American Journal of Cardiology*.)

**Table 12.** ST-segment amplitudes and T-wave amplitudes in the optimal BSPM channels for ST depression and T-wave amplitude decrease, Study II.

Group	ST amplitude			T-wave amplitude		
	At cessation of stress			4 minutes' recovery		
	DI	Patients ( $\mu\text{V}$ )	Controls ( $\mu\text{V}$ )	DI	Patients ( $\mu\text{V}$ )	Controls ( $\mu\text{V}$ )
CAD	-1.19	$-39 \pm 61\ddagger$	$38 \pm 38$	-0.80	$33 \pm 130^*$	$139 \pm 110$
LAD	-1.15	$-24 \pm 113^{**}$	$88 \pm 68$	-0.96	$120 \pm 205^{**}$	$354 \pm 161$
LCX	-1.24	$-45 \pm 24^*$	$-7 \pm 27$	-1.09	$-3 \pm 72$	$67 \pm 47$
RCA	-1.89	$-90 \pm 69\ddagger$	$14 \pm 35$	-1.70	$-86 \pm 123\ddagger$	$139 \pm 110$

\*  $p < 0.05$ , \*\*  $p < 0.01$ , †  $p < 0.005$ , and ‡  $p < 0.001$  comparing patient group to control group, Mann-Whitney U-test. Mean  $\pm$  SD. DI = discriminant index. Abbreviations as in Table 3.

**Table 13.** ST amplitudes and ST slopes at cessation of stress in the optimal BSPM lead for ST depression and ST slope decrease, Study III.

Group	All CAD patients	LAD area ischemic	LCX area ischemic	RCA area ischemic
ST amplitude				
Discriminant index	-1.4	-1.28	-1.54	-1.76
Patients ( $\mu\text{V}$ )	$-70 \pm 70\ddagger$	$-60 \pm 90\ddagger$	$-90 \pm 90\ddagger$	$-100 \pm 70\ddagger$
Controls ( $\mu\text{V}$ )	$70 \pm 80$	$80 \pm 90$	$80 \pm 90$	$40 \pm 70$
ST slope				
Discriminant index	-1.62	-1.42	-1.69	-1.89
Patients ( $\mu\text{V/s}$ )	$20 \pm 240\ddagger$	$110 \pm 290\ddagger$	$20 \pm 170\ddagger$	$-100 \pm 220\ddagger$
Controls ( $\mu\text{V/s}$ )	$720 \pm 320$	$720 \pm 320$	$900 \pm 430$	$720 \pm 320$

‡  $p < 0.001$  comparing patient group to control group; Mann-Whitney U-test. Mean  $\pm$  SD. Abbreviations as in Table 3. (Reprinted with permission from *The American Journal of Cardiology*.)

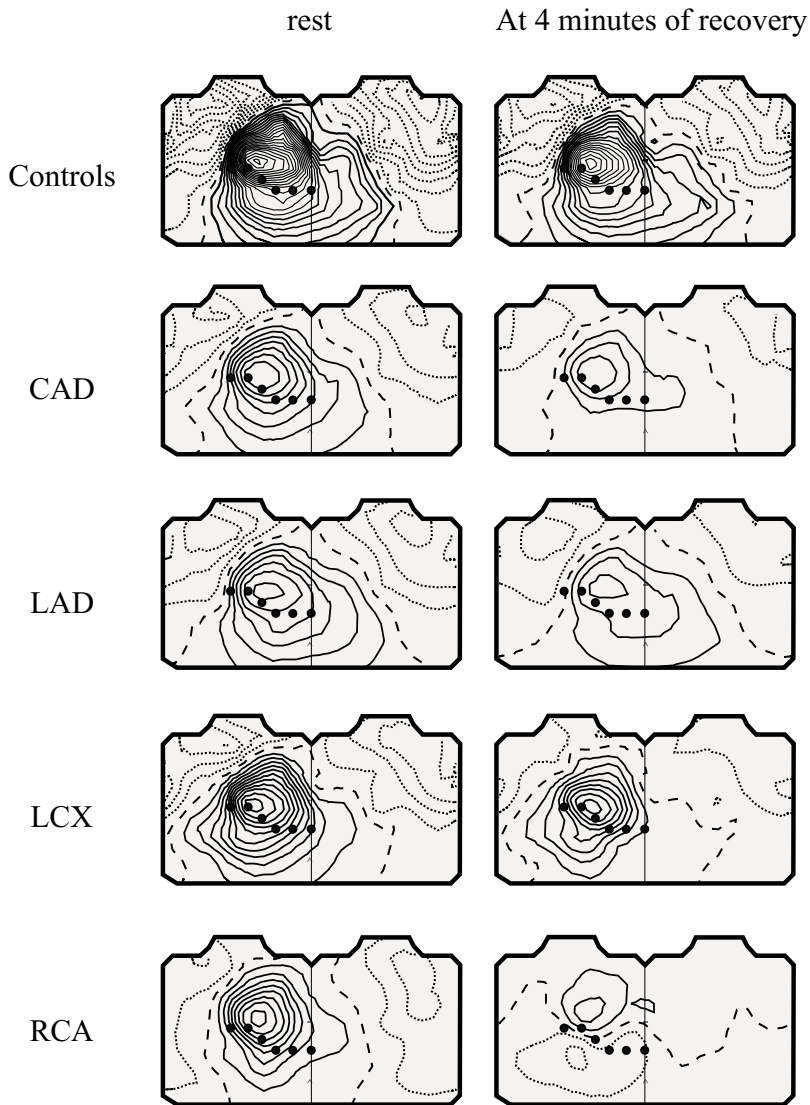


**Figure 9.** Study II. Group mean electric isopotential maps of patient subgroups at the T-wave apex. Left to right: Spatial distribution of the electric potentials at rest and 4 minutes' recovery. See Fig. 7 for subjects. T-wave changes were most prominent in the RCA subgroup at 4 minutes' recovery. Negative T-waves occurred in the inferior abdominal part of the thorax, and the zero potential line turned from vertical to horizontal after stress. The step between any two isocontour lines is 25  $\mu$ V. — positive, ..... negative, - - - zero line, • leads V<sub>1</sub>-V<sub>6</sub>.

**Table 14.** *ST-T areas and T-wave amplitudes at 2 minutes' recovery in the optimal BSPM leads, Study V.*

Group	All CAD patients	LAD area ischemic	LCX area ischemic	RCA area ischemic
<b>Decrease in ST-T isointegral area</b>				
Lead	74	69	71	70
Discriminant index	-1.42	-1.18	-1.59	-1.80
Patients ( $\mu$ Vs)	$-3.8 \pm 14\ddagger$	$3.6 \pm 20\ddagger$	$-15 \pm 29\ddagger$	$-11 \pm 17\ddagger$
Controls ( $\mu$ Vs)	$24 \pm 14$	$37 \pm 20$	$26 \pm 13$	$29 \pm 17$
<b>Decrease in positive ST-T area</b>				
Lead	72	73	71	73
Discriminant index	-1.48	-1.36	-1.52	-1.71
Patients ( $\mu$ Vs)	$9 \pm 8\ddagger$	$10 \pm 7\ddagger$	$8 \pm 9\ddagger$	$5 \pm 6\ddagger$
Controls ( $\mu$ Vs)	$31 \pm 14$	$31 \pm 15$	$28 \pm 12$	$31 \pm 15$
<b>T-wave amplitude decrease</b>				
Lead	74	70	71	70
Discriminant index	-1.37	-1.03	-1.52	-1.79
Patients ( $\mu$ V)	$3 \pm 110\ddagger$	$60 \pm 100\ddagger$	$-40 \pm 230\ddagger$	$-50 \pm 100\ddagger$
Controls ( $\mu$ V)	$190 \pm 90$	$220 \pm 120$	$260 \pm 110$	$220 \pm 120$

Leads refer to locations in Figure 2.  $\ddagger$   $p < 0.001$  comparing patient groups to control group; Mann-Whitney U-test. Mean  $\pm$  SD. Abbreviations as in Table 3.

### 6.2.2. Optimal recording locations

**ST amplitude (II, III, V).** In Study II, the optimal location for ST depression was, for the pooled CAD group, on the inferior thorax 5 cm right from the left midclavicular line; it was, for the LAD subgroup, on the height of the fourth intercostal space and lateral to the left midclavicular line; for the RCA subgroup, on the left inferior thorax lateral to the left midclavicular line; and for the LCX subgroup, on the height of the fifth intercostal space, posterior to the left midaxillar line. In Studies III and V, the optimal sites for ST depression were roughly the same for the pooled CAD group and the RCA subgroup, on the inferior thorax lateral to the left midclavicular line. The optimal site for the LAD and LCX subgroups was on the height of the fourth intercostal space lateral to the left midclavicular line (Figure 10, Tables 12 and 13). The optimal locations for detecting the reciprocal ST elevation were found over the right shoulder (Figure 10).

**ST slope (III).** The optimal location for the decrease in ST slope was over the left side on the height of the fifth intercostal space, posterior to the left midaxillar line in all patient subgroups. The ST slope was more horizontal in all patient groups than in the control group (Figure 8, Table 13). The optimal location for the reciprocal increase in ST slope was located over the right shoulder (Figure 10).

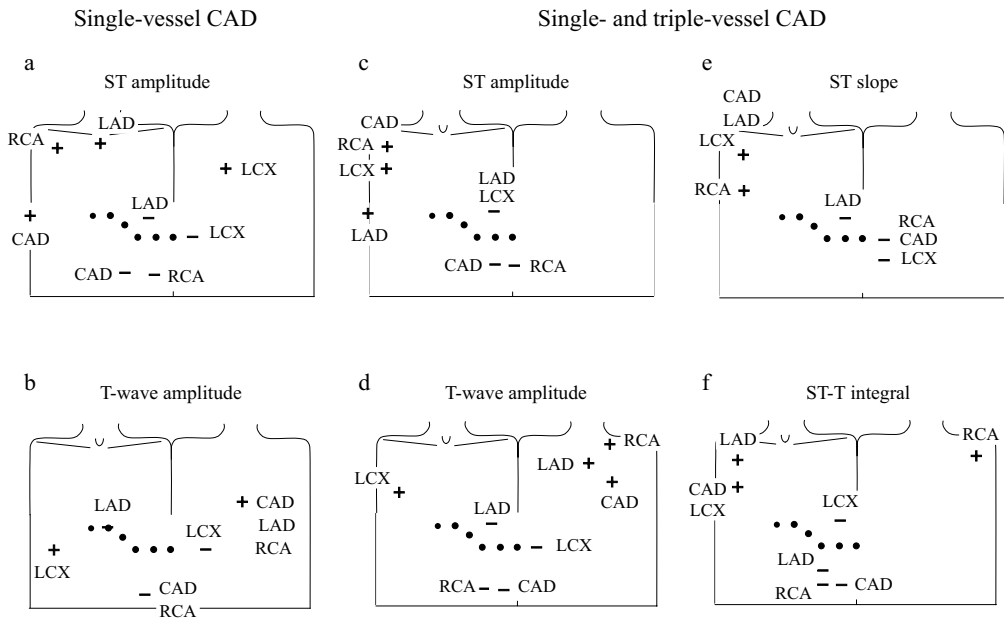


**Figure 10.** Studies II, III, and V. Recording locations in body surface potential mapping with the highest and the lowest discriminant index value in the pooled CAD group and in all patient subgroups with patients with single-vessel coronary artery disease (Study II) or with single- and triple-vessel CAD (Studies III and V). a) ST amplitude immediately after cessation of exercise, b) T-wave amplitude at 4 minutes' recovery, c) ST amplitude immediately after cessation of exercise, d) T-wave apex at 2 minutes' recovery, e) ST slope immediately after cessation of exercise, f) ST-T integral at 2 minutes' recovery. See Figure 7 for subjects. + highest values, - lowest values, • leads V<sub>1</sub>-V<sub>6</sub>.

**T-wave amplitude (II, V).** In Study II, the optimal location for T-wave amplitude decrease was, for the pooled CAD group and for the RCA subgroup, on the left inferior thorax, lateral to the left midclavicular line; for the LAD subgroup, on the level of the fourth intercostal space, left from the midsternal line; and for the LCX subgroup, on the level of the fifth intercostal space, posterior to the left midaxillary line on the back (Figure 10, Tables 12 and 14). The variation between the optimal locations in vessel subgroups was not as extensive in Study V as in Study II (Figure 10, Table 13).

**ST-T integral (V).** The optimal location for decrease in ST-T isointegral area was lateral to the left midclavicular line in all patient groups, on the inferior thorax for the pooled CAD group and for the LAD and RCA subgroups, and on the level of the fourth intercostal space for the LCX subgroup (Figure 10, Table 14). The optimal location for reciprocal increase in ST-T isointegral area was over the right shoulder (Figure 10).

#### 6.2.4. Performance of ischemia parameters in BSPM (III, V)

**Receiver operating characteristic curves.** At cessation of exercise, the ST slope had a slightly higher area under the receiver operating characteristic curve than did ST depression (97% vs. 93%), but this difference was not statistically significant (Table 15). Overall, in the pooled CAD group, the ST slope showed a trend toward better performance than did ST depression. The decrease in ST-T isointegral area, T-wave amplitude, and ST depression performed in a comparable way in ischemia detection in the pooled CAD group, yielding areas under the receiver operating curves of 94%, 92%, and 93%, respectively. T-wave amplitude performed particularly well in the post-MI patients with multi-vessel disease, with areas under the curve of 98% for decrease in T-wave amplitude, in ST-T isointegral area, and in ST-T positive area, all three (Table 15).

**Table 15.** Areas under the receiver operating characteristic curves for ST depression, ST slope, decrease in ST-T areas, and for T-wave amplitude decrease in patient subgroups in BSPM, Studies III and V.

Group	CAD	No MI single- vessel	Post-MI multi- vessel	LAD	LCX	RCA
Immediately after cessation of stress						
ST depression	93 %	93 %	94 %	94 %	92 %	94 %
ST slope	97 %	95 %	99 %	94 %	99 %	99 %
At 2 minutes' recovery						
Decrease in ST-T isointegral area	94 %	93 %	94 %	92 %	92 %	97 %
Decrease in positive ST-T area	95 %	94 %	96 %	92 %	95 %	98 %
T-wave amplitude decrease	92 %	90 %	95 %	87 %	91 %	99 %

Abbreviations as in Table 3.

**Logistic regression analysis (V).** In Study V, a stepwise logistic regression analysis was performed to study the independent discriminative power of the parameters in identification of the CAD patients. The parameters were entered into the model stepwise, and the presence of CAD served as the dependent value. Testing all the parameters, the decrease in positive ST-T area and ST depression entered the model. When the decrease in positive ST-T area was removed from the model, the decrease in ST-T isointegral area and ST depression entered the model. Altogether, the decrease in positive ST-T area, the decrease in ST-T isointegral area, and the T-wave amplitude decrease had discriminant value additive to ST depression, but not to each other.

### 6.3. Spatial comparison of MCG and BSPM

MCG was capable of detecting reciprocal ischemia-induced changes in the ST-segment and T-wave parameters, despite the smaller spatial mapping area of the MCG than of the BSPM. Over the frontal chest, on the mapping region closest to the heart, the optimal recording locations evaluated visually from the maps were orthogonal, i.e., showing a spatial angle of approximately 90° between the MCG and BSPM. This was first evaluated in Study II, comprising patients with single-vessel CAD, and remained constant in Studies III, IV, and V, comprising more heterogeneous CAD populations: both single- and triple-vessel CAD patients and patients with remote MI.

### 6.4. Optimal time phases of exercise testing

**ST amplitude (I-V) and ST slope (III, IV).** Of the phases of the exercise test, ST slope (in Studies III and IV) and ST amplitude (in all studies) performed best in ischemia detection immediately after cessation of exercise.

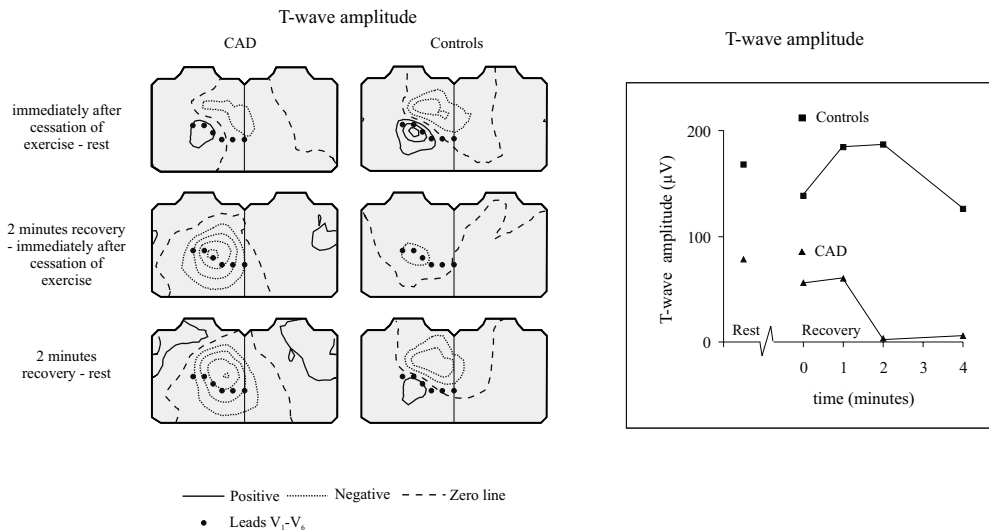
**T-wave amplitude (I, II, IV, V).** In Studies I and II, T-wave amplitude performed best in detection of ischemia at 4 minutes of recovery. The findings at 2 minutes of recovery resembled those at 4 minutes, although they were in general less pronounced. In Studies IV and V, T-wave amplitude performed best at 2 minutes of recovery, and the findings at 4 minutes resembled those at 2 minutes, although they were less pronounced (Figure 11). In Study V, the phase-difference maps of the T-wave amplitude showed that during the first minutes of the recovery phase of the exercise test, T-wave amplitude decreased over the left anterior thorax in CAD patients but not in healthy controls (Figure 11).

**ST-T integral (IV, V).** In Studies IV and V, the ST-T integral performed best in ischemia detection at 2 minutes of recovery.

### 6.5. 12-lead ECG in detection of exercise-induced myocardial ischemia

In 12-lead ECG, recorded simultaneously with MCG, the average ST depression measured at 60 ms after the J point was in patients with single-vessel disease  $83 \pm 74 \mu\text{V}$  and in the pooled CAD patient group  $120 \pm 97 \mu\text{V}$ . None of the healthy controls showed  $\geq 100 \mu\text{V}$  ST depression. Of the 27 patients with single-vessel disease and the pooled CAD patient group of 47 patients, 7 (26%) and 21 (46%) showed  $\geq 100 \mu\text{V}$  ST depression, yielding a sensitivity of 26% and 46% at the specificity level of 100% for detection of single-vessel disease and CAD.

a



b

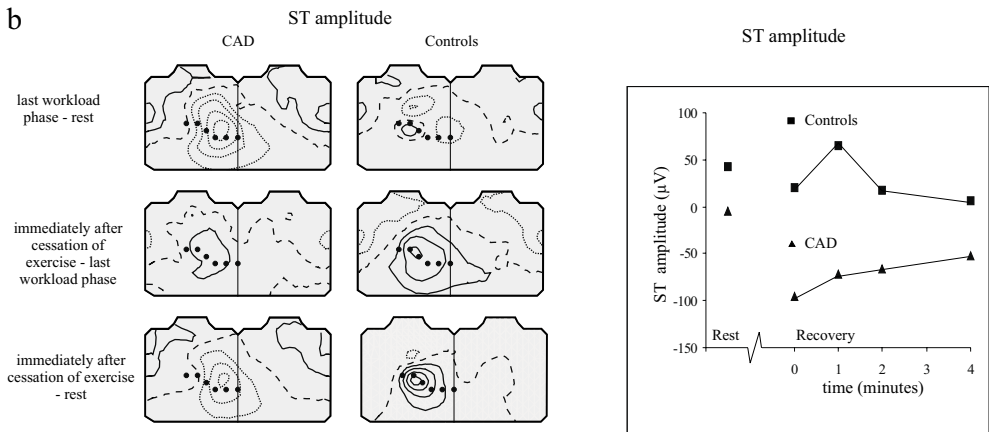


**Figure 11.** Study V. a) Left: Phase-difference maps of the T-wave amplitude for patients with CAD and for healthy Controls. Top: T-wave amplitude at rest was subtracted from the corresponding amplitude immediately after cessation of exercise. Middle: T-wave amplitude immediately after cessation of exercise was subtracted from the amplitude at 2 minutes' recovery. Bottom: T-wave amplitude at rest was subtracted from the amplitude at 2 minutes' recovery. The step between two isocontour lines is 50  $\mu\text{V}$  in T-wave maps. Right: Group mean T-wave amplitudes in the optimal site, lead 74, for T-wave amplitude decrease. On the X-axis, 0 corresponds to the last workload phase, 1 is immediately after cessation of exercise, and 2 and 4 are the corresponding minutes of recovery. b) Left: Phase-difference maps of ST amplitude for patients with CAD and healthy controls. Top: ST amplitude at rest subtracted from corresponding amplitude at last workload phase. Middle: ST amplitude at last workload phase subtracted from amplitude immediately after cessation of exercise. Bottom: ST amplitude at rest subtracted from amplitude immediately after

*cessation of exercise. The step between two isocontour lines is 25  $\mu$ V in ST amplitude maps. Right: Group mean ST amplitudes in the optimal site, lead 73, for ST depression. As in Figure 11a.*

## **7. DISCUSSION**

### **7.1. Main findings**

Multichannel MCG and BSPM were able to detect exercise-induced myocardial ischemia caused by stenosis in any of the main coronary artery branches, regardless of the presence or absence of a remote myocardial infarction.

In MCG, exercise-induced myocardial ischemia induced a change in the magnetic field orientation during ST segment and T-wave. This rotation, i.e., change in the orientation of the magnetic field, could be quantified either by estimating the angle manually or by determining the two-dimensional direction of the maximum spatial field gradient. The change in T-wave field orientation was most profound in patients with inferior ischemia due to a stenosis in the right coronary artery.

In MCG, the optimal locations for ischemia-induced ST depression, decrease in ST slope, decrease in T-wave amplitude, and decrease in ST-T integral area were over the middle inferior thorax and abdomen. The optimal locations for the reciprocal increase in these variables were over the left parasternal area and left anterior shoulder. These locations were roughly the same for all patient groups, irrespective of the culprit vessel or the presence or absence of a history of MI.

In BSPM, the optimal locations for ischemia-induced ST depression, decrease in ST slope, decrease in T-wave amplitude, and decrease in ST-T integral area were over the left anterior and posterior thorax, cranial to, caudal to, or on the level of the fourth intercostal space. The optimal locations for the reciprocal increase in these parameters were over the right shoulder and on the middle back. The variation in location of these optimal sites was more extensive in BSPM than in MCG.

Variation in the optimal locations in subgroups of patients with different anatomic ischemic regions was more extensive for the T-wave parameters than for the ST-segment parameters. The optimal locations for detection of exercise-induced myocardial ischemia by use of ST-segment and T-wave parameters were orthogonal in both MCG and BSPM, i.e., showed a spatial angle of approximately 90° between them.

The ST-segment parameters and the T-wave parameters performed best in different phases of the formal exercise test. The best time-phase for the ST-segment parameters: ST amplitude and ST slope, to separate the CAD patient groups from the control group was immediately after cessation of exercise. In contrast, the best time-phase for the T-wave

amplitude and for the ST-T integral area to separate the CAD patient groups from the control group was two to four minutes after cessation of exercise.

In the heterogeneous CAD population, the morphology of the ST segment, as reflected in the ST slope, appeared to be a sensitive and specific marker for transient myocardial ischemia assessed in MCG and BSPM. Despite variation in the ischemic regions in the heart and the presence or absence of a history of MI, two nearby regions in BSPM could be identified, one sensitive for ST depression and the other for ST slope decrease. In MCG, the optimal locations for ST depression and ST slope decrease were roughly the same.

The new ischemia parameters ST-T integral area and T-wave amplitude, as evaluated in MCG and in BSPM, were sensitive and specific markers for exercise-induced myocardial ischemia. In BSPM, the ST-T area showed information additional to ST depression in logistic regression analysis, and thus had independent discriminative value in ischemia detection.

## **7.2. Contribution to previous investigations**

### **7.2.1. Myocardial ischemia in MCG**

The present studies systematically evaluated the detection of exercise-induced myocardial ischemia in patients with well-defined CAD who showed a diverse extent of disease and variation in culprit vessel distribution. Previous MCG studies have focused mainly on distinguishing CAD patients from healthy subjects in rest measurements, focusing on either QRS changes or repolarization abnormalities secondary to remote MIs. The present thesis also assessed the optimal time-phases of various ST-segment and T-wave parameters to detect transient ischemia during the exercise test; time-phases have not been examined in other MCG studies. Furthermore, the present studies evaluated the optimal recording locations for ST-segment and T-wave indexes to detect exercise-induced ischemia by use of discriminant index analysis, an analysis previously not applied to exercise MCG recordings.

#### **7.2.1.1. *Magnetic field orientation***

The capability of magnetic field orientation to detect myocardial ischemia seems not to have been previously evaluated in exercise testing. In rest measurements, magnetic field orientation has differed both in non-MI CAD patients with normal ECGs and in post-MI patients from that of the control group (van Leeuwen et al. 1999c). Evaluated throughout the whole QRST interval, the T-wave field orientation diverged from that of the controls, with more prominent changes in severe disease. It separated the MI and CAD groups from the control group with a sensitivity of 85% and 68% both with a specificity of 90%. Field orientation was defined as the angle between the line joining the field extrema and the right-left line of the torso: a method closely resembling the measurement of field polarity

or orientation of the spatial field gradient presented in Study I. Since no stress was induced in the former study, the better sensitivity and specificity gained for the post-MI group compared to patients without prior MI could be due to the infarction scar rather than to acute ischemia.

#### **7.2.1.2. *QRST analysis in MCG***

Tsukada et al. (2000) evaluated the capability of the QRS and ST-T integrals in MCG to separate 10 CAD patients from 12 healthy controls at rest. The CAD patient group showed a reduced ratio of maximum repolarization and depolarization values in ST-T and QRS isointegral maxima compared to those of the control group. Since seven of their ten CAD patients had a history of remote MI, the reduced current ratio could have been caused by current perturbations due to remote MIs. Kandori et al. (2001b) recorded 64-channel MCG in six patients with effort angina pectoris and in two patients with variant angina at rest and after a two-step exercise test. In the former six, the current-ratio maps of the QRS complex showed three distinct patterns for each stenosed main coronary artery. The maximum current ratios of these three patterns differed from those of normal patterns; the abnormalities were reduced after PCI treatment. Obvious fundamental differences exist between rest and stress studies focused on QRS analysis and those exercise studies focused on repolarization indexes. In the former, macroscopic QRS changes associated with permanent myocardial damage are utilized, whereas the latter exploit transient exercise-induced ST-T-amplitude shifts representing true ischemia. Thus, the electrophysiological differences between these two pathophysiological states: the permanent myocardial infarction scar and the transient myocardial ischemia, should be appreciated.

#### **7.2.1.3. *ST-segment- and T-wave parameters in MCG***

The present studies evaluated the performance of ST amplitude, ST slope, T-wave amplitude, and ST-T integral area in detection of exercise-induced myocardial ischemia in MCG, performance not assessed in previous multichannel MCG studies.

Saarinen et al. (1974) performed the first human exercise MCG study in a CAD patient. Single-channel MCG showed manifest ST-segment depression after exercise testing. In direct-current MCG, TQ-baseline elevation and ST depression were registered in a CAD patient after a two-step exercise test; the diastolic "apparent" ST shift disappeared more rapidly than did the "true" systolic ST shift (Cohen et al. 1983). Hailer et al. (1999) studied seven CAD patients with normal 12-lead ECG and eight healthy controls with 37-channel MCG at rest and during pharmacological stress. Spatial evaluation of QT dispersion in MCG improved the separation of the CAD group from the control group compared to the QT dispersion assessed in 12-lead ECG. Their study, however, evaluated only the temporal QT parameters, not ST-segment or T-wave amplitude changes.

#### **7.2.1.4. Optimal locations of ST-segment and T-wave parameters**

In the single-channel MCG pilot study of Saarinen et al. (1974), two of their three MCG measurement locations were on the thoracic midline over the inferior part of the sternum, and the third was on the left side of the sternum. Based on the multichannel recordings presented in this thesis, these recording sites actually were located over the optimal sites to detect ischemia-induced ST depression in MCG.

#### **7.2.2. Myocardial ischemia in BSPM**

The present studies systematically compared MCG and BSPM in detection of exercise-induced myocardial ischemia in the same well-defined CAD patient cohort with a diverse extent of disease showing variation in culprit vessel distribution; these factors seem not to have been evaluated in previous studies. The optimal time-phases of various ST-segment and T-wave indexes to detect transient ischemia during an exercise test were identified, ones seemingly not previously assessed in any other BSPM studies. Although optimal recording sites for acute and remote MIs and for transmural ischemia provoked during PCI have been identified in BSPM, no other study seems to have evaluated the optimal recording locations for detection of exercise-induced myocardial ischemia.

##### **7.2.2.1. ST-segment parameters in BSPM**

In the present series of studies, the location of the maximal exercise-induced ST depression was only slightly more caudal in the RCA subgroup than in the LAD or LCX subgroups. The site of the maximal ST depression thus did not localize the culprit coronary artery. These findings are in accord with earlier BSPM findings, some showing marked overlap of the patterns of exercise-induced ST deviation (Simoons and Block 1981, Kubota et al. 1985 and 1989, Nakajima et al. 1988, Hosoya et al. 1990, Montague et al 1990), and others only modest success in localization of ischemia (Wada et al. 1981, Yanowitz et al. 1982, Kubota et al. 1989).

In a pilot BSPM study of CAD patients with solitary LAD or RCA stenosis, a stepwise discriminant analysis by the jackknife statistical method has improved ischemia localization (Farr et al. 1987). Since patients with LCX stenosis were not included, the capability of this method to localize ischemia in the region of any of the main coronary artery branches remained unevaluated.

Fox et al. (1979a) demonstrated the improved localizing accuracy of ischemic ST depression in BSPM compared to that of 12-lead ECG. In 16-lead precordial isopotential mapping, ST depression took place in different areas for the three main stenotic coronary artery branches (Fox et al. 1979b). They considered  $\geq 0.1$  mV of ST-segment depression diagnostic, neglecting any lesser degree of ST deviation. In contrast to the supine exercise testing employed in the present series of studies, Fox et al. employed upright bicycle exercise testing. Thadani et al. (1977) demonstrated that CAD patients in a supine bicycle

exercise test show higher LV end-diastolic pressures than in an upright bicycle exercise test. These higher pressures may contribute to the early development of the global subendocardial ischemia suggested to explain the lack of ischemia localization capacity (Kubota et al. 1985). The present results support the idea of a more diffuse nature of exercise-induced ischemia than is seen in the transmural ischemia produced by coronary artery occlusion in acute MI or in PCI.

#### **7.2.2.2. *T-wave parameters in BSPM***

In the present series of studies, the ischemic T-wave amplitude deviations were emphasized during the recovery phase of the exercise test. In BSPM, the most profound ischemia-induced changes in T-wave apex amplitude and ST-T integral area were demonstrated in different spatial areas of the chest surface for each patient subgroup with different ischemic regions in the heart.

In accord with the results of this thesis, other BSPM studies have also demonstrated the capability of T-wave parameters to localize the ischemic region (Ishikawa et al. 1988, Nakajima et al. 1988, Kubota et al. 1989, Tseng et al. 1999). Rest BSPM studies have applied T-wave apex amplitude (Tseng et al. 1999) or T-wave maps at 4 ms time intervals (Ishikawa et al. 1988), whereas exercise BSPM studies have mostly used ST-T isointegral analysis (Nakajima et al. 1988, Kubota et al. 1989). At rest, the T-wave maps have displayed differing patterns related to the coronary artery which is diseased, with negative T-waves anteriorly for LAD disease, but inferiorly or over the back for LCX or RCA disease (Ishikawa et al. 1988). In exercise BSPM, the ST-T isointegral maps have demonstrated negative values over the thorax: anteriorly for LAD disease, inferiorly for RCA disease, and posteriorly for LCX disease (Nakajima et al. 1988, Kubota et al. 1989). No other study seems, however, to have evaluated the optimal time-phases of the T-wave indexes to detect ischemia in exercise testing.

#### **7.2.2.3. *Optimal locations of ST-segment and T-wave parameters***

No similar studies have evaluated the optimal recording locations of BSPM, identified by discriminant index analysis, to detect exercise-induced myocardial ischemia in patient cohorts. In patients with acute or remote MIs, of the six optimal recordings sites identified for detection of MI, five were outside the standard precordial leads (Kornreich et al. 1993). The optimal sites for exercise-induced ST depression in the present studies displayed much less spatial variation in the three main culprit coronary arteries than in those identified for acute or remote MIs (Kornreich et al. 1991 and 1993) or the ones for acute ischemia in PCI studies (Shenasa et al. 1993, Lux et al. 1995, MacLeod et al. 1995, Horáček et al. 2001). The present findings support the fact that the poorer ischemia-localization capability in the exercise-induced ischemia may be due to a global subendocardial ischemia caused by elevated LV end-diastolic pressure, as previously suggested by Kubota et al. (1985).

### **7.2.3. Comparison of MCG and BSPM**

The ST-segment and T-wave parameters evaluated in the present series of studies were capable of detecting ischemia both in MCG and in BSPM. These parameters showed a trend toward a slightly better performance in electric than in magnetic mapping. Noteworthy is the fact that in both methods the ST slope and the T-wave indexes performed as well as did the standard ST depression.

MCG is less affected than is ECG by inhomogeneities and conductivity variations in the thorax. The optimal recording sites to detect ischemia in MCG and in BSPM were approximately orthogonal over the frontal chest. This finding is consistent with the fact that the spatial MCG and BSPM patterns are similar but rotated by 90 degrees in respect to each other. Thus, BSPM demonstrates accuracy in manifesting the cardiac signals to the body surface, despite all these confounding factors.

In MCG, both axial and planar hardware gradiometers had very similar noise levels, but axial sensors showed much larger signal amplitudes and thus had a superior signal-to-noise ratio. The 33 axial gradiometers simulated from the measured MCG data in turn exhibited signal amplitudes similar to those of the axial hardware gradiometers but also higher noise due to the signal interpolation. Their signal-to-noise ratio therefore became approximately a weighted average of those in the hardware axial and planar gradiometers. On the other hand, the mean signal-to-noise ratio of the BSPM leads was very close to the corresponding mean of the 33 simulated axial channels. This signal-to-noise ratio thus does not explain the differences between MCG and BSPM results. The larger spatial coverage of the thorax in electric than in magnetic mapping can, however, explain the differences in ischemia detection between these methods.

MCG and BSPM have not been previously compared in detection of exercise-induced myocardial ischemia, but in healthy individuals, the physiological response of MCG and BSPM to exercise and to pharmacological stress has been compared (Brockmeier et al. 1994, 1997, Takala et al. 2001a). ST depression and T-wave inversion in MCG, not detected in simultaneous BSPM, can possibly be explained by circular vortex currents (Brockmeier et al. 1997). When Lant et al. (1990) compared MCG and BSPM in post-MI patients and in healthy controls at rest, the largest differences between the groups appeared in magnetic mapping during repolarization and in electric mapping during depolarization. The repolarization changes were more prominent in patients with inferior than with anterior Q-wave MI. In concordance with this, Study I showed that repolarization changes were most prominent in patients with inferior ischemia.

### **7.2.4. Time scale of ST-segment and T-wave parameters**

Due to its better signal-to-noise ratio, the ST segment was examined immediately after cessation of exercise. With progressive exercise, the depth of ST-segment depression

increases (Chaitman 1997), persisting well after exercise into the immediate recovery phase (Montaque et al. 1988 and 1990). The time-dependency of the T-wave amplitude changes during exercise testing has not been evaluated earlier. In 12-lead ECG exercise testing, the downsloping ST depression with T-wave inversion during the recovery phase is considered an ischemic response (Chaitman 1997). On the basis of the present studies, the time-dependency of the optimal performance of ST-segment and T-wave parameters should be considered. The comparable performance of T-wave amplitude and ST-T integral area to ST depression—the former two analyzed later during recovery than was ST depression—supports the idea that combining the observations over different phases of a formal exercise test enhances detection of myocardial ischemia.

### 7.3. Methodological considerations

**Patient selection.** Studies I and II included only patients with single-vessel CAD without prior MI. The results of these two studies may therefore not be applicable to patients with multi-vessel disease and a history of MI. Patients with triple-vessel disease and prior MI were included in Studies III to V in order to have findings more applicable to CAD patients in general. Nevertheless, patients were excluded if they had two-vessel disease, single-vessel disease and prior MI, or triple-vessel disease without prior MI. The patients with triple-vessel disease and prior MI were not systematically screened for local or overall LV hypertrophy. None of the patients included were, however, diagnosed with valvular disease.

**Anti-anginal medication during the study.** All CAD patients were on appropriate anti-anginal medication: most CAD patients were on beta blockers and on long-acting nitrates, and some on Ca<sup>2+</sup> channel-blocking drugs. For safety reasons, these medications were continued during the study. Anti-ischemic drug therapy with beta-blocking drugs, nitrates, or Ca<sup>2+</sup> channel-blocking drugs prolongs the time onset of ischemic ST depression, increases exercise tolerance, and in a small minority of patients with documented CAD (from 10% to 15%), may normalize the exercise ECG response (Chaitman 1997). Beta blockers reduce the amount of ST depression (Gianelly et al. 1969) and the peak exercise heart rate (Epstein et al. 1965, Gianelly et al. 1969), but not the overall heart rate change during exercise testing (Kligfield et al. 1993). The continuous anti-anginal medication during the study thus might have been disadvantageous for detection of ischemia by MCG and BSPM. On the basis of the 12-lead ECG studies, however, it seems unlikely that in exercise testing it would have induced false-positive responses.

**Ischemia localization by <sup>201</sup>Tl SPECT imaging.** In patients with triple-vessel disease, because determining the myocardial region limiting the performance in exercise testing is difficult, the most severely ischemic myocardial region was determined by both <sup>201</sup>Tl

SPECT imaging and coronary angiography. The variables that reduce the sensitivity of  $^{201}\text{Tl}$  SPECT imaging for detection of CAD are single-vessel disease, LCX stenosis, branch-vessel or distal stenosis, mild degree of stenosis, inadequate heart-rate response, and anti-anginal therapy with nitrates or  $\text{Ca}^{2+}$  channel-blockers (Beller and Zaret 2000). Sensitivity is, however, enhanced in patients with prior MI, more extensive CAD, high-grade stenosis, proximal location of stenosis, and presence of regional wall-motion abnormalities, features present in the subpopulation of triple-vessel CAD patients in Studies III to V. Especially in women, the overall specificity of  $^{201}\text{Tl}$  SPECT imaging is suboptimal due to an attenuation artifact in the anterior wall and septum caused by overlying breast tissue (Beller and Zaret 2000, Lee and Boucher 2001).

**Repeated exercise testing.** The study subjects underwent two separate exercise tests on the same day. The exercise tests were purposely performed in random order, meaning every other CAD patient and healthy control underwent the MCG, and all others underwent BSPM exercise testing first. Because relatively few episodes or even one burst of short-lived severe ischemia followed by complete reperfusion may cause preconditioning, protecting the myocardium against a greater subsequent ischemic insult (Opie 1997), ischemic preconditioning may have had some effect on the latter exercise test.

**Limb lead placement.** In the present study, arm leads were attached to the base of each shoulder against the deltoid border, below the clavicle, according to the "correct" modified Mason-Likar placement (Gamble et al. 1984). This placement is preferable to the original Mason-Likar formula in which the arm electrodes are attached to the frontal chest (Gamble et al. 1984). Differences between the standard and the exercise ECG can be minimized by placing the arm electrodes as close to the shoulders as possible, and by recording the ECG with the patient in supine posture. The correct modified Mason-Likar leads have produced an average QRS axis rightward shift of only  $9^\circ$  compared to  $26^\circ$  with the original Mason-Likar system (Gamble et al. 1984). In comparing the standard 12-lead ECG to the original Mason-Likar system, Rautaharju et al. (1980) found that the QRS axis shifted on average  $16^\circ$  towards a more vertical position, and P, R, and T-wave amplitudes decreased in lead aVL, and increased in leads II, III, and aVF. The reduction in ST slope and T-wave amplitude in aVL, and the opposite increase in the inferior leads II, III, and aVF may also affect the interpretation of exercise ECG (Rautaharju et al. 1980). Kleiner et al. (1978) found that the Mason-Likar system showed Q-waves and T-wave inversions in lead aVL which were suggestive of lateral wall infarction in 15% of the patients without prior history or ECG evidence of MI. Of the patients with prior inferior MI, 41% had diagnostic inferior Q-waves erased by the rightward axis shift on the modified ECG. The exact location of their shoulder electrodes was not stated by Kleiner et al. (1978).

**Supine exercise position.** The geometry of the current studies' MCG device allows exercise measurement only in the supine position. In order to make possible a comparison between two exercise tests, the same protocol was also applied to BSPM measurements.

The upright position produce a net effect on exercise performance of an approximate 10% increase in exercise time, cardiac index, heart rate, and rate pressure product at peak exercise compared with figures for the supine position (Chaitman 1997). It has been suggested that LV preload would be augmented by increased venous return during supine exercise with the legs above atrial level (Currie et al. 1983). The supine position could thus increase myocardial wall tension, and hence, myocardial oxygen requirements, by elevating LV volumes and end-diastolic pressures and increasing arterial pressures. In most studies, the ischemic ST depression has been greater in the supine than in the upright position at similar heart rates or rate-pressure products (Currie et al. 1983, Wetherbee et al. 1988). Since upright exercise is associated with greater exercise time, peak heart rate, and peak rate-pressure product, an increased incidence of ischemic ST deviations occurs in exercise performed upright rather than supine (Shaw et al. 1990). The present studies demonstrated that fewer patients fulfilled the ischemic ECG criterion in supine than in upright bicycle ergometry, supporting the findings that supine bicycle ergometry may be less sensitive in provoking myocardial ischemia and ischemic ECG findings than is the upright version. The position of the heart with respect to the chest surface may vary according to body posture. Since the present study identified the optimal locations to detect ischemia in supine recordings, these results may not be directly applicable to measurements in the upright position.

**Ischemia localization.** In multi-vessel disease, ischemia at a distance, developing because of inadequate blood flow through collaterals from one stenotic main coronary branch to the region of other stenotic branches, may reduce blood flow to regions dependent on the collateral flow, complicating ischemia localization (Katz 1992). Ischemia at a distance does not, however, explain the inability to localize exercise-induced ischemia in single-vessel disease. This lack of correlation may be related to various factors, including the presence or absence of collateral circulation, and individual differences in coronary anatomy and heart position in relation to electrode positions (Kubota et al. 1985). Differences in ischemia localization capacity may depend on differences between transmural ischemia, occurring in response to total interruption of blood flow due to coronary thrombosis or spasm, and subendocardial ischemia, occurring in a controlled manner during exercise testing (Katz 1992). Experimental studies comparing pacing-induced with flow-limited ischemia have shown that changes in systolic and diastolic function occur earlier and to a greater extent during coronary occlusion, but qualitatively similar changes are also observable during the pacing-induced ischemia. The LV response to ischemia should therefore not be classified simply based on whether “supply” or “demand” ischemia is present, but rather on a complex interaction between duration, extent and severity, and type of ischemia elicited (Applegate et al. 1990).

## 7.4. Clinical implications

Results of the present studies imply that exercise-induced myocardial ischemia causes identifiable changes in MCG and in BSPM. In addition to ST depression, changes in ST slope, T-wave amplitude, and ST-T integral area are associated with exercise-induced ischemia.

In BSPM, the optimal recording locations for the decrease in these ischemia parameters are reasonably well covered by the standard precordial leads  $V_1$ - $V_6$  of the 12-lead ECG. Thus, ST slope (independently of ST depression) and the novel ischemia markers T-wave amplitude and ST-T integral area can all serve in ischemia detection also in standard 12-lead ECG exercise testing. Although location of the maximum ST depression cannot identify the anatomic site of coronary artery obstruction, T-wave amplitude changes during the recovery phase of an exercise test may be useful in localization of the culprit coronary artery. Larger studies could confirm all these preliminary results and establish reference values for clinical use. Identification of the optimal sites for ischemia detection may aid in developing systems for improved ischemia monitoring in cardiac care units.

At present, exercise MCG is a research tool, not feasible for clinical use due to its high cost and need for magnetic shielding. Thus far, MCG ischemia studies have focused either on acute exercise-induced ischemia or on chronic ischemia and the infarct scar in rest measurements. In the future, the SQUID systems operating without expensive magnetic shielding will permit less expensive MCG measurements without technical limitations even in the clinical environment. Such developments will allow study also of transmural ischemia due to acute MI or to transmural ischemia produced in PCI. BSPM studies have demonstrated that the electrocardiographic manifestations of myocardial ischemia during acute coronary occlusion or physical or pharmacological stress show fundamental differences, the former allowing more accurate ischemia localization. Meanwhile, studies comparing MCG with the pre-existing methods of ischemia assessment are needed to evaluate its future value in clinical practice.

## 8. CONCLUSIONS

Magnetocardiography and body surface potential mapping can detect exercise-induced myocardial ischemia caused by stenosis in any of the main coronary artery branches, regardless of the presence or absence of a remote myocardial infarction.

In CAD patients, exercise-induced myocardial ischemia induces a change in orientation of the cardiac magnetic field, a change quantifiable by use of the two-dimensional orientation of the maximum spatial field gradient.

In MCG and in BSPM, various ST-segment and T-wave parameters are sensitive and specific markers of exercise-induced myocardial ischemia. As expected, the optimal recording sites in BSPM to detect ischemia were in locations orthogonal to the ones in MCG.

In MCG and in BSPM, neither the ST amplitude nor the ST slope can localize the culprit coronary artery during exercise, possibly due to the suggested global nature of exercise-induced subendocardial ischemia. In BSPM, the ischemia-induced changes in T-wave amplitude and the ST-T integral area were demonstrated in different spatial areas of the chest surface for each patient subgroup with different ischemic regions in the heart.

During exercise testing, the ST-segment and T-wave ischemia indexes contain information on separate physiological stages of ischemia development and resolution. The detection of myocardial ischemia could thus be enhanced by analysis of the signals over the ST segment to the end of the T-wave and combination of the observations over different phases of the exercise test.

## 9. ACKNOWLEDGEMENTS

This study was carried out from 1996 to 2002 at the Cardiovascular Laboratory of the Division of Cardiology, Department of Medicine, and at the BioMag Laboratory of the Helsinki University Central Hospital. I am very grateful to Professor Markku S. Nieminen, M.D., Ph.D., Head of the Division of Cardiology, for placing its excellent research facilities at my disposal and for supporting me in my endeavors throughout the years. I wish to thank Professor Juhani Heikkilä, M.D., Ph.D., the former Head of the Cardiovascular Laboratory, and Docent Markku Kupari, M.D., Ph.D., the present Head, for their encouragement and interest in my study during these years.

I am indebted to Professor Toivo Katila, D.Sc. (Tech.), for providing me with excellent research facilities at the Laboratory of Biomedical Engineering at the Helsinki University of Technology. As the Head of the interdisciplinary graduate school "Functional Research in Medicine" he has provided continuous encouragement and support which have been important for me. I wish to express my warmest gratitude to Docent Risto Ilmoniemi, D.Sc. (Tech.), Head of the BioMag Laboratory, for the excellent research facilities in the BioMag Laboratory, and for his continuous encouragement and interest in my work.

I have had the great privilege to work under the firm guidance of a distinguished clinical electrophysiologist and scientist, Docent Lauri Toivonen, M.D., Ph.D., who taught me how to do scientific work. His enthusiastic guidance, never-ending patience, optimism, humor, support, and true interest toward my work have been invaluable during these years. I am especially grateful to him for always being there to give expert advice on my numerous scientific problems, often sacrificing his evenings and weekends. I wish to extend my deepest gratitude to my other supervisor, Docent Markku Mäkijärvi, M.D., Ph.D., for his encouragement and continuous positive attitude toward my work, for introducing me to numerous highly acknowledged scientists from all over the world, for diligently keeping together our interdisciplinary research group, and for teaching me the basic rules of scientific travel.

I express my warmest gratitude to Docent Kari Virtanen, M.D., Ph.D., for his sound support and his expert advice on nuclear cardiology.

I extend my gratitude to Docent Juhani Airaksinen, M.D., Ph.D., and Professor Hannu Eskola, D.Sc. (Tech.), the reviewers of this thesis, for their constructive criticism and valuable advice concerning the final manuscript. I am grateful to Carol Norris, Ph.D., for author-editing the language of this thesis.

I am sincerely grateful to Panu Takala, D.Sc. (Tech.), for constructing the custom-made non-magnetic exercise bicycle, for designing the computer software for the data analysis, and for numerous innovative and fruitful scientific discussions during all these

years. I am deeply indebted to him also for kindly and patiently introducing me to the world of computers.

The heart and the soul of the Laboratory of Biomedical Engineering, Jukka Nenonen, D.Sc. (Tech.), a brilliant scientist and an excellent team player, deserves my warmest gratitude for the pleasant co-operation during these years. I am deeply indebted to him not only for his strenuous efforts in creation of the analysis software and in modifying its features to fit my needs, but for his absolutely endless research ideas and optimism, and for bringing together our interdisciplinary research group.

I express my warmest thanks to Lasse Oikarinen, M.D., Ph.D., for his contribution to the sometimes exhausting patient measurements, and his expert advice in many practical and statistical problems I encountered. I wish to thank my fellow researcher Juha Rantonen, M.D., for his contribution to the patient studies.

Kim Simelius, Lic.Sc. (Tech.), and Tommi Jokiniemi, M.Sc. (Tech.), deserve my warmest gratitude for reconstructing the body surface mapping system, and for the 24-hour phone services during the patient measurements. I wish to thank my fellow medical researchers Ilkka Tierala, M.D., Petri Haapalahti, M.D., and Paula Vesterinen, M.D., for sharing the sun and rain of a researcher's life; and researchers Juha Montonen, D.Sc. (Tech.), Katja Pesola, D.Sc. (Tech.), Milla Karvonen, M.Sc. (Tech.), Mats Lindholm, M.Sc. (Tech.), Timo Mäkelä, Lic. Sc. (Tech.), and Heikki Väänänen, Lic.Sc. (Tech.), for teaching me facts about physics and sharing some good humor. I am grateful to Matti Stenroos, M.Sc. (Tech.), for helping me in the final preparation of the manuscript.

I am deeply indebted to the personnel of the Cardiovascular Laboratory and the BioMag Laboratory for their friendly help and support during this study. I wish to thank our research assistants Rea Katajisto, R.N., and Leila Sikanen, R.N., for patiently assisting me in the patient studies, Helena Siljander, R.N., for her friendly help with thallium imaging, and Leena Lajunen for the excellent library services.

I wish to express my warmest gratitude to the numerous coronary artery disease patients and healthy volunteers who participated in this study. Without their brave and positive attitude toward clinical research, this thesis would not exist. I am deeply indebted to all these people.

I wish to extend my warmest thanks to all my friends for sharing numerous good moments of laughter that allowed me to relax and temporarily forget about the work. I would especially like to thank Eeva, Jari, Kaisa, Kati, Marjo, and Taneli and their spouses, The Consensus, for the lovely Midsummer excursions and the traditional Christmas parties; and Eini, Kisu, Marja, Paula, and Päivi–The Levi's Ladies–for The Boogie Nights.

My parents, Helvi and Ilmari, deserve my warmest gratitude for their continuous love and support throughout my life. I am deeply indebted to my big brother Hannu for always being there for me.

Finally, I wish to express my heartfelt gratitude to my fellow researcher, dear husband, and best friend Petri, not only for his contribution to the patient measurements during the research, but for his own patience, understanding, and support throughout all this work, and for bringing happiness and meaning to my life every day. To him I dedicate this book.

This work was financially supported by the Finnish Foundation for Cardiovascular Research, the Aarne Koskelo Foundation, and the Finnish Medical Society Duodecim, which I gratefully acknowledge.

Helsinki, September 2002

A handwritten signature in black ink, consisting of a cursive name that appears to be 'Helena Hänninen'.

Helena Hänninen

## 10. REFERENCES

- Abildskov JA, Burgess MJ, Urie PM, Lux RL, Wyatt RF. The unidentified information content of the electrocardiogram. *Circ Res* 1977; 40: 3-7.
- Antzelevitch C, Shimizu W, Yan G-X, Sicouri S, Weissenburger J, Nesterenko VV, Burasnikov A, Di Diego J, Saffitz J, Thomas GP. The M Cell: its contribution to the ECG and to normal and abnormal electrical function of the heart. *J Cardiovasc Electrophysiol* 1999; 10: 1124-1152.
- Applegate RJ, Walsh RA, O'Rourke RA. Comparative effects of pacing-induced and flow-limited ischemia on left ventricular function. *Circulation* 1990; 81: 1380-1392.
- Aravindakshan V, Surawicz B, Allen RD. Electrocardiographic exercise test in patients with abnormal T-waves at rest. *Am Heart J* 1977; 93: 706-714.
- Arnold AER, Simoons ML, Detry JMR, von Essen R, Van de Werf F, Deckers JW, Lubsen J, Verstraete M. Prediction of mortality following hospital discharge after thrombolysis for acute myocardial infarction: is there a need for coronary angiography? *Eur Heart J* 1993; 14: 306-315.
- Baule G, McFee R. Detection of the magnetic field of the heart. *Am Heart J* 1963; 95-96.
- Barr RC. Genesis of the electrocardiogram. In: Macfarlane PW, Lawrie TDV, eds. *Comprehensive Electrocardiology Volume I*. Pergamon Press, Oxford 1989: 129-151.
- Beller GA, Zaret BL. Contributions of nuclear cardiology to diagnosis and prognosis of patients with coronary artery disease. *Circulation* 2000; 101: 1465-1478.
- Blackburn H, Katigbak R. What electrocardiographic leads to take after exercise? *Am Heart J* 1963; 67: 184-188.
- Bosimini E, Galli M, Guagliumi G, Giubbini R, Tavazzi L. Electrocardiographic markers of ischemia during mental stress testing in postinfarction patients. Role of body surface mapping. *Circulation* 1991; 83[suppl II]:II-115-II-127.
- Boudik F, Anger Z, Aschermann M, Vojáčěk J, Tomečková M. Dipyridamole body surface potential mapping: noninvasive differentiation of syndrome X from coronary artery disease. *J Electrocardiol* 2002; 35: 181-191.
- Braat SH, Kingma JH, Brugada P, Wellens HJJ. Value of lead V<sub>4</sub>R in exercise testing to predict the proximal stenosis of the right coronary artery. *J Am Coll Cardiol* 1985; 5: 1308-1311.
- Brockmeier K, Comani S, Erne SN, Di Luzio S, Pasquarelli A, Romani GL. Magnetocardiography and exercise testing. *J Electrocardiol* 1994; 27: 137-142.

- Brockmeier K, Schmitz L, Chavez JJB, Burghoff M, Koch H, Zimmermann R, Trahms L. Magnetocardiography and 32-lead potential mapping: repolarization in normal subjects during pharmacologically induced stress. *J Cardiovasc Electrophysiol* 1997; 8: 615-626.
- Bruce RA. Exercise testing of patients with coronary heart disease. Principles and normal standards for evaluation. *Ann Clin Res* 1971; 3: 323-332.
- Bruce RA. Methods of exercise testing. Step test, bicycle, treadmill, isometrics. *Am J Cardiol* 1974; 33: 715-720.
- Bruce RA. Exercise testing for evaluation of ventricular function. *N Engl J Med* 1977; 296: 671-675.
- Bruce RA, Fisher LD, Pettinger M, Weiner DA, Chaitman BR. ST segment elevation with exercise: a marker for poor ventricular function and poor prognosis. Coronary Artery Surgery Study (CASS) confirmation of Seattle Heart Watch results. *Circulation* 1988; 77: 897-905.
- Brunken R, Schwaiger M, Grover-McKay M, Phelps ME, Tillisch J, Schelbert HR. Positron emission tomography detects tissue metabolic activity in myocardial segments with persistent thallium perfusion defects. *J Am Coll Cardiol* 1987; 10: 557-567.
- Burgess MJ, Green LS, Millar K, Wyatt R, Abildskov JA. The sequence of normal ventricular recovery. *Am Heart J* 1972; 84: 660-669.
- Burghoff M, Nenonen J, Trahms L, Katila T. Conversion of magnetocardiographic recordings between two different multichannel SQUID devices. *IEEE Trans Biomed Eng* 2000; 47: 869-875.
- Chaitman BR, Bourassa MG, Wagniar P, Corbara F, Ferguson RJ. Improved efficiency of treadmill exercise testing using a multiple lead ECG system and basic hemodynamic exercise response. *Circulation* 1978; 57: 71-79.
- Chaitman BR. The changing role of the exercise electrocardiogram as a diagnostic and prognostic test for chronic ischemic heart disease. *J Am Coll Cardiol* 1986; 8: 1195-1210.
- Chaitman BR, McMahon RP, Terrin M, Younis LT, Shaw LJ, Weiner DA, Frederick MM, Knatterud GL, Sopko G, Braunwald E. Impact of treatment strategy on pre-discharge exercise test in the thrombolysis in myocardial infarction (TIMI) II trial. *Am J Cardiol* 1993; 71: 131-138.
- Chaitman BR. Exercise testing. In: Braunwald E, ed. *Heart Disease. A textbook of cardiovascular medicine*. Philadelphia: W.B. Saunders Company, 1997: 153-176.
- Chouhan L, Krone RJ, Keller A, Eisenkramer G. Utility of lead V<sub>4</sub>R in exercise testing for detection of coronary artery disease. *Am J Cardiol* 1989; 64: 938-939.

- Cohen D. Magnetic fields around the torso: production by electrical activity of the human heart. *Science* 1967; 156: 652-654.
- Cohen D, Edelsack EA, Zimmerman JE. Magnetocardiograms taken inside a shielded room with superconducting point-contact magnetometer. *Appl Phys Lett* 1970; 16: 278-280.
- Cohen D, Norman JC, Molokhia F, Hood W Jr. Magnetocardiography of direct currents: S-T segment and baseline shifts during experimental myocardial infarction. *Science* 1971; 172: 1329-1333.
- Cohen D, McCaughan D. Magnetocardiograms and their variation over the chest in normal subjects. *Am J Cardiol* 1972; 29: 678-685.
- Cohen D, Kaufman LA. Magnetic determination of the relationship between the S-T segment shift and the injury current produced by coronary artery occlusion. *Circ Res* 1975; 36: 414-424.
- Cohen D, Lepeschkin E, Hosaka H, Massell BF, Myers G. Part I. Abnormal patterns and physiological variations in magnetocardiograms. *J Electrocardiol* 1976; 9: 398-409.
- Cohen D, Hosaka H. Magnetic field produced by a current dipole. *J Electrocardiol* 1976; 9: 409-417.
- Cohen D, Savard P, Rifkin RD, Lepeschkin E, Strauss WE. Magnetic measurement of S-T and T-Q segment shifts in humans. Part II: exercise-induced S-T segment depression. *Circ Res* 1983; 53: 274-279.
- Cole CR, Blackstone EH, Pashkow FJ, Snader CE, Lauer MS. Heart-rate recovery immediately after exercise as a predictor of mortality. *N Engl J Med* 1999; 341: 1351-1357.
- Cowan JC, Hiltón CJ, Griffiths CJ, Tansuphaswadikul S, Bourke JP, Murray A, Campbell RWF. Sequence of epicardial repolarization and configuration of the T wave. *Br Heart J* 1988; 60: 424-433.
- Currie PJ, Kelly MJ, Pitt A. Comparison of supine and erect bicycle exercise electrocardiography in coronary heart disease: accentuation of exercise-induced ischemic ST depression by supine posture. *Am J Cardiol* 1983; 52: 1167-1173.
- Dagenais GR, Rouleau JR, Christen A, Fabia J. Survival of patients with a strongly positive exercise electrocardiogram. *Circulation* 1982; 65: 452-456.
- Desai MY, De la Peña-Almaguer E, Mannting F. Abnormal heart rate recovery after exercise as a reflection of an abnormal chronotropic response. *Am J Cardiol* 2001; 87: 1164-1169.

- Detrano R, Gianrossi R, Mulvihill D, Lehmann K, Dubach P, Colombo A, Froelicher V. Exercise-induced ST segment depression in the diagnosis of multivessel coronary artery disease: a meta analysis. *J Am Coll Cardiol* 1989; 14: 1501-1508.
- Diamond GA. Reverend Bayes' silent majority: an alternative factor affecting sensitivity and specificity of exercise electrocardiography. *Am J Cardiol* 1986; 57: 1175-1180.
- Downar E, Janse MJ, Durrer D. The effect of acute coronary artery occlusion on subepicardial transmembrane potentials in the intact porcine heart. *Circulation* 1977; 56: 217-224.
- Dubuc M, Nadeau R, Tremblay G, Kus T, Molin F, Savard P. Pace mapping using body surface potential maps to guide catheter ablation of accessory pathways in patients with Wolff-Parkinson-White syndrome. *Circulation* 1993; 87: 135-143.
- Dunn RF, Freedman B, Bailey IK, Uren RF, Kelly DT. Localization of coronary artery disease with exercise electrocardiography: correlation with thallium-201 myocardial perfusion scanning. *Am J Cardiol* 1981; 48: 837-843.
- Ellestad MH, Wan MKC. Predictive implications of stress testing. Follow-up of 2700 subjects after maximum treadmill stress testing. *Circulation* 1975; 51: 363-369.
- Elamin MS, Boyle R, Kardash MM, Smith DR, Stoker JB, Whitaker W, Mary DASG, Linden RJ. Accurate detection of coronary heart disease by new exercise test. *Br Heart J* 1982; 48: 311-320.
- Epstein SE, Robinson BF, Kahler RL, Braunwald E. Effects of beta-adrenergic blockade on the cardiac response to maximal and submaximal exercise in man. *J Clin Invest* 1965; 44: 1745-1753.
- Epstein SE, Beiser GD, Stampfer M, Braunwald E. Exercise in patients with heart disease. Effects of body position and type and intensity of exercise. *Am J Cardiol* 1969; 23: 572-576.
- Farr BR, Vondenbusch B, Silny J, Rau G, Effert S. Localization of significant coronary arterial narrowing using body surface potential mapping during exercise stress testing. *Am J Cardiol* 1987; 59: 528-530.
- Fletcher G, Flipse T, Kligfield P, Malouf J. Current status of ECG stress testing. *Curr Probl Cardiol* 1998; 23: 353-428.
- Fletcher GF, Balady GJ, Amsterdam EA, Chaitman B, Eckel R, Fleg J, Froelicher VF, Leon AS, Piña IL, Rodney R, Simons-Morton DA, Williams MA, Bazzarre T. Exercise standards for testing and training: a statement for healthcare professionals from the American Heart Association. *Circulation* 2001; 104: 1694-1740.

- Flowers NC, Horan LG, Johnson JC. Anterior infarctional changes occurring during mid and late ventricular activation detectable by surface mapping techniques. *Circulation* 1976; 54: 906-913.
- Flowers NC, Horan LG. Body surface potential mapping. In: In: Zipes DP, Jalife J, eds. *Cardiac Electrophysiology: from cell to bedside*. 2<sup>nd</sup> edition, W. B. Saunders Company, Philadelphia 1995: 1049-1067.
- Fox K, Selwyn A, Shillingford J. Precordial exercise mapping: improved diagnosis of coronary artery disease. *Br Med J* 1978a; 2: 1596-1598.
- Fox KM, Selwyn AP, Shillingford JP. A method for praecordial surface mapping of the exercise electrocardiogram. *Br Heart J* 1978b; 40: 1339-1343.
- Fox KM, Selwyn A, Shillingford JP. Precordial electrocardiographic mapping after exercise in the diagnosis of coronary artery disease. *Am J Cardiol* 1979a; 43: 541-546.
- Fox KM, Selwyn A, Oakley D, Shillingford JP. Relation between the precordial projection of the S-T segment changes after exercise and coronary angiographic findings. *Am J Cardiol* 1979b; 44: 1068-1075.
- Fozzard HA, Makielski JC. The electrophysiology of acute myocardial ischemia. *Ann Rev Med* 1985; 36: 275-284.
- Franz MR, Bargheer K, Rafflenbeul W, Haverich A, Lichtlen PR. Monophasic action potential mapping in human subjects with normal electrocardiograms: direct evidence for the genesis of the T wave. *Circulation* 1987; 75: 379-386.
- Franz MR, Bargheer K, Costard-Jäckle A, Miller CD, Lichtlen PR. Human ventricular repolarization and T wave genesis. *Progr Cardiovasc Dis* 1991; 33: 369-384.
- Froelicher ES. Usefulness of exercise testing shortly after acute myocardial infarction for predicting 10-year mortality. *Am J Cardiol* 1994; 74: 318-323.
- Fuchs RM, Achuff SC, Grunwald L, Yin FCP, Griffith LSC. Electrocardiographic localization of coronary artery narrowing: studies during myocardial ischemia and infarction in patients with one-vessel disease. *Circulation* 1982; 66: 1168-1176.
- Fujino K, Sumi M, Saito K, Murakami M, Higuchi T, Nakaya Y, Mori H. Magnetocardiograms of patients with left ventricular overloading recorded with a second-derivative SQUID gradiometer. *J Electrocardiol* 1984; 17: 219-228.
- Fuller MS, Dustman TJ, Sharp S, Green LS, Lux R. Optimal lead selection for detection of ST segment shifts. *Pacing Clin Electrophysiol* 1996; 19: 920-928.
- Gamble P, McManus H, Jensen D, Froelicher V. A comparison of the standard 12-lead electrocardiogram to exercise electrode placements. *Chest* 1984; 85: 616-622.

- Gianelly RE, Treister BL, Harrison DC. The effect of propranolol on exercise-induced ischemic S-T segment depression. *Am J Cardiol* 1969; 24: 161-165.
- Gianrossi R, Detrano R, Mulvihill D, Lehmann K, Dubach P, Colombo A, McArthur D, Froelicher V. Exercise-induced ST depression in the diagnosis of coronary artery disease: a meta-analysis. *Circulation* 1989; 80: 87-98.
- Goraya TY, Jacobsen SJ, Pellikka PA, Miller TD, Khan A, Weston SA, Gersh BJ, Roger VL. Prognostic value of treadmill exercise testing in elderly persons. *Ann Intern Med* 2000; 132: 862-870.
- Gorgels APM, Vos MA, Mulleneers R, de Zwaan C, Bär FWHM, Wellens HJJ. Value of the electrocardiogram in diagnosing the number of severely narrowed coronary arteries in rest angina pectoris. *Am J Cardiol* 1993; 72: 999-1003.
- Green LS, Lux RL, Stilli D, Haws CW, Taccardi B. Fine detail in body surface potential maps: accuracy of maps using a limited lead array and spatial and temporal data representation. *J Electrocardiol* 1987a; 20: 21-26.
- Green LS, Lux RL, Haws CW. Detection and localization of coronary artery disease with body surface mapping in patients with normal electrocardiograms. *Circulation* 1987b; 76: 1290-1297.
- Hailer B, Van Leeuwen P, Lange S, Wehr M. Spatial distribution of QT dispersion measured by magnetocardiography under stress in coronary artery disease. *J Electrocardiol* 1999; 32: 207-216.
- Hanley JA, McNeil BJ. The meaning and use of the area under a receiver operating characteristic (ROC) curve. *Radiology* 1982; 143: 29-36.
- Hanley JA, McNeil BJ. A method of comparing the areas under receiver operating characteristic curves derived from the same cases. *Radiology* 1983; 148: 839-843.
- Hecht HS, DeBord L, Sotomayor N, Shaw R, Ryan C. Truly silent ischemia and the relationship of chest pain and ST segment changes to the amount of ischemic myocardium: evaluation by supine bicycle stress echocardiography. *J Am Coll Cardiol* 1994; 23: 369-376.
- Hoffman I. Clinical vectorcardiography in adults. Part I. *Am Heart J* 1980; 100: 239-254.
- Holland RP, Arnsdorf MF. Solid angle theory and the electrocardiogram: physiologic and quantitative interpretations. *Progr Cardiovasc Dis* 1977; 19: 431-457.
- Holland RP, Brooks H. TQ-ST segment mapping: critical review and analysis of current concepts. *Am J Cardiol* 1977; 40: 110-129.

- Holt JH Jr, Barnard ACL, Kramer JO Jr. Multiple dipole electrocardiography. A comparison of electrically and angiographically determined left ventricular masses. *Circulation* 1978; 57: 1129-1133.
- Horan LG, Sridharan MR, Killam HAW, Flowers NC. Patterns of body surface potential and ventriculograms specific to occlusion of subdivisions of the coronary arteries. *Circ Res* 1990; 67: 683-693.
- Horáček BM, Warren JW, Penney CJ, MacLeod RS, Title LM, Gardner MJ, Feldman CL. Optimal electrocardiographic leads for detecting acute myocardial ischemia. *J Electrocardiol* 2001; 34(suppl): 97-111.
- Horáček BM, Wagner GS. Electrocardiographic ST-segment changes during acute myocardial ischemia. *Card Electrophysiol Rev* 2002; 6: 196-203.
- Hosoya Y, Ikeda K, Yamaki M, Tsuiki K, Yasui S. The clinical significance of exercise-induced ST segment changes in patients with previous myocardial infarction. *Am Heart J* 1990; 120: 554-561.
- Ikeda K, Kawashima S, Kubota I, Igarashi A, Yamaki M, Yasumura S, Tsuiki K, Yasui S. Non-invasive detection of coronary artery disease by body surface electrocardiographic mapping after dipyridamole infusion. *J Electrocardiol* 1986; 19: 213-224.
- Ishikawa T, Watabe S, Yamada Y, Miyachi K, Sakai Y, Ito A, Sotobata I. New diagnostic evidence on the T wave map indicating involved coronary artery in patients with angina pectoris. *Circulation* 1988; 77: 301-310.
- Janse MJ, Wit AL. Electrophysiological mechanisms of ventricular arrhythmias resulting from myocardial ischemia and infarction. Electrophysiological effects of acute myocardial ischemia. *Physiol Rev* 1989; 69: 1058-1076.
- Janse MJ, Opthof T. Mechanisms of ischemia-induced arrhythmias. In: Zipes DP, Jalife J, eds. *Cardiac Electrophysiology: from cell to bedside*. 2<sup>nd</sup> edition, W. B. Saunders Company, Philadelphia 1995: 490-496.
- Kandori A, Kanzaki H, Miyatake K, Hashimoto S, Itoh S, Tanaka N, Miyashita T, Tsukada K. A method for detecting myocardial abnormality by using a total current-vector calculated from ST-segment deviation of a magnetocardiogram signal. *Med Biol Eng Comput* 2001a; 39: 21-28.
- Kandori A, Kanzaki H, Miyatake K, Hashimoto S, Itoh S, Tanaka N, Miyashita T, Tsukada K. A method for detecting myocardial abnormality by using a current-ratio map calculated from an exercise-induced magnetocardiogram. *Med Biol Eng Comput* 2001b; 39: 29-34.

- Karvonen M, Oikarinen L, Takala P, Kaartinen M, Rossinen J, Hänninen H, Montonen J, Nenonen J, Mäkijärvi M, Keto P, Toivonen L, Nieminen MS, Katila T. Magnetocardiographic indices of left ventricular hypertrophy. *J Hypertension*, in press.
- Katz AM. The ischemic heart. *Physiology of the heart*, second edition. Raven Press, New York 1992: 609-668.
- Kittnar O, Slavíček J, Vávrová M, Barna M, Dohnalová A, Málková A, Aschermann M, Humhal J, Hradec J, Kral J. Repolarization pattern of body surface potential maps (BSPM) in coronary artery disease. *Physiol Res* 1993; 42: 123-130.
- Kléber AG, Janse MJ, van Chapelle FJL, Durrer D. Mechanism and time course of S-T and T-Q segment changes during acute regional myocardial ischemia in the pig heart determined by extracellular and intracellular recordings. *Circ Res* 1978; 42: 603-613.
- Kléber AG, Fleischhauer J, Cascio WE. Ischemia-induced propagation failure in the heart. In: Zipes DP, Jalife J, eds. *Cardiac Electrophysiology: From cell to bedside*. 2<sup>nd</sup> edition, W.B. Saunders Company, Philadelphia 1995: 175-182.
- Kleiner JP, Nelson WP, Boland MJ. The 12-lead electrocardiogram in exercise testing. A misleading baseline? *Arch Intern Med* 1978; 138: 1572-1573.
- Kligfield P, Okin PM, Goldberg HL. Value and limitations of heart rate-adjusted ST segment depression criteria for the identification of anatomically severe coronary obstruction: test performance in relation to method of rate correction, definition of extent of disease, and  $\beta$ -blockade. *Am Heart J* 1993; 125: 1262-1268.
- Korhonen P, Montonen J, Mäkijärvi M, Katila T, Nieminen MS, Toivonen L. Late fields of the magnetocardiographic QRS complex as indicators of propensity to sustained ventricular tachycardia after myocardial infarction. *J Cardiovasc Electrophysiol* 2000; 11: 413-420.
- Korhonen P, Montonen J, Endt P, Mäkijärvi M, Trahms L, Katila T, Toivonen L. Magnetocardiographic intra-QRS fragmentation analysis in the identification of patients with sustained ventricular tachycardia after myocardial infarction. *Pacing Clin Electrophysiol* 2001; 24: 1179-1186.
- Kornreich F, Montague TJ, Rautaharju PM. Identification of first acute Q wave and non-Q wave myocardial infarction by multivariate analysis of body surface potential maps. *Circulation* 1991; 84: 2442-2453.
- Kornreich F, Montague TJ, Rautaharju PM. Body surface potential mapping of ST segment changes in acute myocardial infarction. Implications for ECG enrollment criteria for thrombolytic therapy. *Circulation* 1993; 87: 773-782.

- Kubota I, Ikeda K, Ohyama T, Yamaki M, Kawashima S, Igarashi A, Tsuiki K, Yasui S. Body surface distributions of ST segment changes after exercise in effort angina pectoris without myocardial infarction. *Am Heart J* 1985; 110: 949-955.
- Kubota I, Hanashima K, Ikeda K, Tsuiki K, Yasui S. Detection of diseased coronary artery by exercise ST-T maps in patients with effort angina pectoris, single-vessel disease, and normal ST-T wave on electrocardiogram at rest. *Circulation* 1989; 80: 120-127.
- Lachterman B, Lehmann KG, Abrahamson D, Froelicher VF. "Recovery only" ST-segment depression and the predictive accuracy of the exercise test. *Ann Intern Med* 1990; 112: 11-16.
- Lant J, Stroink G, ten Voorde B, Horáček BM, Montague TJ. Complementary nature of electrocardiographic and magnetocardiographic data in patients with ischemic heart disease. *J Electrocardiol* 1990; 23: 315-322.
- Laukkanen JA, Kurl S, Lakka TA, Tuomainen T-P, Rauramaa R, Salonen R, Eränen J, Salonen JT. Exercise-induced silent myocardial ischemia and coronary morbidity and mortality in middle-aged men. *J Am Coll Cardiol* 2001a; 38: 72-79.
- Laukkanen JA, Lakka TA, Rauramaa R, Kuhanen R, Venäläinen JM, Salonen R, Salonen JT. Cardiovascular fitness as a predictor of mortality in men. *Arch Intern Med* 2001b; 161: 825-831.
- Leder U, Hauelsen J, Huck M, Nowak H. Non-invasive imaging of arrhythmogenic left ventricular myocardium after infarction. *Lancet* 1998a; 352: 1825.
- Leder U, Pohl HP, Michaelsen S, Fritschi T, Huck M, Eichhorn J, Müller S, Nowak H. Noninvasive biomagnetic imaging in coronary artery disease based on individual current density maps of the heart. *Int J Cardiol* 1998b; 64: 83-92.
- Lee TH, Boucher CA. Noninvasive tests in patients with stable coronary artery disease. *New Engl J Med* 2001; 344: 1840-1845.
- Lehtinen R, Sievänen H, Viik J, Turjanmaa V, Niemelä K, Malmivuo J. Accurate detection of coronary artery disease by integrated analysis of the ST-segment depression/heart rate patterns during the exercise and recovery phases of the exercise electrocardiography test. *Am J Cardiol* 1996; 78: 1002-1006.
- Lukas A, Antzelevitch C. Differences in the electrophysiological response of canine ventricular epicardium and endocardium to ischemia: role of the transient outward current. *Circulation* 1993; 88: 2903-2915.
- Lux RL, Burgess MJ, Wyatt RF, Evans AK, Vincent GM, Abildskov JA. Clinically practical lead systems for improved electrocardiography: comparison with precordial grids and conventional lead systems. *Circulation* 1979; 59: 356-363.

- Lux RL. Mapping techniques. In: Macfarlane PW, Lawrie TDV, eds. *Comprehensive Electrocardiology Volume II*. Pergamon Press, Oxford 1989: 1001-1014.
- Lux RL, MacLeod RS, Fuller M, Green LS, Kornreich F. Estimating ECG distributions from small number of leads. *J Electrocardiol* 1995; 28(suppl): 92-97.
- MacDougall JD. Blood pressure responses to resistive static and dynamic exercise. In: Fletcher GF, ed. *Cardiovascular Response to Exercise*. Futura Publishing Co, Mount Kisco, NY 1994: 155-173.
- Macfarlane PW. Lead systems. In: Macfarlane PW, Lawrie TDV, eds. *Comprehensive Electrocardiology Volume I*. Pergamon Press, Oxford 1989: 315-352.
- MacLeod RS, Gardner M, Miller RM, Horáček BM. Application of an electrocardiographic inverse solution to localize ischemia during coronary angioplasty. *J Cardiovasc Electrophysiol* 1995; 6: 2-18.
- MacLeod RS, Lux RL, Taccardi B. A possible mechanism for electrocardiographically silent changes in cardiac repolarization. *J Electrocardiol* 1998; 30(suppl): 114-121.
- Mark DB, Hlatky MA, Lee KL, Harrell FE, Califf RM, Pryor DB. Localizing coronary artery obstructions with the exercise treadmill test. *Ann Intern Med* 1987a; 106: 53-55.
- Mark DB, Hlatky MA, Harrell FE, Lee KL, Califf RM, Pryor DB. Exercise treadmill score for predicting prognosis in coronary artery disease. *Ann Intern Med* 1987b; 106: 793-800.
- Mark DB, Shaw L, Harrell FE Jr, Hlatky MA, Lee KL, Bengtson JR, McCants CB, Califf RM, Pryor DB. Prognostic value of a treadmill exercise score in outpatients with suspected coronary artery disease. *N Eng J Med* 1991; 325: 849-853.
- Marcovitz PA. Prognostic issues in stress echocardiography. *Prog Cardiovasc Dis* 1997; 39: 533-542.
- Mason RE, Likar I. A new system of multiple-lead exercise electrocardiography. *Am Heart J* 1966; 71: 196-205.
- Mason RE, Likar I, Biern RO, Ross RS. Multiple-lead exercise electrocardiography. Experience in 107 normal subjects and in 67 patients with angina pectoris, and comparison with coronary cinearteriography in 84 patients. *Circulation* 1967; 36: 517-525.
- McGregor M, Adam W, Sekelj P. Influence of posture on cardiac output and minute ventilation during exercise. *Circ Res* 1961; 9: 1089-1092.
- Medvegy M, Préda I, Savard P, Pintér A, Tremblay G, Nasmith JB, Palisaitis D, Nadeau RA. New body surface isopotential map evaluation method to detect minor potential losses in non-Q-wave myocardial infarction. *Circulation* 2000; 101: 1115-1121.

- Menéndez T, Achenbach S, Hofbeck M, Beinder E, Schmid O, Moshage W, Singer H, Daniel WG. Prenatal diagnosis of QT prolongation by magnetocardiography. *Pacing Clin Electrophysiol* 2000; 23: 1305-1307.
- Menéndez T, Achenbach S, Beinder E, Hofbeck M, Klinghammer L, Singer H, Moshage W, Daniel WG. Usefulness of magnetocardiography for the investigation of fetal arrhythmias. *Am J Cardiol* 2001; 88: 334-336.
- Menown IBA, Allen J, Anderson J, Adgey AAJ. Early diagnosis of right ventricular or posterior infarction associated with inferior wall left ventricular acute myocardial infarction. *Am J Cardiol* 2000a; 85: 934-938.
- Menown IBA, Allen J, Anderson J, Adgey AAJ. Noninvasive assessment of reperfusion after fibrinolytic therapy for acute myocardial infarction. *Am J Cardiol* 2000b; 86: 736-741.
- Menown IBA, Allen J, Anderson J, Adgey AAJ. ST depression only on the initial 12-lead ECG: early diagnosis of acute myocardial infarction. *Eur Heart J* 2001; 22: 218-227.
- Michaelides AP, Psodamaki ZD, Dilaveris PE, Richter DJ, Andrikopoulos GK, Aggeli KD, Stefanidis CI, Toutouzas PK. Improved detection of coronary artery disease by exercise electrocardiography with the use of right precordial leads. *N Engl J Med* 1999; 340: 340-345.
- Mickley H, Pless P, Nielsen JR, Berning J, Møller M. Transient myocardial ischemia after a first acute myocardial infarction and its relation to clinical characteristics, predischARGE exercise testing and cardiac events at one-year follow-up. *Am J Cardiol* 1993; 71: 139-144.
- Mirvis DM, Keller FW, Cox JW, Zettergren DG, Dowdie RF, Ideker RE. Left precordial isopotential mapping during supine exercise. *Circulation* 1977; 56: 245-252.
- Mirvis DM. Body surface distributions of repolarization forces during acute myocardial infarction. I. Isopotential and isoarea mapping. *Circulation* 1980; 62: 878-887.
- Mirvis DM, Ramanathan KB, Wilson JL. Regional blood flow correlates of ST segment depression in tachycardia-induced myocardial ischemia. *Circulation* 1986; 73: 365-373.
- Mirvis DM. Current status of body surface electrocardiographic mapping. *Circulation* 1987; 75: 684-688.
- Mirvis DM, El-Zeky F, Vander Zwaag R, Ramanathan KB, Crenshaw JH, Kroetz FW, Sullivan JM. Clinical and pathophysiologic correlates of ST-T-wave abnormalities in coronary artery disease. *Am J Cardiol* 1990; 66: 699-704.
- Miyakoda H, Kinugawa T, Ogino K, Mori M, Endo A, Kato M, Kato T, Osaki S, Hisatome I, Shigemasa C. QRST integral analysis of body surface electrocardiographic mapping for assessing exercise-induced changes in the spatial distribution of local repolarization

- properties in patients with coronary artery disease and in patients with previous anterior infarction. *J Electrocardiol* 1999; 32: 123-136.
- Montague TJ, Johnstone DE, Spencer CA, Lalonde LD, Gardner MJ, O'Reilly MG, Horáček BM. Non-Q-wave acute myocardial infarction: body surface potential map and ventriculographic patterns. *Am J Cardiol* 1986; 58: 1173-1180.
- Montague TJ, Johnstone DE, Spencer CA, Miller RM, MacKenzie BR, Gardner MJ, Horáček BM. Body surface potential maps with low-level exercise in isolated left anterior descending coronary artery disease. *Am J Cardiol* 1988; 61: 273-282.
- Montague TJ, Witkowski FX. The clinical utility of body surface potential mapping in coronary artery disease. *Am J Cardiol* 1989; 64: 378-383.
- Montague TJ, Witkowski FX, Miller RM, Johnstone DE, MacKenzie RB, Spencer CA, Horáček BM. Exercise body surface potential mapping in single and multiple coronary artery disease. *Chest* 1990; 97: 1333-1342.
- Moshage W, Achenbach S, Göhl K, Bachmann K. Evaluation of the non-invasive localization accuracy of the cardiac arrhythmias attainable by multichannel magnetocardiography (MCG). *Int J Cardiac Imaging* 1996; 12: 47-59.
- Moss AJ, Goldstein RE, Hall WJ, Bigger JT, Fleiss JL, Greenberg H, Bodenheimer M, Krone RJ, Marcus FI, Wackers FJTh, Benhorin J, Brown MW, Case R, Coromilas J, Dwyer EM, Gillespie JA, Gregory JJ, Kleiger R, Lichstein E, Parker JO, Raubertas RF, Stern S, Tzivoni D, Van Voorhees L. Detection and significance of myocardial ischemia in stable patients after recovery from an acute coronary event. *JAMA* 1993; 269: 2379-2385.
- Murayama M, Kawakubo K, Nakajima T, Sakamoto S, Ono S, Itai T, Kato N. Different recovery process of ST depression on postexercise electrocardiograms in women in standing and supine positions. *Am J Cardiol* 1985; 55: 1474-1477.
- Myers J, Prakash M, Froelicher V, Do D, Partington S, Atwood JE. Exercise capacity and mortality among men referred for exercise testing. *New Engl J Med* 2002; 346: 793-801.
- Mäkijärvi M, Nenonen J, Toivonen L, Montonen J, Leiniö M, Nieminen MS, Siltanen P, Katila T. Localization of accessory pathways in Wolff-Parkinson-White syndrome by high-resolution magnetocardiographic mapping. *J Electrocardiol* 1992; 25: 143-155.
- Mäkijärvi M, Montonen J, Toivonen L, Siltanen P, Nieminen MS, Leiniö M, Katila T. Identification of patients with ventricular tachycardia after myocardial infarction by high-resolution magnetocardiography and electrocardiography. *J Electrocardiol* 1993; 26: 117-124.

- Nakajima T, Kawakubo K, Toda I, Mashima S, Ohtake T, Iio M, Sugimoto T. ST-T isointegral analysis of exercise stress body surface mapping for identifying ischemic areas in patients with angina pectoris. *Am Heart J* 1988; 115: 1013-1021.
- Nenonen JT. Solving the inverse problem in magnetocardiography. *IEEE Eng Med Biol* 1994; 13: 487-496.
- Nenonen J. Magnetocardiography. In: Braginski A, Clarke J, eds. *SQUID handbook*. Wiley-VCH Verlag, Berlin 2002a.
- Nenonen J, Montonen J, Mäkijärvi M. Principles of magnetocardiographic mapping. In: Shenasa M, Borggreffe M, Breithardt G, eds. *Futura Publishing Co, Mount Kisco, NY* 2002b.
- Nishime EO, Cole CR, Blackstone EH, Pashkow FJ, Lauer MS. Heart rate recovery and treadmill exercise score as predictors of mortality in patients referred for exercise ECG. *JAMA* 2000; 284: 1392-1398.
- O'Donnell J, Lovelace DE, Knoebel SB, McHenry PL. Behavior of the terminal T-wave during exercise in normal subjects, patients with symptomatic coronary artery disease and apparently healthy subjects with abnormal ST segment depression. *J Am Coll Cardiol* 1985; 5: 78-84.
- Oeff M, Burghoff M. Magnetocardiographic localization of the origin of ventricular ectopic beats. *Pacing Clin Electrophysiol* 1994; 17: 517-522.
- Oikarinen L, Viitasalo M, Korhonen P, Väänänen H, Hänninen H, Montonen J, Mäkijärvi M, Katila T, Toivonen L. Postmyocardial infarction patients susceptible to ventricular tachycardia show increased T wave dispersion independent of delayed ventricular conduction. *J Cardiovasc Electrophysiol* 2001; 12: 1115-1120.
- Okin PM, Anderson KM, Levy D, Kligfield P. Heart rate adjustment of exercise-induced ST segment depression. Improved risk stratification in the Framingham Offspring Study. *Circulation* 1991; 83: 866-874.
- Okin PM, Kligfield P. Heart rate adjustment of ST segment depression and performance of the exercise electrocardiogram: a critical evaluation. *J Am Coll Cardiol* 1995; 25: 1726-1735.
- Okin PM, Grandits G, Rautaharju PM, Prineas RJ, Cohen JD, Crow RS, Kligfield P. Prognostic value of heart rate adjustment of exercise-induced ST segment depression in the multiple risk factor intervention trial. *J Am Coll Cardiol* 1996; 27: 1437-1443.
- Opie L. Mechanisms of cardiac contraction and relaxation. Effects of ischemia and reperfusion on contraction and relaxation. In: Braunwald E, ed. *Heart Disease. A textbook of cardiovascular medicine*. W.B. Saunders Company, Philadelphia 1997: 386-389.

- Pesola K, Nenonen J, Fenici R, Lötjönen J, Mäkijärvi M, Fenici P, Korhonen P, Lauerma K, Valkonen M, Toivonen L, Katila T. Bioelectromagnetic localization of a pacing catheter in the heart. *Phys Med Biol* 1999a; 44: 2565-2578.
- Pesola K, Hänninen H, Lauerma K, Lötjönen J, Mäkijärvi M, Nenonen J, Takala P, Voipio-Pulkki L-M, Toivonen L, Katila T. Current density estimation on the left ventricular epicardium: a potential method for ischemia localization. *Biomed Tech (Berl)* 1999b; 44(suppl.2): 143-146.
- Pilote L, Silberberg J, Lisbona R, Sniderman A. Prognosis in patients with low left ventricular ejection fraction after myocardial infarction. Importance of exercise capacity. *Circulation* 1989; 80: 1636-1641.
- Plonsey R. Comparative capabilities of electrocardiography and magnetocardiography. *Am J Cardiol* 1972; 29: 735-736.
- Quyyumi AA, Crake T, Mockus LJ, Wright CA, Rickards AF, Fox KM. Value of the bipolar lead CM5 in electrocardiography. *Br Heart J* 1986; 56: 372-376.
- Rautaharju PM, Prineas RJ, Crow RS, Seale D, Furberg C. The effect of modified limb electrode positions on electrocardiographic wave amplitudes. *J Electrocardiol* 1980; 13: 109-114.
- Rautaharju PM, Prineas RJ, Eifler WJ, Furberg CD, Neaton JD, Crow RS, Stamler J, Cutler JA. Prognostic value of exercise electrocardiogram in men at high risk of future coronary heart disease: multiple risk factor intervention trial experience. *J Am Coll Cardiol* 1986; 8: 1-10.
- Ribisl PM, Liu J, Mousa I, Herbert WG, Miranda CP, Froning JN, Froelicher VF. Comparison of computed ST criteria for diagnosis of severe coronary artery disease. *Am J Cardiol* 1993; 71: 546-551.
- Roger VL, Jacobsen SJ, Pellikka PA, Miller TD, Bailey KR, Gersh BJ. Prognostic value of treadmill exercise testing: a population-based study in Olmsted County, Minnesota. *Circulation* 1998; 98: 2836-2841.
- Ryan TJ, Weiner DA, McCabe CH, Davis KB, Sheffield LT, Chaitman BR, Tristani FE, Fisher LD. Exercise testing in the Coronary Artery Surgery Study randomized population. *Circulation* 1985; 72(suppl V): V31-38.
- Saarinen M, Karp PJ, Katila TE, Siltanen P. The magnetocardiogram in cardiac disorders. *Cardiovasc Res* 1974; 8: 820-834.
- Saarinen M, Siltanen P, Karp PJ, Katila TE. The normal magnetocardiogram: I Morphology. *Ann Clin Res* 1978; 10(suppl 21): 1-22.

- Savage MP, Squires LS, Hopkins JT, Raichlen JS, Park CH, Chung EK. Usefulness of ST-segment depression as a sign of coronary artery disease when confined to the postexercise recovery period. *Am J Cardiol* 1987; 60: 1405-1406.
- Savard P, Cohen D, Lepeschkin E, Cuffin BN, Madias JE. Magnetic measurement of S-T and T-Q segment shifts in humans. Part I: early repolarization and left bundle branch block. *Circ Res* 1983; 53: 264-273.
- Selker HP. Coronary care unit triage decision aids: how do we know when they work? *Am J Med* 1989; 87: 491-493.
- Selzer A. The Bayes theorem and clinical electrocardiography. *Am Heart J* 1981; 101: 360-363.
- Shaw LJ, Younis LT, Stocke KS, Sharma AK, Chaitman BR. Effects of posture on metabolic and hemodynamic predischarge exercise response after acute myocardial infarction. *Am J Cardiol* 1990; 66: 134-139.
- Shenasa M, Hamel D, Nasmith J, Nadeau R, Savard P. Body surface potential mapping of ST segment shift in patients undergoing percutaneous transluminal coronary angioplasty: correlations with the electrocardiogram and vectorcardiogram. In: Shenasa M, Borggreffe M and Breithardt G, eds. *Cardiac mapping*. Futura Publishing Co, Mount Kisco, NY 1993: 325-334.
- Siltanen P. Magnetocardiography. In: Macfarlane PW, Lawrie TDV, eds. *Comprehensive Electrocardiology Volume II*. Pergamon Press, Oxford 1989: 1408-1438.
- Simelius K, Tierala I, Jokiniemi T, Nenonen J, Toivonen L, Katila T: A Body surface mapping system in clinical use. *Med & Biol Eng* 1996; 34(suppl): 107-108.
- Simoons ML, Block P. Toward the optimal lead system and optimal criteria for exercise electrocardiography. *Am J Cardiol* 1981; 47: 1366-1374.
- SippensGroenewegen A, Peeters HAP, Jessurun ER, Linnenbank AC, Robles de Medina EO, Lesh MD, van Hemel NM. Body surface mapping during pacing at multiple sites in the human atrium. P-wave morphology of ectopic right atrial activation. *Circulation* 1998; 97: 369-380.
- Sohi GS, Flowers NC. Body surface map patterns of altered depolarization and repolarization in right bundle branch block. *Circulation* 1980; 61: 634-640.
- Sohi GS, Flowers NC, Horan LG, Sridharan MR, Johnson JC. Comparison of total body surface map depolarization patterns of left bundle branch block and normal axis with left bundle branch block and left axis deviation. *Circulation* 1983; 67: 660-664.
- Surawicz B, Saito S. Exercise testing for detection of myocardial ischemia in patients with abnormal electrocardiograms at rest. *Am J Cardiol* 1978; 41: 943-951.

- Surawicz B. Electrophysiology of myocardial ischemia. *Electrophysiological basis of ECG and cardiac arrhythmias*. Williams and Wilkins, Philadelphia 1995a: 378-401.
- Surawicz B. Abnormalities of ventricular repolarization. *Electrophysiological basis of ECG and cardiac arrhythmias*. Williams and Wilkins, Philadelphia 1995b: 566-607.
- Surawicz B. Electrocardiographic theory and methods of recording. *Electro-physiological basis of ECG and cardiac arrhythmias*. Williams and Wilkins, Philadelphia 1995c: 494-507.
- Taggart P, Sutton PMI, Spear DW, Drake HF, Swanton RH, Emanuel RW. Simultaneous endocardial and epicardial monophasic action potential recordings during brief periods of coronary artery ligation in the dog: influence of adrenaline, beta blockade, and alpha blockade. *Cardiovasc Res* 1988; 22: 900-909.
- Takala P, Hänninen H, Montonen J, Mäkijärvi M, Nenonen J, Oikarinen L, Simelius K, Toivonen L, Katila T. Magnetocardiographic and electrocardiographic exercise mapping in healthy subjects. *Ann Biomed Eng* 2001a; 29: 501-509.
- Takala P, Hänninen H, Montonen J, Mäkijärvi M, Nenonen J, Toivonen L, Katila T. Beat-to-beat analysis method for magnetocardiographic recordings during interventions. *Phys Med Biol* 2001b; 46: 975-982.
- Takala P, Hänninen H, Montonen J, Korhonen P, Mäkijärvi M, Nenonen J, Oikarinen L, Toivonen L, Katila T. Heart rate adjustment of magnetic field map rotation in detection of myocardial ischemia in exercise magnetocardiography. *Basic Res Cardiol* 2002; 97: 88-96.
- Tavarozzi I, Comani S, Del Gratta C, Luca Romani G, Di Lucio S, Brisinda D, Gallina S, Zimarino M, Fenici R, De Caterina R. Magnetocardiography: current status and perspectives. Part I: physical principles and instrumentation. *Ital Heart J* 2002a; 3: 75-85.
- Tavarozzi I, Comani S, Del Gratta C, Di Luzio S, Luca Romani G, Gallina S, Zimarino M, Brisinda D, Fenici R, De Caterina R. Magnetocardiography: current status and perspectives. Part II: clinical applications. *Ital Heart J* 2002b; 3: 151-165.
- Thadani U, West RO, Mathew TM, Parker JO. Hemodynamics at rest and during supine and sitting bicycle exercise in patients with coronary artery disease. *Am J Cardiol* 1977; 39: 776-783.
- Théroux P, Waters DD, Halphen C, Debaisieux J-C, Mizgala HF. Prognostic value of exercise testing soon after myocardial infarction. *N Engl J Med* 1979; 301: 341-345.
- Tseng YZ, Hsu KL, Chiang FT, Lo HM, Hwang JJ, Lai LP, Lin JL, Tseng CD. Characteristic findings of body surface potential map during ventricular repolarization in patients with coronary artery disease. *Jpn Heart J* 1999; 40: 391-404.

- Tsukada K, Miyashita T, Kandori A, Mitsui T, Terada Y, Sato M, Shiono J, Horigome H, Yamada S, Yamaguchi I. An iso-integral mapping technique using magnetocardiogram, and its possible use for diagnosis of ischemic heart disease. *Int J Card Imaging* 2000; 16: 55-66.
- Van Leeuwen P, Hailer B, Wehr M. Spatial distribution of QT intervals: An alternative approach to QT dispersion. *Pacing Clin Electrophysiol* 1996; 19[Pt.II]: 1894-1899.
- Van Leeuwen P, Hailer B, Wehr M. Changes in current dipole parameters in patients with coronary artery disease with and without myocardial infarction. *Biomed Tech (Berl)* 1997; 42: 132-135.
- Van Leeuwen P, Hailer B, Bader W, Geissler J, Trowitsch E, Gronemeyer DH. Magnetocardiography in the diagnosis of fetal arrhythmia. *Br J Obstet Gynaecol* 1999a; 106: 1200-1208.
- Van Leeuwen P, Stroink G, Hailer B, Adams A, Lange S, Grönemeyer D. Rest and stress magnetocardiography in coronary artery disease. *Med Biol Eng Comput* 1999b; 37: 1482-1483.
- Van Leeuwen P, Hailer B, Lange S, Donker D, Grönemeyer D. Spatial and temporal changes during the QT-interval in the magnetic field of patients with coronary artery disease. *Biomed Tech (Berl)* 1999c; 44: 139-142.
- Viik J, Lehtinen R, Turjanmaa V, Niemelä K, Malmivuo J. The effect of lead selection on traditional and heart rate-adjusted ST-segment analysis in the detection of coronary artery disease during exercise testing. *Am Heart J* 1997; 134: 488-494.
- Viik J, Lehtinen R, Turjanmaa V, Niemelä K, Malmivuo J. Correct utilization of exercise electrocardiographic leads in differentiation of men with coronary artery disease from patients with a low likelihood of coronary artery disease using peak exercise ST-segment depression. *Am J Cardiol* 1998; 81: 964-969.
- Viik J, Lehtinen R, Malmivuo J. Detection of coronary artery disease using maximum value of ST/HR hysteresis over different number of leads. *J Electrocardiol* 1999; 32(suppl): 70-75.
- Vincent GM, Abildskov JA, Burgess MJ. Mechanisms of ischemic ST-segment displacement. Evaluation by direct current recordings. *Circulation* 1977; 56: 559-566.
- Wada M, Kaneko K, Teshigawara H, Kondo T, Ohashi S, Miyagi Y, Nomura M, Okajima S, Hishida H, Takeuchi A, Mizuno Y. Exercise stress body surface isopotential map in patients with coronary artery disease: comparison with coronary angiographic and stress myocardial perfusion scintigraphic findings. *Jpn Circ J* 1981; 45: 1203-1207.

- Weiner DA, Ryan TJ, Parsons L, Fisher LD, Chaitman BR, Sheffield LT, Tristani FE. Long-term prognostic value of exercise testing in men and women from the Coronary Artery Surgery Study (CASS) registry. *Am J Cardiol* 1995; 75: 865-870.
- Weiss J, Shine KI. Extracellular  $K^+$  accumulation during myocardial ischemia in isolated rabbit heart. *Am J Physiol* 1982; 242: H619-H628.
- Wetherbee JN, Bamrah VS, Ptacin MJ, Kalbfleisch JH. Comparison of ST segment depression in upright treadmill and supine bicycle exercise testing. *J Am Coll Cardiol* 1988; 11: 330-337.
- Wung SF, Drew B. Comparison of 18-lead ECG and selected body surface potential mapping leads in determining maximally deviated ST lead and efficacy in detecting acute myocardial ischemia during coronary occlusion. *J Electrocardiol* 1999; 32(suppl): 30-37.
- Yamaki M, Kubota I, Endo T, Hosoya Y, Ikeda K, Tomoike H. Relation between recovery sequence estimated from body surface potentials and T wave shape in patients with negative T waves and normal subjects. *Circulation* 1992; 82: 1768-1774.
- Yan G-X, Yamada KA, Kléber AG, McHowat J, Corr PB. Dissociation between cellular  $K^+$  loss, reduction in repolarization time, and tissue ATP levels during myocardial hypoxia and ischemia. *Circ Res* 1993; 72: 560-570.
- Yan G-X, Antzelevitch C. Cellular basis for the electrocardiographic J wave. *Circulation* 1996; 93: 372-379.
- Yan G-X, Antzelevitch C. Cellular basis for the normal T wave and electrocardiographic manifestations of the long-QT syndrome. *Circulation* 1998; 98: 1928-1936.
- Yan G-X, Antzelevitch C. Cellular basis for the Brugada syndrome and other mechanisms of arrhythmogenesis associated with ST-segment elevation. *Circulation* 1999; 100: 1660-1666.
- Yanowitz FG, Vincent GM, Lux RL, Merchant M, Green LS, Abildskov JA. Application of body surface mapping to exercise testing: S-T<sub>80</sub> isorearea maps in patients with coronary artery disease. *Am J Cardiol* 1982; 50: 1109-1113.
- Yasumura S, Kubota I, Ikeda K, Yamaki M, Tsuiki K, Yasui S. ST segment changes in exercise body surface mapping after myocardial infarction in patients with isolated left anterior descending coronary artery disease. *Am Heart J* 1987; 114: 1120-1128.